

R-95-12



# LAKE OROVILLE RUNOFF ENHANCEMENT PROJECT

FINAL REPORT

Submitted to  
California Department of Water Resources  
Division of Operations and Maintenance

Under  
Cooperative Agreement Contract No. B-57788

September 1995

**U.S. DEPARTMENT OF THE INTERIOR**  
Bureau of Reclamation  
Technical Service Center  
River Systems and Meteorology Group

T  
45.7  
.R4  
No.R-95-12  
C.2



# REPORT DOCUMENTATION PAGE

Form Approved  
OMB No. 0704-0188

Public reporting burden for this collection of information is estimated to average 1 hour per response, including the time for reviewing instructions, searching existing data sources, gathering and maintaining the data needed, and completing and reviewing the collection of information. Send comments regarding this burden estimate or any other aspect of this collection of information, including suggestions for reducing this burden to Washington Headquarters Services, Directorate for Information Operations and Reports, 1215 Jefferson Davis Highway, Suite 1204, Arlington VA 22202-4302, and to the Office of Management and Budget, Paperwork Reduction Report (0704-0188), Washington DC 20503.

<b>1. AGENCY USE ONLY (Leave Blank)</b>		<b>2. REPORT DATE</b> September 1995	<b>3. REPORT TYPE AND DATES COVERED</b> Final	
<b>4. TITLE AND SUBTITLE</b> Lake Oroville Runoff Enhancement Project			<b>5. FUNDING NUMBERS</b>  PR	
<b>6. AUTHOR(S)</b> David W. Reynolds and Curtis L. Hartzell				
<b>7. PERFORMING ORGANIZATION NAME(S) AND ADDRESS(ES)</b> Bureau of Reclamation Technical Service Center Denver CO 80225			<b>8. PERFORMING ORGANIZATION REPORT NUMBER</b>  R-95-12	
<b>9. SPONSORING/MONITORING AGENCY NAME(S) AND ADDRESS(ES)</b> Bureau of Reclamation Denver Federal Center PO Box 25007 Denver CO 80225-0007			<b>10. SPONSORING/MONITORING AGENCY REPORT NUMBER</b>  DIBR	
<b>11. SUPPLEMENTARY NOTES</b> Microfiche and hard copy available at the Technical Service Center, Denver, Colorado				
<b>12a. DISTRIBUTION/AVAILABILITY STATEMENT</b> Available from the National Technical Information Service, Operations Division, 5285 Port Royal Road, Springfield, Virginia 22161			<b>12b. DISTRIBUTION CODE</b>	
<b>13. ABSTRACT (Maximum 200 words)</b> Bureau of Reclamation cooperated with California Department of Water Resources to design and implement a snowpack augmentation program to increase runoff to Oroville Reservoir. The program involves collection of data to document physical processes leading to increased precipitation. This report summarizes main results from 3 yr of in-situ physical studies and statistical analysis of precipitation data collected during 87 randomized seeding cases. Liquid propane released from high elevation sites has proven to be a viable, reliable method of seeding wintertime clouds in the Sierra Nevada. Targeting of seeded crystals produced from the propane dispenser has proven difficult. Based on these findings, project suspension is appropriate after 3 yr and project redesign is necessary. Propane seeding can increase snowfall when excess supercooled water is available. The questions yet to be answered are: what propane release rate is required to produce significant snowfall, is such a release rate economical, and can dispenser sites be located that will allow upward transport of ice crystals and adequate time for particle growth and fallout in the target area? The potential importance of being able to seed slightly supercooled clouds, which are found in abundance during the winter in northern California, is too great to ignore these questions.				
<b>14. SUBJECT TERMS</b> --atmospheric research/ meteorology/ weather modification/ cloud seeding/ precipitation augmentation/ meteorological instruments/ Sierra Nevada/ Middle Fork Feather River Watershed/ Lake Oroville/ Plumas County, CA/ Wasatch Plateau, UT/			<b>15. NUMBER OF PAGES</b> 133	
			<b>16. PRICE CODE</b>	
<b>17. SECURITY CLASSIFICATION OF REPORT</b>  UL	<b>18. SECURITY CLASSIFICATION OF THIS PAGE</b>  UL	<b>19. SECURITY CLASSIFICATION OF ABSTRACT</b>  UL	<b>20. LIMITATION OF ABSTRACT</b>  UL	

**R-95-12**

**LAKE OROVILLE RUNOFF  
ENHANCEMENT PROJECT**

**Final Report**

**by**

**David W. Reynolds\*  
Curtis L. Hartzell**

River Systems and Meteorology Group  
Technical Service Center  
Denver, Colorado

September 1995

\*Present affiliation: DOC/NOAA/NWS-WFO, Monterey, CA

## ACKNOWLEDGMENTS

Each individual who contributed to or directly participated in the LOREP cannot possibly be acknowledged. Mr. Don Finlayson and Mr. Maury Roos at the California DWR (Department of Water Resources) inspired the project's beginning in 1985. Mr. Larry Mullnix, former Deputy Director of DWR, was the driving force behind the program implementation. Mr. Richard Lallatin worked for almost three years before his retirement to draft the first environmental document and manage the initial procurement phase of the program. Mr. Gerry Boles and Mr. Dave Bogner of the Northern District saw the environmental process to its completion. Ms. Laura Shaw and Mr. Bill Anderson of the General Services Telecommunications office were instrumental in developing the communications network required to remotely operate the propane dispensers from Sacramento. DWR staff out of Oroville, including Mr. Bruce Gillette and Mr. Ron Vance, were critical to the development of the remote propane dispenser. The entire DWR staff of the Beckwourth field office provided dedicated field work support. This staff includes Conrad Lahr, Jim Hespen, Don Hand, and Ralph Howell. This team was truly instrumental in ensuring the success of the field operations. Thanks to the DWR staff in the Sacramento Project Operations Center for operating the propane dispensers during each of the seeding experiments.

A great deal of appreciation is given to the DWR management team who provided guidance and support during the last four years of the project (1991 through 1994), during which the field research operations were conducted. This team includes Mr. John Silveira, Deputy Director of DWR; Mr. Keith Barrett, Chief, Division of Operations and Maintenance; and LOREP's program manager, Mr. Clay Magonigal. Several members of the Flood Forecasting Section of DWR are to be thanked for their support. Mr. David Parker provided continuous support in assuring that all field data entered into the California Data Exchange Center were properly archived. Mr. Gary Hester was not only instrumental in helping to finalize an important section of the environmental document, but provided many hours of support and encouragement. Finally, Mr. Mark Heggli provided significant contributions in forecasting support, field support, and in data management.

Mr. John Lease from the Bureau of Reclamation's Technical Service Center, Denver, Colorado, provided vital leadership and oversight for the project. Mr. Jack McPartland and Mr. Glenn Cascino provided critical support on the installation and calibration of equipment in the field. Dr. Arlin B. Super authored appendix E, which discusses observations from liquid propane seeding Utah's Wasatch Plateau. Special thanks is due to Mr. Tom Hovland for his technical editing of the draft report.

### *U.S. Department of the Interior Mission Statement*

As the Nation's principal conservation agency, the Department of the Interior has responsibility for most of our nationally-owned public lands and natural resources. This includes fostering sound use of our land and water resources; protecting our fish, wildlife, and biological diversity; preserving the environmental and cultural values of our national parks and historical places; and providing for the enjoyment of life through outdoor recreation. The Department assesses our energy and mineral resources and works to ensure that their development is in the best interests of all our people by encouraging stewardship and citizen participation in their care. The Department also has a major responsibility for American Indian reservation communities and for people who live in island territories under U.S. administration.

The information contained in this report regarding commercial products or firms may not be used for advertising or promotional purposes and is not to be construed as an endorsement of any product or firm by the Bureau of Reclamation.

## FOREWORD

The California DWR (Department of Water Resources) has the responsibility to help protect, conserve, develop and manage California's water for present and future needs. Paramount in this responsibility is the examination of current water use and supply, and development of plans to meet the water needs of a continually increasing population that has grown from 24 million to 30 million between 1980 and 1990, and is expected to increase to 40 million by 2010.

Snowpack augmentation through cloud seeding is a nonstructural and environmentally preferred alternative for increasing water supplies. Cloud seeding in California has been used for over 40 years. From 1987 through 1991, the DWR, in cooperation with Reclamation (Bureau of Reclamation), designed a snowpack augmentation research project and prepared the required EIS (Environmental Impact Statement). Three preliminary field programs were conducted during the winters of 1988-89, 1989-90, and 1990-91. During these three winters, remote liquid propane dispenser testing was conducted under actual field conditions.

The winter of 1991-92 marked the commencement of the planned five-year experimental LOREP (Lake Oroville Runoff Enhancement Project). The LOREP, funded by the California SWP (State Water Project) contractors, was designed to increase runoff to Oroville Reservoir, the largest reservoir of the SWP, through seeding of wintertime orographic clouds. Seeding was performed along the Sierra crest above the Middle Fork Feather River, using ten remotely operated liquid propane dispensers, during the 1991-92, 1992-93, and 1993-94 winter seasons.

The LOREP was suspended after completion of only three years of the intended five-year project. DWR management suspended the project prematurely because of circumstances that indicated that the LOREP could not be successfully completed on schedule.

This report constitutes the final report on the LOREP (Lake Oroville Runoff Enhancement Project). Appendix A provides the 1993-94 field season budget breakdown for the LOREP.

## GLOSSARY AND ACRONYMS

AgI: silver iodide

BAG: Bagley Pass

C: columns

DAV: Lake Davis

DCP: data collection platform

Dispersion: in this report, the horizontal and vertical spreading or mixing of a substance like silver iodide or tracer gas caused by turbulent motions in the atmosphere; the turbulence can be mechanically induced, when set off by interactions between the airflow and rugged terrain, or convectively induced, or both.

DWR: Department of Water Resources

EIR/EIS: Environmental Impact Review/Environmental Impact Statement

EIS: Environmental Impact Statement

FAA: Federal Aviation Administration

free lift: volume of helium put in a balloon

G.m.t.: Greenwich mean time (UTC)

GOES: Geostationary Orbital Earth Satellite

GPS: global positioning system

GRZ: Grizzly Ridge

GUIDE: seeding guidance model

IFR: instrument flight rules

ING: Mt. Ingalls

in situ: Latin—in its original place (e.g., within a cloud)

JCC: Jackson Creek

JVL: Johnsville

LOREP: Lake Oroville Runoff Enhancement Project

m: meter

MHH: Mt. Hough

min: minutes

MLS: Mills Peak

m.s.l.: mean sea level

NOAA: National Oceanic and Atmospheric Administration

Orographic: mountain-induced, as orographic clouds are formed by the forced uplift and cooling of moist air over mountains

P: plates

pct: percent

PMS: Particle Measure System

POC: Project Operations Center

P.s.t: Pacific standard time

Radar wind profiler: a complete NOAA 915-MHz radar wind profiler system that measures winds in three fixed directions ( $u, v, w$ ) with along-beam resolutions of 100 and 400 m. Typical minimum range measurement is 100 to 300 m (depending on local radar clutter conditions) and maximum range is 1.5 to 5.0 km depending on atmospheric moisture.

Radiometer: in this report, a passive instrument that measures natural radiation in two specific microwave wavelengths related to emissions from water vapor and liquid water; the instrument is capable of estimating the vertically integrated amounts of water vapor and liquid water above it, but no ranging information is provided as from radar or lidar measurements.

Rawinsonde: a method of obtaining upper-air measurements of the wind, temperature, humidity, and pressure structure of the atmosphere; a balloon-borne instrument called a radiosonde is tracked as it ascends by radar or radio direction finder. The radiosonde and its balloon are commonly called a "weather balloon."

RDH: Red Hill

Reclamation: Bureau of Reclamation

SF<sub>6</sub>: sulfur hexafluoride

Snowfall: For appendix E, snowfall is defined as the rate at which snow falls.

Supercooled liquid water (SLW): water in the liquid state at temperatures below the freezing point of bulk water (0 °C); supercooled cloud droplets are common in many winter clouds over the intermountain West between temperatures of 0 and -15 °C, and sometimes exist at significantly lower temperatures.

SWP: State Water Project

UTC: Universal time coordinated

V: volt

2D-C: two-dimensional crystal

# CONTENTS

	Page
Foreword . . . . .	iii
Glossary and acronyms . . . . .	iv
Executive summary . . . . .	xi
1. Introduction . . . . .	1
2. Operation of ground-based equipment . . . . .	4
2.1 Mountaintop weather stations . . . . .	4
2.2 Propane dispensers . . . . .	7
2.3 Rawinsonde observations . . . . .	8
2.4 Precipitation gauge network . . . . .	10
2.5 SF <sub>6</sub> tracer operations . . . . .	13
2.5.1 Remote SF <sub>6</sub> release . . . . .	14
2.5.2 SF <sub>6</sub> analyzer . . . . .	14
2.5.3 SF <sub>6</sub> sequential samplers . . . . .	14
2.6 Radiometer measurements . . . . .	15
2.7 Radar wind profiler . . . . .	17
2.8 Ground microphysics sites . . . . .	18
3. Research aircraft operations . . . . .	20
4. Seeding operations . . . . .	23
5. Discussion of mountaintop icing data . . . . .	26
6. Application of a radar wind profiler . . . . .	32
7. Statistical analysis of randomized seeding . . . . .	43
8. The effects of mountain lee waves on the transport of liquid propane generated ice crystals . . . . .	48
8.1 Introduction to lee wave effects study . . . . .	48
8.2 Rawinsonde observations of mountain lee waves . . . . .	48
8.3 Aircraft tracer studies . . . . .	54
8.3.1 Experimental procedures . . . . .	54
8.3.2 Plume analyses . . . . .	54
8.3.2.1 Valley track plume intersections . . . . .	54
8.3.2.2 Ridge track plume intersections . . . . .	62
8.3.2.3 Downwind plume intersections . . . . .	64
8.4 Seeding studies and targeting model verification . . . . .	65
8.4.1 February 17, 1993, seeding studies . . . . .	65
8.4.2 GUIDE model plume and crystal trajectory simulations for February 17, 1993 . . . . .	74
8.5 Summary of lee wave effects study results . . . . .	80
9. Summary and conclusions . . . . .	81
10. Bibliography . . . . .	83

## TABLES

### Table

2.1	Mountaintop weather stations . . . . .	4
2.2	Propane dispenser site locations . . . . .	8
2.3	Precipitation gauge locations . . . . .	11
2.4	Syringe sampler locations . . . . .	14
4.1	Seeding log from November 8, 1993, to March 1, 1994 . . . . .	25
5.1	Mt. Hough icing data for 1993-94 . . . . .	27
5.2	Red Hill icing data for 1993-94 . . . . .	28
8.1	SF <sub>6</sub> experiments conducted during early 1993 . . . . .	56
8.2	SF <sub>6</sub> plume characteristics from site d7 observed by aircraft for valley track . . . . .	57
8.3	Site d9 plume characteristics observed by aircraft for valley track . . . . .	59

## CONTENTS — CONTINUED

### TABLES — CONTINUED

Table		Page
8.4	SF <sub>6</sub> plume characteristics from site d7 as observed by aircraft for ridge pass . . . . .	63
8.5	SF <sub>6</sub> plume characteristics from site d9 as observed by aircraft for ridge pass . . . . .	63
8.6	SF <sub>6</sub> plume characteristics from site d7 as observed by aircraft for downwind track . . . . .	65
8.7	SF <sub>6</sub> plume characteristics from site d9 as observed by aircraft for downwind track . . . . .	65

### FIGURES

Figure		
2.1	LOREP project area and location of field operations and observation equipment. . . . .	5
2.2	Environmental sensors mounted on tower at a mountaintop weather station . . . . .	6
2.3	LOREP target area showing 100-m contours of terrain . . . . .	7
2.4	Typical dispenser site installation showing tanks and dual tower assembly . . . . .	9
2.5	Rawinsonde tracking antenna at the Johnsville site . . . . .	10
2.6	Locations of propane seeding dispensers on the Sierra crest and downwind precipitation gauges . . . . .	12
2.7	Typical precipitation gauge site showing shielded gauge and GOES antenna . . . . .	13
2.8	Example of vertically integrated liquid water (bottom) and water vapor (top) observed by the radiometer on February 18, 1992, over Johnsville . . . . .	16
2.9	Microwave radiometer (trailer) located at Jackson Creek site . . . . .	17
2.10	Radar wind profiler at Blairsdens site . . . . .	18
3.1	NOAA King-Air C-90 research aircraft . . . . .	21
3.2	Nominal flight tracks used by the NOAA research aircraft during the 1993 tracer and seeding experiments superimposed over the project area . . . . .	22
4.1	Example of GUIDE model output . . . . .	24
5.1a	Water year (Oct. 1 to Sept. 30) averages derived from the Red Hill mountaintop icing station . . . . .	29
5.1b	Same as a) but for Mt. Hough . . . . .	29
5.2	Masses of growing ice crystals at various times as a function of temperature . . . . .	30
5.3	Terminal speeds of ice crystals and snowflakes . . . . .	31
6.1	Time-height plot of Blairsdens hourly profiler consensus wind vectors for January 24, 1994 . . . . .	33
6.2	Precipitation measured in the gauge network for January 24, 1994 . . . . .	34
6.3	Comparison of the hourly profiler winds with the rawinsonde winds for 1700 UTC (0900 P.s.t) on January 24, 1994 . . . . .	35
6.4	Rawinsonde derived vertical velocity vectors along path of ascending balloon for 1700 UTC (0900 P.s.t.) on January 24, 1994 . . . . .	37
6.5	The 24-h wind profile from the profiler along with the observed precipitation in the gauge network for February 7, 1994 (UTC) . . . . .	38
6.6	Comparison of the hourly profiler winds with the rawinsonde winds for 0600 and 1100 UTC on February 7, 1994 . . . . .	39
6.7	The 24-h wind profile from the profiler along with the observed precipitation in the gauge network for February 18, 1994 . . . . .	40
6.8	Comparison of the hourly profiler winds with the rawinsonde winds for 0000 and 0500 UTC on February 18, 1994 . . . . .	42
7.1	Gauge network and time lag used for each gauge in the analysis of seeded and nonseeded periods . . . . .	44

## CONTENTS — CONTINUED

### FIGURES — CONTINUED

Figure	Page
7.2	Results of target versus control mean precipitation regression analysis for all 87 randomized cases . . . . . 46
7.3	Results of target versus control mean precipitation regression analysis for 60 randomized cases where GUIDE model predicted seeding effects in the target area . . . . 47
8.1	Schematic illustration of mountain waves forming over and to the lee of the project area . . . . . 49
8.2	Rawinsonde determined vertical velocities measured along the path of the ascending balloon for February 10, 1994 . . . . . 49
8.3	Balloon derived vertical velocities plotted with respect to distance from Johnsville for February 10, 1994 . . . . . 50
8.4	Rawinsonde derived vertical velocities for soundings taken during storm events prior to the passage of the surface cold front . . . . . 52
8.5	Same as figure 8.4 but for soundings taken after surface frontal passage . . . . . 53
8.6	Nominal flight tracks used by the NOAA research aircraft during the mid-January to mid-March 1993 tracer and seeding experiments superimposed over the project area . . . 55
8.7	Average SF <sub>6</sub> concentrations plotted with respect to altitude for all SF <sub>6</sub> plume penetrations from site d7 (EL 2225 m) along the valley track . . . . . 58
8.8	Variables observed or calculated from aircraft observations made during plume tracing experiments during VFR conditions on March 9 along the valley track . . . . . 61
8.9	Average SF <sub>6</sub> concentrations plotted with respect to altitude for all SF <sub>6</sub> plume penetrations from site d9 (EL 2146 m) along the valley track . . . . . 62
8.10	Rawinsonde derived vertical velocities for March 17 showing well defined lee wave pattern which influenced the transport of SF <sub>6</sub> on this day . . . . . 64
8.11	Same as figure 8.8 but for March 9 downwind (northeast) from the flight track shown on figure 8.6 . . . . . 66
8.12	Aircraft-observed SF <sub>6</sub> concentrations above 10 p/t plotted over target area terrain contours for March 9, 1993 . . . . . 67
8.13	Various parameters observed at the Jackson Creek Observatory for February 17, 1993 . . . . . 68
8.14	Temporal plot of meteorological variables measured at Mt. Hough for February 17, 1993 . . . . . 69
8.15	Temporal plots of measurements made by the NOAA aircraft on pass 13 for February 17, 1993 . . . . . 71
8.16	Same as figure 8.15 but for February 9, 1993, along ridge pass for seeded plume initiated from site d7 . . . . . 72
8.17	Guide predicted plume from site d7 overlaid onto terrain contours for February 9, 1993 . . . . . 73
8.18a	Guide model predicted particle trajectories from sites d7 and d9 using rawinsonde horizontal wind field and the vertical velocities from figure 8.18a for 1800 UTC February 17, 1993 . . . . . 75
8.18b	Same as (a) but for 2100 UTC for site d7 only . . . . . 75
8.19	GUIDE model contoured vertical velocities (m s <sup>-1</sup> ) across the project area for 1800 UTC, February 17, 1993 . . . . . 76
8.20	GUIDE model predicted plume from site d7 along with actual aircraft observed SF <sub>6</sub> plume . . . . . 77
8.21	GUIDE model predicted plume from site d9 along with actual aircraft observed SF <sub>6</sub> plume . . . . . 78
8.22	SF <sub>6</sub> measured by sequential sampler located at site No. 8 on figure 2.3 (near JCC) . . . . 79

## CONTENTS — CONTINUED

### APPENDIXES

Appendix	Page
A	LOREP cost estimates for FY94 field program and FY95 report . . . . . 87
B	LOREP suspension criteria . . . . . 93
C	Liquid propane dispenser design documentation . . . . . 97
D	Calculations estimating increased runoff from an augmented snowpack in the Middle Fork Feather River catchment area . . . . . 103
E	Observations of microphysical effects of liquid propane seeding on Utah's Wasatch Plateau during early 1995, by Arlin B. Super . . . . . 109

### APPENDIX FIGURES

Figure	
C.1	Liquid propane dispenser configuration . . . . . 101
E.1	Map of the Wasatch Plateau Experimental Area for the 1994-95 field program . . . . . 112
E.2	HAS temporal distributions of wind direction, air temperature, icing detector trips, and propane release rates during two seeding experiments of March 5, 1995 . . . . . 116
E.3	TAR temporal distributions of wind speed and direction, air temperature and icing detector trips during two seeding experiments of March 5, 1995 . . . . . 117
E.4	Temporal distributions of the IPC and precipitation intensity, both calculated from the TAR 2D-C probe observations and the NCAR IN counter observations of $\text{IN L}^{-1}$ , effective at $-20^\circ\text{C}$ , for two seeding experiments of March 5, 1995 . . . . . 118
E.5a	Cumulative percentage of IPC, partitioned by size, versus time during March 5, 1995 . . . . . 120
E.5b	Cumulative percentage of IPC, partitioned by crystal habit, versus time during March 5, 1995 . . . . . 120
E.5c	Cumulative percentage of precipitation intensity, partitioned by size, versus time during March 5, 1995 . . . . . 121
E.5d	Cumulative percentage of precipitation intensity, partitioned by crystal habit, versus time during March 5, 1995 . . . . . 121
E.6	TAR 2D-C images of ice particles (100 $\mu\text{m}$ minimum size) for selected periods during March 5, 1995 . . . . . 122
E.7	HAS temporal distributions of wind speed and direction, air temperature, icing detector trips, and propane release rates during three seeding experiments of March 11, 1995 . . . . . 124
E.8	TAR temporal distributions of wind speed and direction, air temperature, and icing detector trips during three seeding experiments of March 11, 1995 . . . . . 124
E.9	Temporal distributions of the IPC and precipitation intensity, both calculated from the TAR 2D-C probe observations, and the NCAR IN counter observations of $\text{IN L}^{-1}$ , effective at $-20^\circ\text{C}$ (middle panel), for three propane seeding experiments of March 11, 1995 . . . . . 125
E.10a	Cumulative percentage of IPC, partitioned by size, versus time during March 11, 1995 . . . . . 127
E.10b	Cumulative percentage of IPC, partitioned by crystal habit, versus time during March 11, 1995 . . . . . 127
E.10c	Cumulative percentage of precipitation intensity, partitioned by size, versus time during March 11, 1995 . . . . . 128
E.10d	Cumulative percentage of precipitation intensity, partitioned by crystal habit, versus time during March 11, 1995 . . . . . 128
E.11	TAR 2D-C images of ice particles (100 $\mu\text{m}$ minimum size) for selected periods during March 11, 1995 . . . . . 130

## EXECUTIVE SUMMARY

The LOREP (Lake Oroville Runoff Enhancement Project) was intended to be a 5-year randomized winter cloud seeding demonstration project conducted by the California Department of Water Resources. The long-term goal of the project was to increase runoff to Oroville Reservoir, the main reservoir of the State Water Project located in northern California. Orographic cold-cloud seeding operations were conducted in 6-h randomized blocks during the 1991-92, 1992-93, and 1993-94 winter seasons. Ground-truth precipitation measurements (snowfall water equivalent) were obtained with a network of up to 11 automatic recording and transmitting precipitation gauges. Statistical analyses of the randomized cases were attempted, but the sample size obtained (87 cases: 56 seed, 31 no seed) during these three winter seasons proved to be too small for obtaining statistically significant results.

Physical studies were conducted in the hope of documenting the magnitude of the increases possible in the seasonal snowpack obtained by seeding winter storms using liquid propane. The field studies conducted emphasized the transport and dispersion of ice crystals produced by the ground-based release of liquid propane from high altitude dispensers along the crest of the northern Sierra Nevada. These studies included a combination of rawinsonde upper-air observations, low altitude research aircraft data collection flights over the target area, a vertically pointing dual-channel microwave radiometer to measure the integrated liquid water and vapor within passing clouds, mountaintop weather stations to measure icing rate and other meteorological parameters, tracer gas release from two propane dispenser sites, both airborne and ground-based tracer sampling measurements, and a radar wind profiler.

The balloon ascent rates for special rawinsonde launches made just downwind from the main Sierra Nevada crest showed a very well defined mountain lee (gravity) wave present during most precipitation events. Strong airflow descent to the lee of the Sierra will thus have a detrimental effect on the growth of ice crystal particles generated on the crest. The tracer SF<sub>6</sub> (sulphur hexafluoride) was used to simulate the transport and dispersion of propane generated ice crystals. Aircraft measurements of SF<sub>6</sub> indicated that at the normal flight altitudes of 2500 m over the downwind valley and 2800 m over the downwind ridge, the aircraft was flying near the top of the tracer gas plumes. When the aircraft was able to fly below cloud base near the release altitude of 2200 m, substantial SF<sub>6</sub> was observed. The lower portion of the plume was also observed to descend into the valley about 700 m below the release altitude.

A simple two-dimensional model (GUIDE) was used to determine the impact these lee waves have on ice crystal trajectories. GUIDE model output is presented for one well documented seeding case (February 17, 1993) to show how such models might be used operationally to predict particle trajectories downwind from the Sierra. The results indicate that the GUIDE model does a good job of predicting the location of seeding plumes downwind from the propane dispensers if the proper wind information can be input to the model.

The physical studies point out the complexities associated with the transport and the successful targeting of seeding induced ice crystals initiated over complex terrain. Nearly continuous horizontal and vertical wind fields along with a vertical profile of temperature are needed to accurately predict particle growth and fallout. The 915-MHz wind profiler with RASS (Radar Acoustic Sounding System) may provide the technology necessary to obtain nearly continuous measurements of the three-dimensional wind field and temperature profile,

if a method can be developed to eliminate the effect of hydrometeor fall speeds on the vertical wind component calculation.

The LOREP was intended to be a 5-year project. It was suspended after 3 years in part because of the limited periods in which lee waves did not have a detrimental effect on particle growth and trajectories. This problem was compounded by the fact that two of the three project years were drought years limiting seeding periods; the other year had record snowfall, which required suspension of seeding operations. This situation severely restricted the number of randomized cases available for statistical analysis.

Results from the 3-year LOREP indicate that a redesign of the project is necessary. Detailed tracer studies from new potential propane dispenser sites, farther south through west of the previous locations, should be completed prior to resuming randomized seeding experiments. In addition, higher propane release rates may be appropriate for the slightly supercooled temperatures (above  $-5^{\circ}\text{C}$ ) that are common at the propane dispenser locations. Propane seeding can increase snowfall at such temperatures when excess supercooled water is available. The questions yet to be answered are: what propane release rate is required to produce significant snowfall, is such a release rate economical, and can dispenser sites be located that will allow upward transport of ice crystals and adequate time for particle growth and fallout in the target area? The potential importance of being able to seed slightly supercooled clouds, which are found in abundance during the winter in northern California, is too great to ignore these questions.

## 1. INTRODUCTION

The LOREP (Lake Oroville Runoff Enhancement Project) was a randomized winter cloud seeding demonstration project that was conducted by the California DWR (Department of Water Resources). The LOREP was located in the Middle Fork Feather River watershed in northern California. The Drought Relief Act of 1991 authorized the Bureau of Reclamation to support the transfer of weather modification technology to the States and to participate with the States on a matching funds basis for a 5-year period. In November 1991, a joint EIR/EIS (Environmental Impact Review and Environmental Impact Statement) was approved by the U.S. Forest Service, Plumas National Forest, which allowed the demonstration project to begin in the 1991-92 winter season. Although the winter of 1991-92 marked the first year of the 5-year program to quantify precipitation increases possible from cloud seeding, DWR had been testing the required program equipment and facilities since 1988. The project plan was for randomized cloud seeding experiments, using liquid propane as the seeding agent, to be conducted during five consecutive winter seasons. Through a Cooperative Agreement between DWR and Reclamation (Bureau of Reclamation), DWR provided funds to Reclamation for technical assistance on this project.

The purpose of the project was to increase snowpack runoff to Lake Oroville, the main reservoir of the State Water Project located in northern California. The goal of the project was to demonstrate through physical and statistical analyses the increases in winter snowpack obtainable by seeding winter storms with liquid propane. The project was hoped to provide additional water to help alleviate drought and provide a working technology for other Western States that need additional water supplies (Sward, 1991).

Propane was tested as the seeding agent instead of the more conventional AgI (silver iodide) because measurement of mountaintop icing showed more hours of SLW (supercooled liquid water) in the -1 to -5 °C temperature window than at the colder temperatures ( $\leq -5$  °C) where AgI is more effective. The use of ground-based liquid propane dispensers is believed to have a better chance to maximize precipitation, given the warm temperature of California storms. This cloud-seeding project is the first of its kind in the country that has used liquid propane to seed winter clouds to increase snowfall (Sward, 1991). The process involved releasing pressurized propane into cold clouds moving up the slope of the Sierra Crest. As propane evaporates, it lowers the surrounding air temperature to well below -40 °C (-40 °F), producing billions of tiny ice crystals. These crystals grow in size at the expense of cloud droplets and eventually form snowflakes. Propane works well because it can drop the ambient air temperature to -100 °F without freezing itself. Reynolds (1989, 1991, 1992a) describes the original design, development and testing of the remote, ground-based liquid propane dispenser used as the seeding device on this project. Reynolds' calculations estimating increased runoff from an augmented snowpack in the study area are included as appendix D.

The LOREP was suspended after completion of only 3 yr of the intended 5-yr project. DWR management suspended this project prematurely because of three overriding considerations. First, the Reclamation project scientist who designed and implemented LOREP took a new position with the National Weather Service. This move was in response to Reclamation's new commitment to transform from a water resources development agency to a premier water resources management agency. Consequently, Reclamation work on research programs to develop water resources, such as weather modification, will be phased out. Secondly, the three winter seasons completed have been extreme, either excessively dry as in 1991-92 and

1993-94, or excessively wet as in 1992-93. This extreme weather has significantly reduced the number of randomized cases obtained after three years (87 actual versus 180 expected). It is anticipated that the project would need to be continued at least two years beyond the five years intended to achieve statistical significance. All of the remaining winter seasons would need to have near normal precipitation. Adding two or more years would require extension of the environmental permits, which may require public review. Thirdly, physical studies relating specifically to the transport of the tracer SF<sub>6</sub> (sulfur hexafluoride) within the target area have shown that moderate to strong downdrafts and updrafts to the lee of the main Sierra crest (mountain lee waves, which often occur prior to storm frontal passage but are much less dominant in post-frontal patterns) have a significant impact on the successful targeting of seeding-produced ice crystals. These results indicate that one solution to this problem would be to move the dispensers farther west and south of their current locations to extend crystal growth time before the crystals pass into this strong vertical motion field. This relocation would require an amendment to the EIR/EIS and a period of public review, and a possible year delay in the project.

The LOREP field activities during 1991-92 and 1992-93 are documented by Reynolds (1992b and 1993) in annual project reports available from DWR. The annual report of 1992-93 field activities (Reynolds, 1993) includes findings from SF<sub>6</sub> tracer studies, verification of the GUIDE (seeding guidance) numerical targeting model, and preliminary results from the statistical analysis of the randomized seeding cases obtained during the first two winter field seasons.

This final report summarizes the field activities conducted during all three winter field seasons. However, more emphasis is given to activities from the 1993-94 field season, which were not reported previously in DWR annual reports.

The effects of mountain gravity waves or "lee waves" will be reviewed based on analysis of the project rawinsonde balloon ascent rate. The combination of the horizontal winds and vertical velocities computed from balloon tracking allows initialization of the Reclamation's GUIDE model. The model computations allow an assessment of the impact these waves have on the successful targeting of seeding effects within the precipitation gauge network.

As has been emphasized repeatedly (Reynolds, 1988; Super 1990), it is imperative that transport and dispersion studies be conducted within any intended cloud seeding project area. These studies are needed to determine whether ground-based seeding can place a sufficient number of ice embryos into supercooled liquid cloud regions long enough to produce substantial crystal growth for fallout within the intended target area.

Results will be provided from the use of a remote radar wind profiler installed within the target area to determine how the wind field changes during seeding operations. Although the profiler was unable to provide continuous vertical velocity data, its ability to accurately measure the horizontal winds hourly demonstrates its value as a tool in assessing the variable nature of the winds during winter storms.

The frequency and magnitude of supercooled liquid water will be reviewed by analysis of the project's mountain-top icing data. Supercooled liquid water is necessary if cloud seeding is to succeed. The magnitude and temperature of the liquid water is critical to the rate of growth of seeded ice particles. This growth rate then impacts how quickly the crystals will fall out of the cloud as precipitation particles, or "snowflakes."

A brief review will be given of the statistical analysis of the randomized precipitation data set obtained through the 1993-94 winter. However, given the small sample size and the complications in targeting, these results should be viewed cautiously.

The design and performance of the remote liquid propane dispenser used on the project will be documented. The current design used during the 1993-94 winter season seems to have solved the loss of battery power during extended stormy periods. The 1993-94 winter season is the first year that all ten dispensers operated throughout the winter season without failure. Brief communications interruptions were noted on several sites. These interruptions prevented use of all ten dispensers during some seeding operations. The use of high gain directional antennas did not completely eliminate these communications problems.

Finally, related observations of microphysical effects of liquid propane seeding on Utah's Wasatch Plateau during early 1995 are discussed in appendix E.

## 2. OPERATION OF GROUND-BASED EQUIPMENT

The LOREP study area was located in the northern Sierra Nevada as shown on figure 2.1. Ground-based equipment for the LOREP consisted of the following:

- Mountaintop weather stations
- Propane dispensers
- Rawinsonde observations (atmospheric soundings)
- Precipitation gauges
- SF<sub>6</sub> (sulfur hexafluoride) tracer gas release, sequential samplers, and analyzer
- Radiometer
- Radar wind profiler
- Microphysics observations

The use of this equipment for the LOREP and related measurement sites are summarized in the following subsections.

### 2.1 Mountaintop Weather Stations

Mountaintop weather stations were installed at four locations within the LOREP study area. The locations of these remote automatic weather stations are shown on figure 2.1 and listed in table 2.1. Handar model 540A DCPs (data collection platforms) were used to collect the data, which were then transmitted hourly through GOES satellite.

Table 2.1. - Mountaintop weather stations. Data are transmitted hourly through GOES satellite.

Station Name	3-letter Ident.	DCP ID	Transmit Time (min)	Data Avg. Interval (min)	Elev. (m)	Lat. North	Long. West
Red Hill	RDH	34243F4A	32	5	1936	40.04°	121.19°
Mills Peak	MLS	34243198	31	5	2248	39.70°	120.62°
Mt. Hough	MHH	34246F36	38	5	2204	40.05°	120.88°
Jackson <sup>1</sup> Creek	JCR	34249FB2	44	5	1951	39.86°	120.63°

<sup>1</sup> No ice detector

The 1993-94 winter was the seventh consecutive winter season in which icing data were collected at the RDH (Red Hill) mountaintop weather station. In addition, 4 winter seasons of data (1990-91 through 1993-94) have been collected at MHH (Mt. Hough) and MLS (Mills Peak). The JCR (Jackson Creek) station was only operated during the last 2 yr of the project (1992-93 and 1993-94).

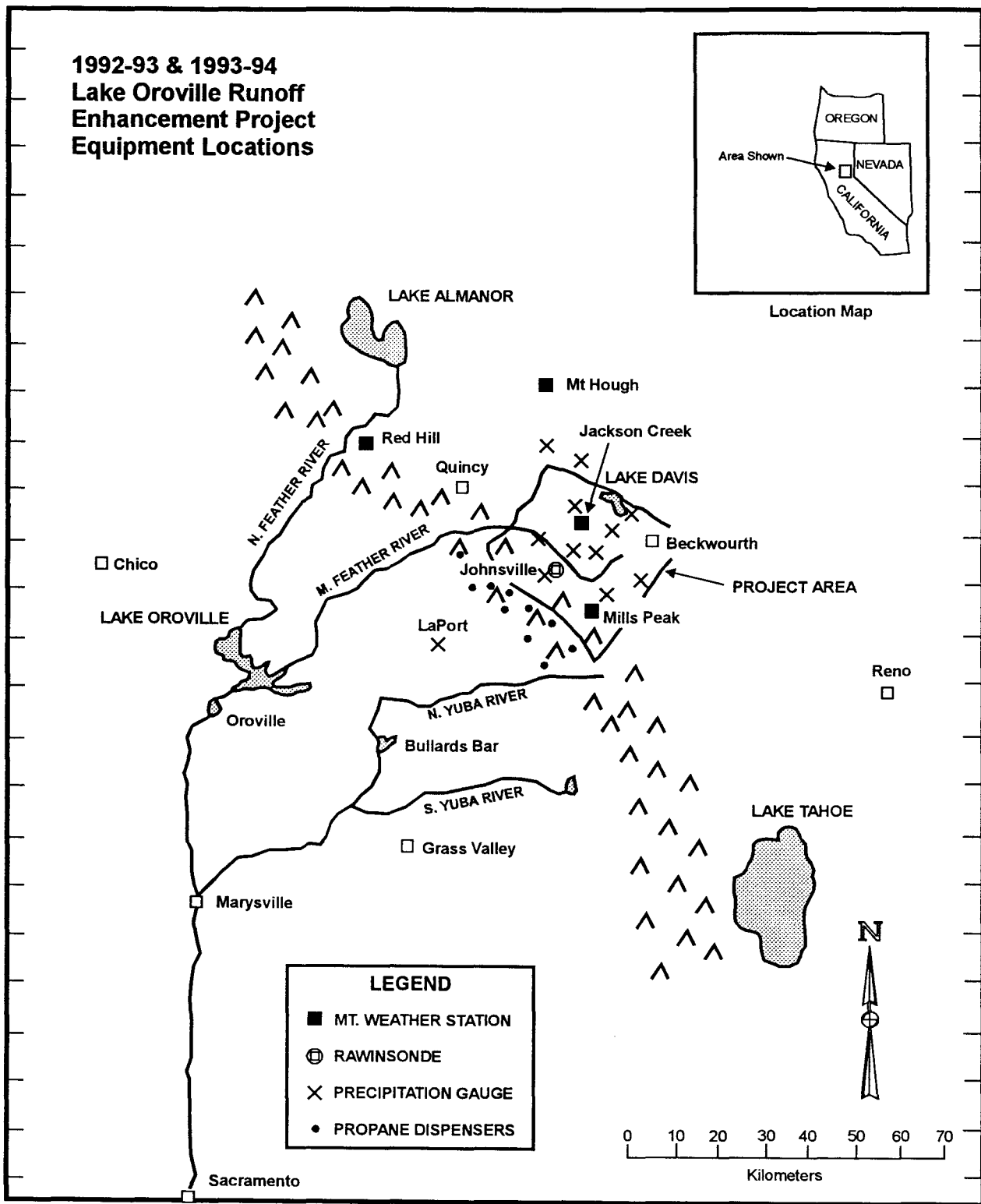


Figure 2.1. - LOREP area and location of field operations and observation equipment.

These data provide critical information for seeding decision making. Each station is equipped with the following sensors:

1. Temperature (Handar model 435A)
2. Relative humidity (Handar model 435A)
3. Wind speed (heated Handar model 430A)
4. Wind direction (heated Handar model 431A)
5. Icing trips (Rosemount model 872B)

Figure 2.2 is a photograph of the sensors mounted on a tower at one of the mountaintop weather stations. The buildup of rime ice on the tower, caused by the presence of SWL, is evident; the heated sensors are free of rime ice.

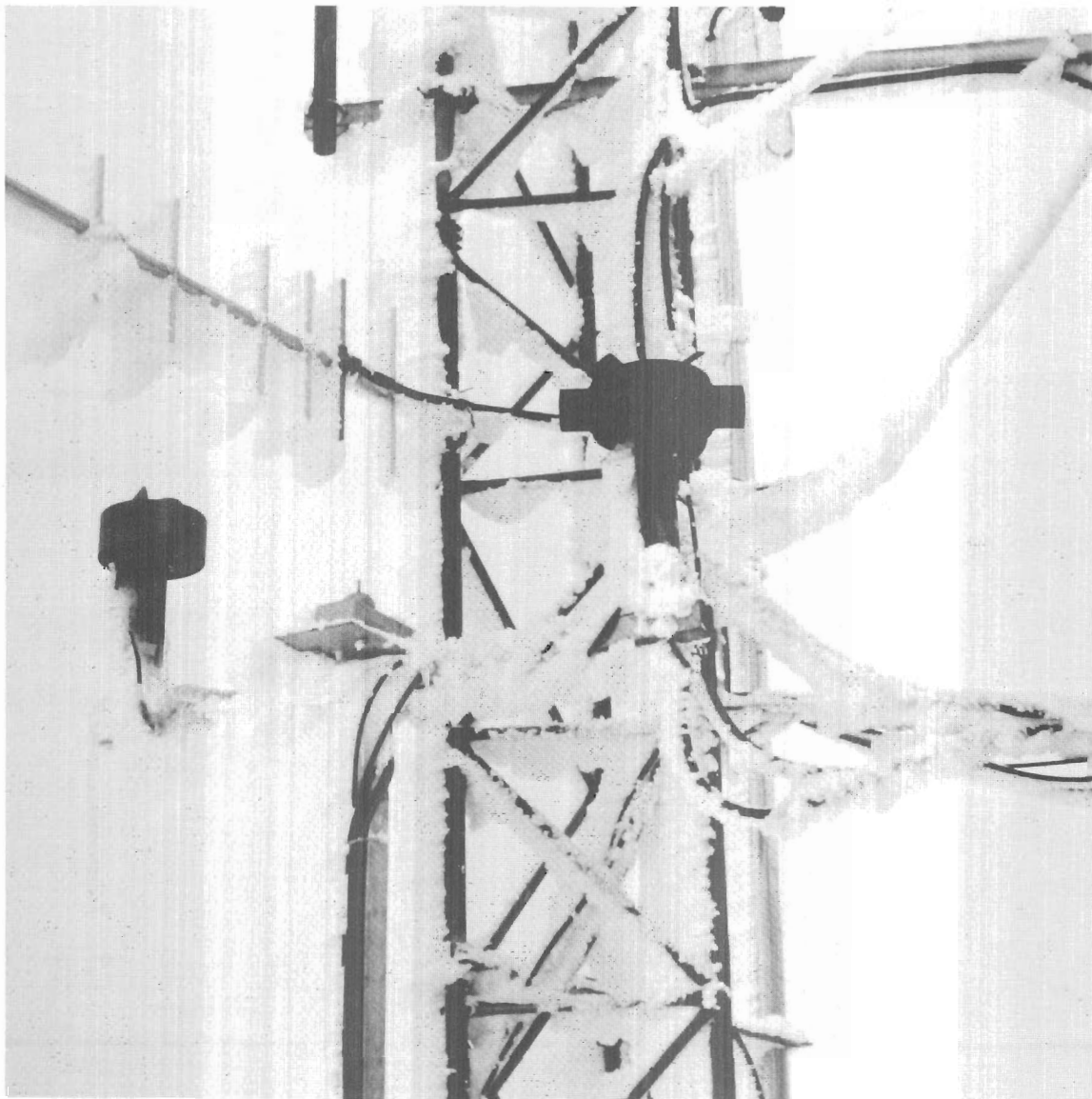


Figure 2.2. - Environmental sensors mounted on tower at a mountaintop weather station.

## 2.2 Propane Dispensers

Ten propane seeding dispensers were installed along the Sierra Crest at the locations shown on figures 2.1 and 2.3 (d1 through d10) and listed in table 2.2. Liquid propane was chosen as the seeding agent because the temperature of the cloud liquid water, as determined from mountaintop icing rate meters, was warmer than  $-4\text{ }^{\circ}\text{C}$  80 pct of the time during the winter season. Conventional silver iodide solutions require temperatures at or below  $-6\text{ }^{\circ}\text{C}$  to be activated as ice nuclei; propane has been shown to be an effective seeding agent at temperatures close to  $0\text{ }^{\circ}\text{C}$  (Hicks and Vali, 1973).

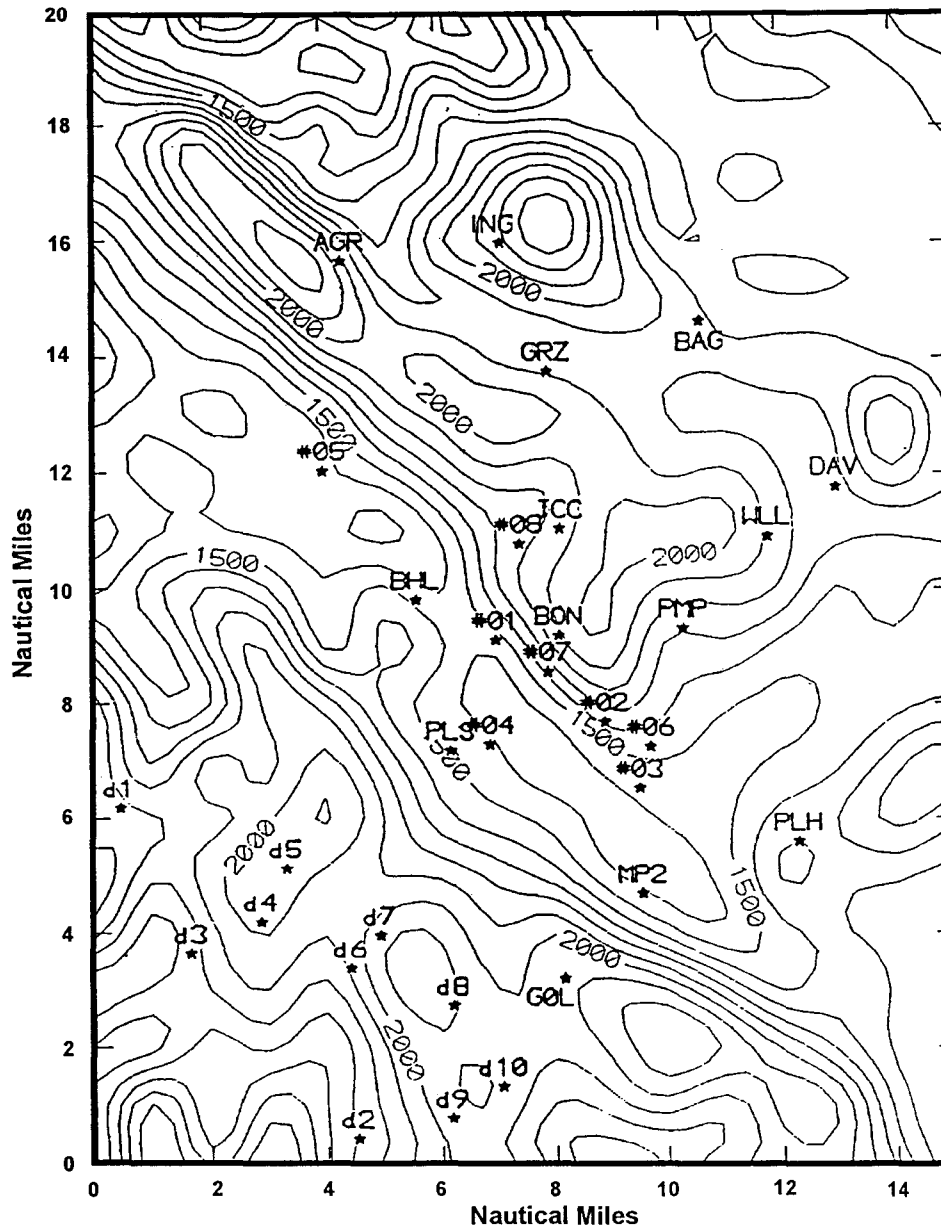


Figure 2.3. - LOREP target area showing 100-m contours of terrain. Location of propane dispensers are labeled d1 through d10, precipitation gauges with three-letter identifiers, and sequential  $\text{SF}_6$  samplers with a number. P2, P3, and P6 are aircraft waypoints along the flight track used for the tracer studies.

Table 2.2. - Propane dispenser site locations.

Station	3-Letter ID	Latitude (N)	Longitude (W)	Elevation (m)
Site d1	MET	39.77	120.84	2122
Site d2	PLC	39.63	120.73	2097
Site d3	PCT	39.69	120.79	2171
Site d4	GIB	39.71	120.78	2239
Site d5	ATR	39.72	120.77	2140
Site d6	SPL	39.70	120.73	2182
Site d7	WDL	39.71	120.72	2225
Site d8	ROL	39.68	120.68	2280
Site d9	BRC	39.64	120.68	2207
Site d10	DRL	39.65	120.66	2220

A typical dispenser site set-up is shown on figure 2.4. The filled propane tanks and dispenser were mounted on a metal pallet and were helicoptered to each site as a single unit. The dispenser has both radio receiving and transmitting capability. This feature provided on-off control of the propane release from the Sacramento POC (Project Operations Center) and confirmation of release by monitoring both nozzle temperature and flow rate.

A coded transmission was used via a microwave repeater atop Beckwourth Peak (see fig. 2.1) to initiate or terminate seeding. The exact details of the transmission sequence and radio system were determined by DWR's Office of Communications. Each station had a separate identification and thus could be interrogated separately. Details on the propane dispensers are given in appendix C.

Minor problems were noted with sites d7 and d10 during the 1992-93 winter season. Site d7 experienced communication problems and site d10 had a microcomputer failure the last 18 hours of seeding. A magnetic latching valve was installed on all dispensers. It required a momentary 12 V to actuate and a second 12 V to deactivate. These momentary power requirements significantly reduced power drain on the dispenser battery, which allowed many more hours of seeding during extended cloudy weather before the battery charge fell below 12 V.

After December 30, 1992, with the continued heavy snowfall, several dispensers were buried, which cut off all light to the solar panels (sites d4 and d9). In addition, several valve boxes were torn off towers because of extreme icing and winds (sites d6 and d8). Before the 1993-94 winter season, all valve boxes were reinforced and a third solar panel was installed looking down at the anti-sun direction so that the panel would not be impacted by falling snow or rime ice.

The 1993-94 winter season was excessively dry; consequently, heavy snowfall or rime icing caused no problems.

### 2.3 Rawinsonde Observations

Rawinsonde systems were used to collect upper-air atmospheric data from the surface to the 300-mb level (if possible) or about 10 km m.s.l. The data collected included pressure, temperature, relative humidity, wind speed, and wind direction.

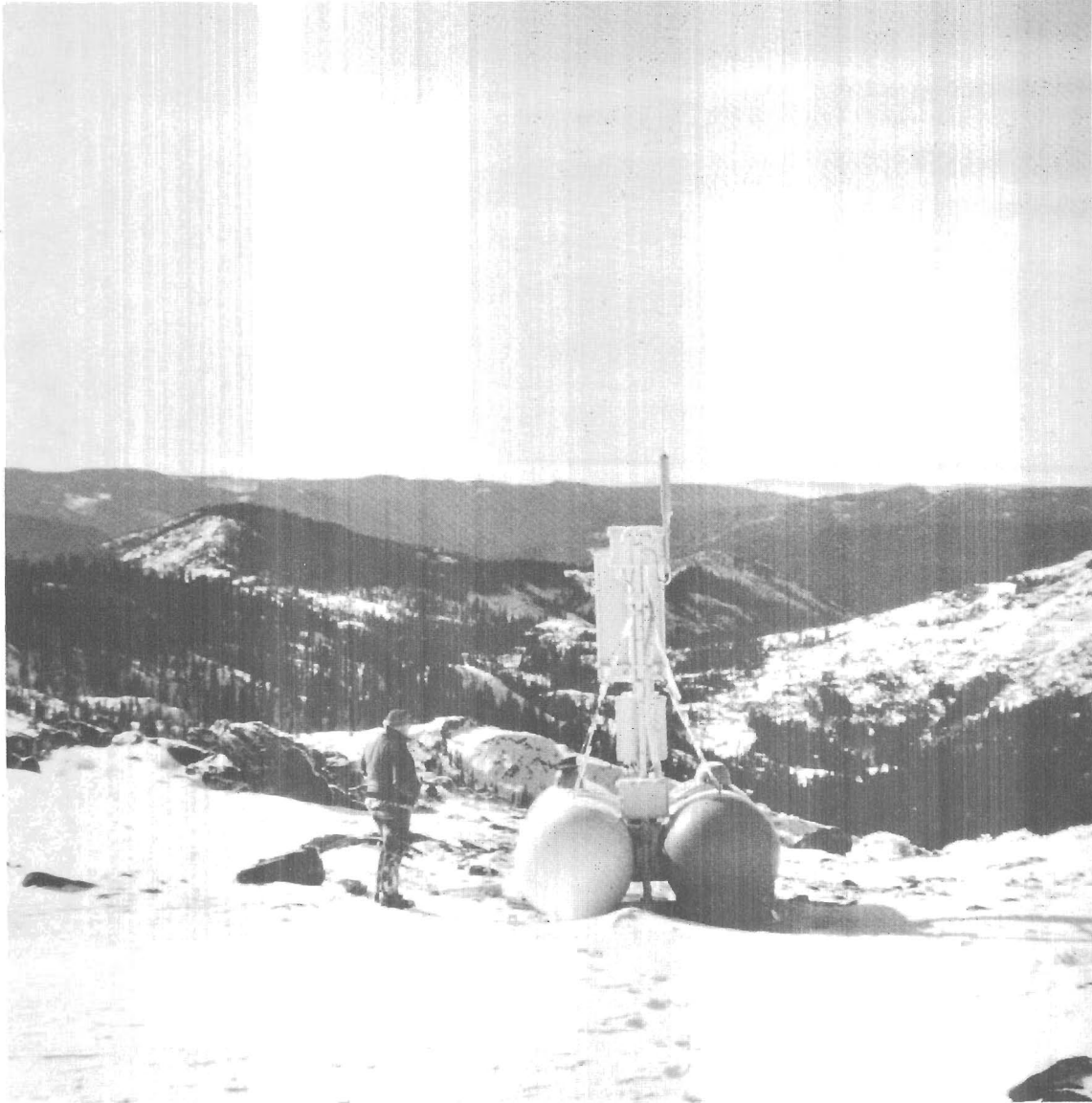


Figure 2.4. - Typical dispenser site installation showing tanks and dual tower assembly.

Two rawinsonde units were operated during the 1991-92 winter season. Rawinsonde launches were made at Plumas-Eureka State Park Headquarters at Johnsville by State Park personnel and at the DWR Thermalito Annex near Oroville by contractor personnel. For the 1992-93 and 1993-94 winter seasons, only the Johnsville site (see figure 2.1) was used for the rawinsonde operations. This rawinsonde system was an AIR (Atmospheric Instrumentation Research, Inc.) Intellisonde Meteorological Rawin System model IS-4A1-MET-UAS-120-MDI.

Rawinsonde upper-air sounding observations were taken at 6-h intervals during favorable (stormy) weather conditions. The information from these upper-air soundings was used in the real-time seeding decision making process, and also for postseason studies.

Figure 2.5 shows the rawinsonde tracking antenna at the Johnsville site, which was located at about 1500 m elevation along the lee slope of the Sierra Nevada.



Figure 2.5. - Rawinsonde tracking antenna at the Johnsville site.

## 2.4 Precipitation Gauge Network

As shown on figure 2.3, the intended target area encompasses a downwind valley and a second ridge line running parallel and at a slightly lower elevation than the main Sierra crest. The original design assumed that liquid water would form along the crest of the Sierra, allowing initial growth of the crystals. The liquid cloud would then begin to dissipate over the valley but reform along the second ridge. It was assumed that along and just over the second ridge, most of the seeding effects would be observed. Thus, most of the precipitation gauges were sited in this area.

The LOREP precipitation gauge network consisted of nine project-installed gauges plus four existing DWR (Department of Water Resources) gauges. Table 2.3 is a list of the gauges installed specifically for the LOREP, as well as the DWR existing gauges. Figure 2.6 shows

the location of all gauges within the target area. The project gauges at PLH and MP2 were moved to ING (Mt. Ingalls) and BAG (Bagley Pass), respectively, prior to the 1993-94 winter season to obtain better measurements of precipitation within the target area.

Table 2.3.- Precipitation gauge locations.

Station Name	3-Letter ID	DCP ID	Transit Time (min)	Data Avg. Int. (min)	Elev. (m)	Lat. (N)	Long. (W)
<b>Project Gauges</b>							
Plumas Eureka	PLS	34244708	33	15	1575	39.77°	120.70°
Big Hill	BHL	342449DA	34	15	1692	39.83°	120.71°
Jackson Creek	JCC	3424547E	35	15	1951	39.86°	120.63°
Willow Creek	WLL	34245AAC	36	15	1966	39.85°	120.53°
Bonta Ridge	BON	342461E4	37	15	1585	39.81°	120.64°
Penman Peak	PMP	34247292	39	15	1783	39.82°	120.58°
Pilot Hill	PLH	34247C40	40	15	1646	39.73°	120.52°
Mills Peak 2	MP2	34248216	41	15	1707	39.71°	120.58°
Argentine Rock	AGR	34249160	43	15	2122	39.96°	120.76°
Bagley Pass	BAG				1963	39.94°	120.55°
Mt. Ingalls	ING				2243	39.96°	120.62°
<b>DWR Gauges</b>							
Gold Lake	GOL				2058	39.67°	120.62°
Grizzly Ridge	GRZ				2104	39.92°	120.65°
Lake Davis	DAV				1759	39.88°	120.47°
Pilot Peak	PLP				2073	39.79°	120.87°

The nine project gauges were fully automated weighing gauges (2.2-kg load cell) with 12-in. orifices. The catchcan was mounted on 11- or 14-ft standpipes and equipped with wind screens. All gauges provide 0.25-mm resolution. Figure 2.7 shows the gauge site.

Using an auto siphon drain-and-fill system and an antifreeze recharge reservoir, the gauge was automatically drained when full (requiring about 120 s to drain and fill) and was recharged with a 20-pct glycerin, 80-pct denatured alcohol nonhazardous antifreeze. The drain-and-fill cycle occurred when 50 to 135 mm (2 to 5 in.) of precipitation had accumulated. The exact amount depends on ambient air temperature. The antifreeze reservoir holds 10, 20, or 30 gal depending on the site. The antifreeze-precipitation mixture was drained periodically into a waste reservoir. For those gauges with a 10-gal antifreeze reservoir, the waste compartment would overflow after 20 in. of water equivalent precipitation had fallen.

The precipitation data were collected on site by a Handar 560A or 540 DCP (data collection platform). Precipitation data were collected at 15-min intervals and transmitted hourly via the GOES satellite to the California Data Exchange Center downlink in Sacramento and the Reclamation downlink in Denver. Two existing DWR gauges were retrofitted with the same load-cell technology as the nine project gauges. These sites are located at DAV (Lake Davis) and GRZ (Grizzly Ridge).

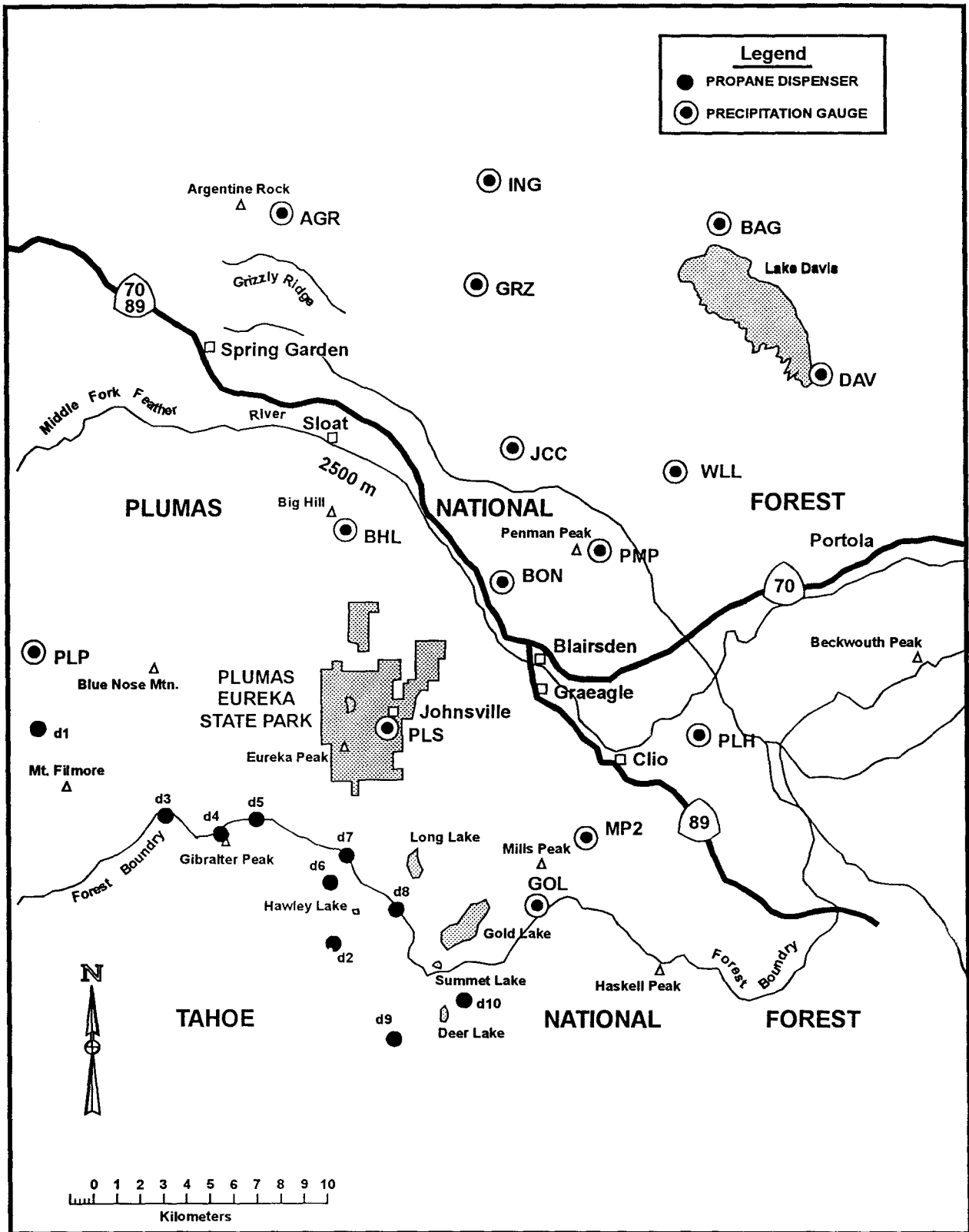


Figure 2.6. - Locations of propane seeding dispensers on the Sierra crest and downwind precipitation gauges.



Figure 2.7. - Typical precipitation gauge site showing shielded gauge and GOES antenna.

## 2.5 SF<sub>6</sub> Tracer Operations

Sulfur hexafluoride (SF<sub>6</sub>), a nontoxic, nonflammable gas, is a well known tracer used in both weather modification and air pollution studies. The tracer gas trajectory will not exactly match the trajectories of propane-generated ice crystals. However, the tracer will indicate the general direction and dispersion patterns of the treated volume of air passing by the dispenser. SF<sub>6</sub> studies conducted during the 1991-92 and 1992-93 winter seasons were summarized in the LOREP Annual Reports of Field Activities (Reynolds, 1992b; 1993). The study discussed in section 8 used SF<sub>6</sub> data from January through March 1993.

### 2.5.1 Remote SF<sub>6</sub> Release

Both propane dispenser sites d7 and d9 were equipped to allow remote release of tracer SF<sub>6</sub>. Site d7 (2225 m) was located on the Sierra crest, and site d9 (2207 m) was positioned about 5 km west of the crest as shown on figure 2.3. Two different locations were used to identify which site transported seeded crystals more reliably into supercooled clouds. Each site had 12 50-kg bottles of SF<sub>6</sub>. Six bottles were manifolded together. The supply line from the bottles was plumbed through a mass flow controller then to a solenoid. A release tube was run up the mast of the propane dispenser to within a few inches of the propane valve box. The solenoid was actuated in the same manner as propane release—by remote-controlled relay activated from Sacramento. The mass flow controller was set to release at 22 kg/h using an electric flow meter. Based on tank weights taken after the field 1992-93 season, flow rates determined by the flow controller were determined to be within 5 pct of actual for site d7 and 1 pct for site d9.

### 2.5.2 SF<sub>6</sub> Analyzer

A continuous SF<sub>6</sub> analyzer (Benner and Lamb, 1985) was provided, installed, and operated by North American Weather Consultants at the Jackson Creek high elevation (1951 m) observatory, located near the JCC precipitation gauge (fig 2.6). The analyzer was mounted in a small, 15-ft office trailer. An external pump was used to draw ambient air through a 5-m-long teflon tube routed through a window and mounted to a support on the trailer roof. This tube was connected to the analyzer inlet port. The analyzer was calibrated before and after each experiment using six calibration gases of known SF<sub>6</sub> concentrations (10.2, 95, 485, 972, 2902, and 4870 p/t [parts per trillion]). Instrument response was nearly linear over the range of calibration gases. Concentrations measured during this project fell well within the first three ranges of test gases. Based on instrument calibrations and stability, it was felt that SF<sub>6</sub> concentrations could be resolved down to 5 p/t.

### 2.5.3 SF<sub>6</sub> Sequential Samplers

Four time-sequential syringe samplers were used to collect 15-min air samples at specified locations within the valley. The eight project sampling sites are noted in table 2.4. Four of these eight sites were selected based on wind direction for each experiment. They were set in place about 30 min prior to data collection. Each sampler had nine 30-cm<sup>3</sup> syringes. The samplers were programmed to start sampling at the same time as the SF<sub>6</sub> gas was to be released. The nine syringes provided 2.25 h of sampling time.

Table 2.4. - Syringe sampler locations.

Site No.	Site Name	Latitude (°N)	Longitude (°W)
1	Two Rivers	39.82	120.66
2	Blairsdan	39.78	120.62
3	Gold Lake Hwy. 89	39.75	120.60
4	Johnsville Rd.	39.77	120.68
5	Lee Summit	39.88	120.76
6	Mohawk Vista	39.77	120.59
7	Bonta Ridge	39.80	120.65
8	Jackson Creek	39.85	120.66

## 2.6 Radiometer Measurements

A dual-frequency (20.6 and 31.54 GHz) microwave radiometer (Hogg et al., 1983), provided by Reclamation, was operated at the Johnsville ski area parking lot from December 30, 1991, through April 30, 1992. During the 1992-93 winter season, the radiometer was moved to the Jackson Creek Observatory (near the JCC precipitation gauge on fig. 2.6) along Grizzly Ridge, where it was operated from February 5 to March 19, 1993. The radiometer was used to measure path-integrated liquid water in millimeters and precipitable water vapor in centimeters passing over the target area. This information is critical to determining seeding effectiveness.

The radiometer is controlled by a mini-computer, which allows both system control and data collection. Data are recorded to hard disk every 2 min. The disk size is sufficient to record a full season of data.

Tipping curves are a means of calibrating the system. They consist of scanning the antenna through various elevation angles that relate to a given number of earth atmospheres (usually 1 to 4). These measurements allow the determination of the attenuation taking place in the entire path from the outside reflector to the microwave detectors. Tipping curves were performed about every 2 weeks under clear sky conditions and a steady water vapor environment.

The outside reflector dish must be kept free of snow or water during radiometer operation. A large exhaust fan was positioned to blow over the dish to help maintain a snow-free surface. However, when wet snow was falling, keeping the dish completely dry was nearly impossible.

At the Johnsville site, the radiometer was normally operated with the antenna pointing vertically. However, elevation scans were made to the east over Grizzly Ridge periodically to determine if supercooled liquid water was more prevalent over this ridge. The radiometer was moved to the Jackson Creek site to sample the integrated liquid and vapor passing over the target ridge. An example of integrated liquid and vapor data is shown on figure 2.8. A photograph of the radiometer and ice crystal collection system is shown on figure 2.9.

The objectives for using the radiometer were:

- a. Provide real-time indications of supercooled liquid water for conducting seeding operations.
- b. Develop a climatology on the frequency and magnitude of supercooled liquid over the target area.
- c. Determine the impact seeding has on the liquid water.

The radiometer experienced a problem throughout the intensive 2-month field program in early 1993. A reference voltage used to compute values of vapor and liquid often drifted outside of specified tolerances. This problem required constant adjustment and compromised data quality. Only a limited set of quality data could be retrieved from this data set.

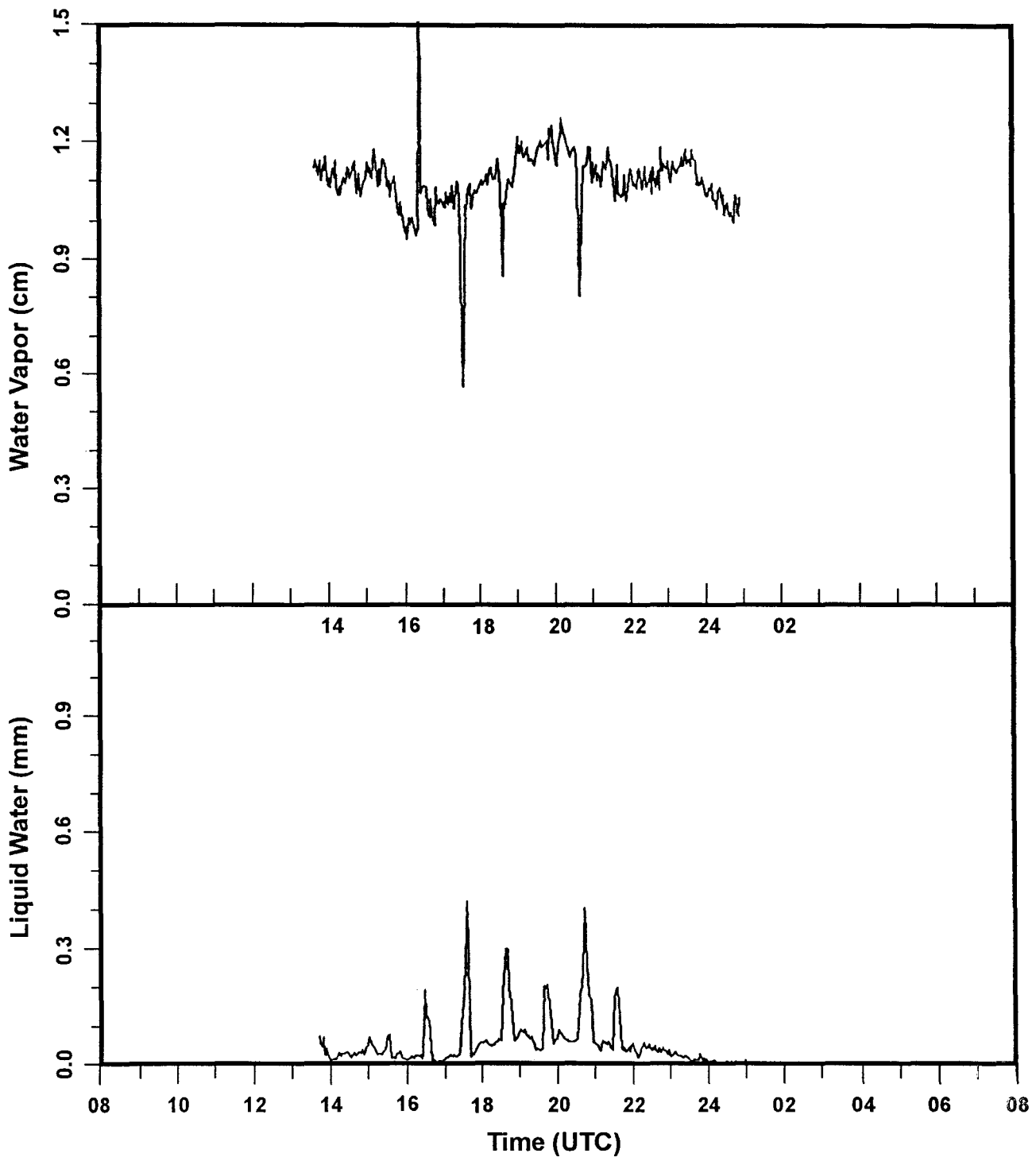


Figure 2.8. - Example of vertically integrated liquid water (bottom) and water vapor (top) observed by the radiometer on February 18, 1992, over Johnsville. The spikes in the liquid data show enhanced liquid over Grizzly Ridge as the antenna scanned over this location. Values have been normalized to the vertical. PST (Pacific standard time) is UTC minus 8 h.



Figure 2.9. - Microwave radiometer (trailer) located at Jackson Creek site.

## 2.7 Radar Wind Profiler

For the 1992-93 winter, a boundary layer radar wind profiler (Rodgers et al., 1993) was obtained for a 4-mo period from the NOAA's Environmental Research Laboratory in Boulder, Colorado. The profiler was installed in Blairsden, about 5 km southeast of Johnsville (fig. 2.6). The profiler is basically a Doppler radar operating at 915 MHz or 32.8 cm. Three separate antennas let the profiler measure both horizontal and vertical components of the wind (fig. 2.10). Antenna beam widths are each 9°. Therefore, the profiler averages over a large spatial volume. The radar has sufficient sensitivity to measure winds within 100-m vertical slices from 100 m above ground up to 3000 m in clear air and up to 5000 m during precipitation. At this wavelength, radar is about as sensitive to light rain as it is to changes in the atmospheric index of refraction. When sampling in clear air, the profiler is tracking



Figure 2.10. - Radar wind profiler at Blairsdan site.

the radial velocities of small "packets of density perturbations," which are common in the atmospheric boundary layer. In precipitation, the profiler simply tracks the horizontal and vertical radial velocities of the falling raindrops or snowflakes.

Section 6 discusses the project's application of the radar wind profiler.

## **2.8 Ground Microphysics Sites**

A microphysics laboratory was installed at the ski area parking lot in Plumas-Eureka State Park for the 1991-92 winter season. Prior to the 1992-93 winter season, the microphysics equipment was moved to a high elevation observatory (1951 m) established near the Jackson Creek (JCC) precipitation gauge site (see fig 2.6).

The microphysics equipment included:

- a. An aspirated PMS (Particle Measuring System) two-dimensional cloud probe used to record hundreds of two-dimensional snow crystal images per second. Images were recorded to magnetic tape which could be processed to determine crystal sizes and concentrations. Temperature, humidity, and wind speed and direction were recorded every 10 s.
- b. A microscope with camera, automatic exposure control, and cold stage attachment allowed photomicrographs of snow crystals collected in petri dishes every 15 min to be taken. These data were used to document crystal habit and degree of rime. Four to five random photos of each dish were taken to characterize the snowfall. Also, a manual record is kept of the crystal habits and riming as a backup to the photos. Tri-X black and white film was used. Negatives of the photomicrographs were contact printed as necessary for future analysis.

### 3. RESEARCH AIRCRAFT OPERATIONS

Through a Cooperative Agreement between the Reclamation and the National Oceanic and Atmospheric Administration, a well-instrumented King-Air C-90 research aircraft was provided to the LOREP for a 2-month field program (January 20 to March 19, 1993). The aircraft was based at Reno-Cannon International Airport in Reno, Nevada (see fig 3.1).

The aircraft carried a full complement of research instruments, including sensors to measure air pressure, ambient temperature and dew point, cloud liquid water content, cloud droplets (forward scattering spectrometer probe [FSSP]) in the size range of 1 to 45  $\mu\text{m}$ , cloud ice particles (2D-C Probe) in the size range from 25 to 800  $\mu\text{m}$ , and aircraft position (Loran-C and GPS). Horizontal wind speed and direction could be derived from aircraft observations of heading and true airspeed. In addition, a ScienTech Inc., precision tracer gas analyzer was operated on the aircraft to provide real-time measurements of  $\text{SF}_6$  tracer gas concentrations (Benner and Lamb, 1985). This analyzer was the same type that was used at the Jackson Creek Observatory. The same calibration procedures were followed for aircraft operation as were used for the ground analyzer. The analyzer is capable of detecting  $\text{SF}_6$  concentrations down to 5 p/t. In-flight testing (injection of calibration gas into the sampling tube) determined that a 10- to 12-s lag time occurred between ingestion of  $\text{SF}_6$  and registration by the analyzer. This lag needs to be accounted for when comparing the aircraft  $\text{SF}_6$  data to other aircraft data. An on-board computer-based data acquisition system recorded all observations at a rate of 1/s.

A waiver obtained from the Federal Aviation Administration permitted flight to within 300 vertical m (1000 ft) of the highest terrain within 2.5 km (5 statute mi) of the flight path during IFR (instrument flight rules) weather conditions. This allowance usually meant the aircraft was within 600 m (2000 ft) of most underlying terrain. All research flights were flown between dawn and dusk. A research flight was terminated at the discretion of the chief pilot when horizontal winds exceeded 20 m/s or when airframe icing became excessive. During VFR (visual flight rules) weather conditions, flight altitudes could be lowered to as close to the terrain as the pilot felt safe to fly.

The flight pattern used during research missions is shown on figure 3.2. The flight leg flown between P1 and P2 was the valley track flown at 2500 m (8300 ft) on a northwest heading. The flight leg between P3 and P4 was the ridge track flown at 2680 m (8800 ft) on a southeast heading. During VFR flights, these same tracks were flown, but at flight levels down to 2100 m (7000 ft). The two  $\text{SF}_6$  release locations are annotated with the numbers d7 and d9, meaning site d7 and site d9 dispenser locations on figure 3.2.

A typical flight operation consisted of takeoff from Reno and climb-out to the west over the Sierra Nevada. The aircraft would then descend from 3960 to 2500 m (13,000 to 8300 ft), entering the project area at P1. A typical flight lasted 3 h, completing about eight valley passes and eight ridge passes. During the early 1993 study period, the aircraft logged 35 research flight hours on 10 separate flights on 10 separate days. LOREP cloud seeding operations were suspended during this period because of excess snowpack. However, the operation of one propane dispenser for a 1-h period was allowed for each research aircraft flight.



Figure 3.1. - NOAA King-Air C-90 research aircraft.

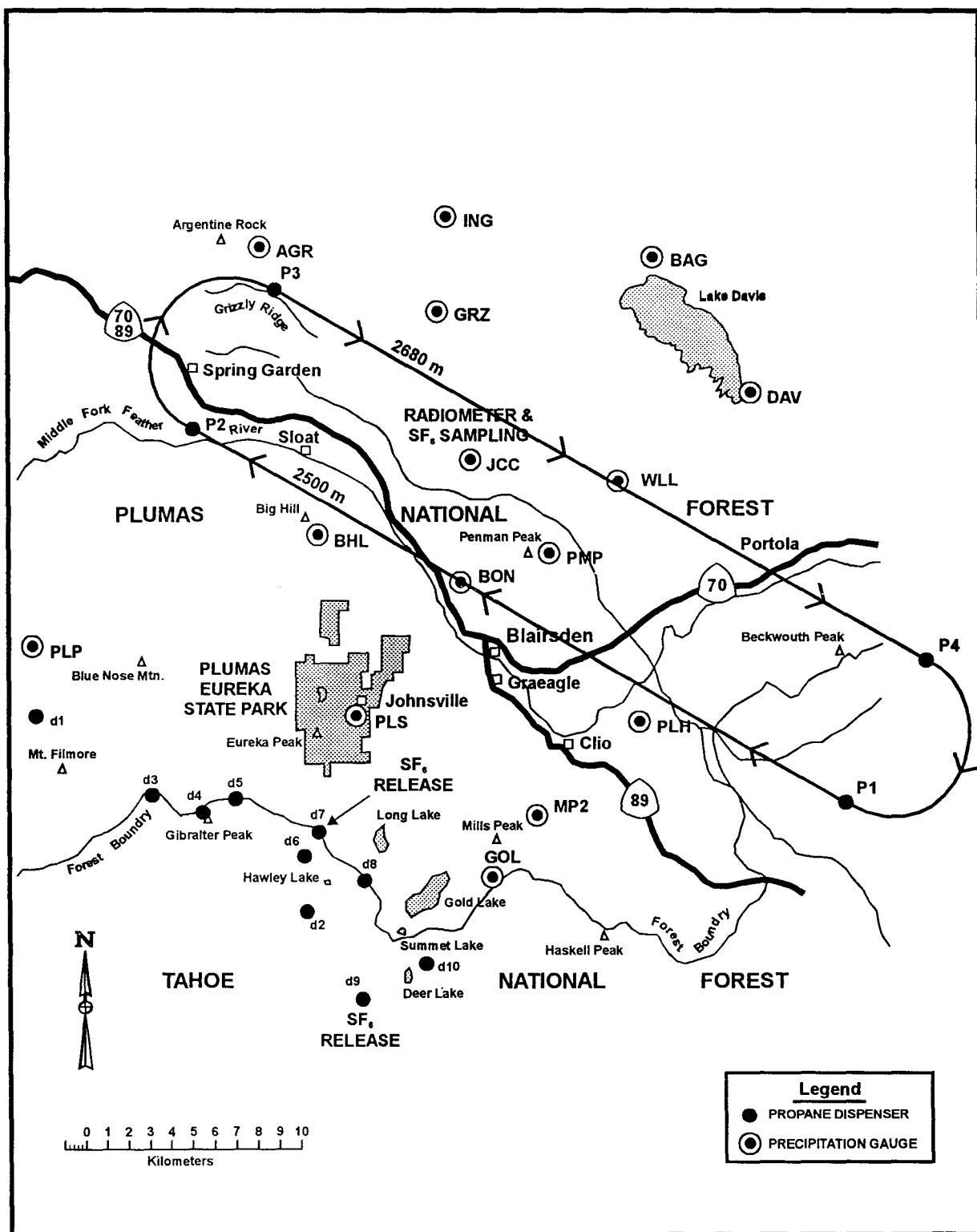


Figure 3.2. - Nominal flight tracks used by the NOAA research aircraft during the 1993 tracer and seeding experiments superimposed over the project area.

## 4. SEEDING OPERATIONS

Winter storm cloud seeding operations for the 3-yr LOREP were conducted in 6-h randomized blocks, based on a simple set of criteria:

1. Indications of rime icing at any of the mountaintop icing stations for at least 1 h.
2. Precipitation falling as snow at or below 5,000 ft m.s.l.
3. The numerical targeting model indicated the target area was being treated.

Each 6-h block meeting these criteria qualified as a "case" to be used in the statistical analysis. If appropriate conditions continued past 6 h, seeding terminated for 1 h and then resumed for 6 h. If a 6-h period was a no-seed, a new 6-h block could begin immediately. This pattern was repeated until cloud conditions were no longer suitable.

Randomization was done on a 3-to-2 basis. On average, for every 5 6-h periods qualifying for seeding, 3 were seeded and 2 were left unseeded for comparison. This ratio was chosen to maximize snow production while still maintaining a similar ratio of seeded and unseeded storms for statistical comparison. An envelope containing the seed or no-seed decision was opened by POC (Project Operations Center) personnel after it was determined that a suitable 6-h period qualified for treatment. On-off times of seeding dispensers were logged by personnel in the POC.

A control gauge was installed at LaPorte (see fig. 2.1), which was upwind of the target area. A 2-yr correlation using 6-h precipitation totals between LaPorte and the target network showed a linear correlation of 0.85. It was anticipated that this control site plus the use of randomization would allow statistical evaluation of the seeding effects (see section 7).

Seeding equipment reliability was documented by recording hourly status information transmitted by each dispenser back to the POC throughout the field season. Tank liquid level measurements were found to be accurate only after liquid levels dropped by several hundred gallons.

The seeding guidance model (GUIDE) was used to determine if seeding would target the gauge network. The model was initialized using the Johnsville sounding (fig. 2.1). The model is a simple two-dimensional Gaussian plume model with parameterized microphysics. The model outputs both the horizontal and vertical dispersion of the seeding plume. In addition, the fallout point of a snow crystal initiated at the dispenser was predicted. Crystal growth was assumed to be in a continuous cloud environment having a liquid water content of  $0.1 \text{ g m}^{-3}$ . A graphical example of GUIDE model output is shown on figure 4.1. Stars at the origin indicate that nucleation occurred at a nuclei source. Downwind stars represent fallout points for fastest growing crystals.

Cloud seeding suspension criteria (listed in appendix B) were developed so that seeding operations would be suspended prior to the development of hazardous situations, e.g., serious flooding and avalanche warnings. No seeding suspensions occurred during the 1991-92 and 1993-94 winter seasons, which were both relatively dry. However, for the 1992-93 winter season, seeding operations were suspended on December 30, 1992, because of excessive snowpack. The suspension remained in effect for the remainder of the field season.

GUIDE Model Plumes 17 Feb 93 1700 UTC

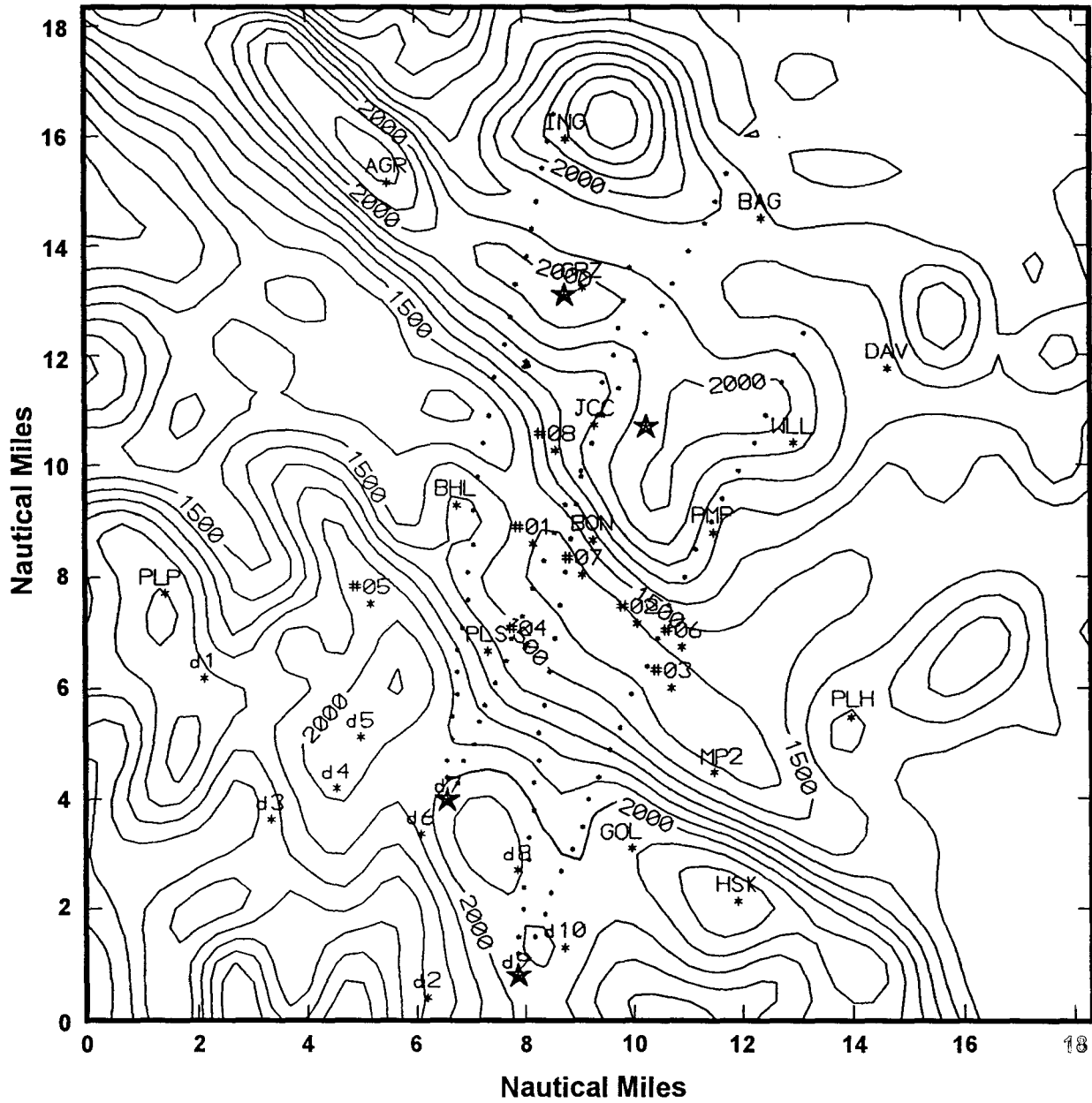


Figure 4.1. - Example of GUIDE model output.

Table 4.1 lists the randomized cases conducted during the 1993-94 winter season. A total of 27 randomized cases were conducted this winter season on 15 different days. The dry winter produced only half of the cases expected. Recall (sec. 1) that the first winter season (1991-92) was also extremely dry. A total of 3,250 gal of propane was dispensed at an average rate of 3.4 gal hr<sup>-1</sup>.

Table 4.1. - Seeding log from November 8, 1993, to March 1, 1994.

Date	No. of Cases	Seeded	Non-Seeded	Hours of Operation	Propane Dispensed (gal)	Gal/h Per Dispenser
11/29/93 (9 of 10)	1	1		1800-0000	196	3.6
12/08/93	3	1 1	1	0000-0600 0830-1430 1645-2245	216 217	3.6 3.6
12/11/93	1	1		1245-1845	216	3.6
12/13-14/93	2	0	1 1	2300-0500 0615-1215	0	0
1/23/94	1	1		1900-2500	209	3.5
1/24/94	3	1 1	1	0200-0800 0900-1500 1600-2200	210 205 0	3.5 3.4 0
2/6/94	1	1		1820-2420	212	3.5
2/7/94	2	1	1	0340-0940 1010-1610	0 214	0 3.6
2/10/94	2	1	1	0500-1100 1230-1830	202 0	3.4 0
2/17/94 (9 of 10)	4	1 1 1	1	0000-0600 0615-1215 1315-1915 2045-2645	0 170 201 196	0 3.1 3.4 3.3
2/18/94	2	1	1	0315-0915 0925-1525	0 196	0 3.3
2/19/94	1		1	1215-1815	0	0
2/20/94 (9 of 10)	2	1	1	0815-1415 2325-2925	0 174e	0 3.2e
2/21/94	1		1	0745-1345	0	0
2/27/94	1	1		0000-0600	216	3.6
e=estimated		16 Seeded	11 No-Seed	96 h Seeding	3,250 gal	3.4 gal/h

## 5. DISCUSSION OF MOUNTAINTOP ICING DATA

The ice detector is a simple 1-in. rod, vibrating at a known frequency. When supercooled liquid water freezes to the rod, the frequency changes. When about 0.08 g of ice accumulates, a heater is activated and melts the ice in about 90 s. This apparatus is referred to as a "trip." Knowing the average wind speed and the number of trips in a 1-h period, the liquid water content can be approximated.

LOREP data show that Red Hill has many more hours of icing than Mills Peak (fig 2.1). This icing occurs because Red Hill is a more prominent peak than is Mills Peak, inducing rapid vertical ascent as moist air passes over the peak. Mt. Hough has similar orography to Red Hill. It is almost 300 m higher, and thus below 0 °C more often. This elevation produces more icing than at Red Hill.

Tables 5.1 and 5.2 summarize icing episodes for Mt. Hough and Red Hill, respectively, for the 1993-94 winter season. The LWC (liquid water concentration) from the icing rate meter was derived using the technique of Hindman (1986) from averages taken over individual storms. The Red Hill wind speed detector failed on December 9 and could not be repaired until January 20. The Red Hill site battery failed on March 5. The Mt. Hough data set was complete for the entire season. The Mills Peak site had no heat to the wind sensors until January 28. This site experienced very little icing, which is typical. Therefore, the data from this will not be discussed.

Figure 5.1a shows yearly averages for four different parameters derived using the Red Hill data set. Values are plotted using the water year, i.e., 1990-91 water year is plotted as 1990. The value plotted for 1994 is the mean for the 7-yr data set for each parameter. Although 1993 had almost 2 mo of missing data, March had very little icing as indicated by Mt. Hough. April had 70 h of icing at Mt. Hough, and thus, based on past comparisons between these two sites, as many as 40 h of icing may have been missed at Red Hill. These lost data would bring the number of hours up to 242, or about the same as the drought year of 1991.

These results contain several key points. First, the number of hours of icing is consistent at about 250 to 300 per season. The mean of 286 for Red Hill is close to the 300 h that was used in the design of the LOREP. However, liquid water concentrations and mean temperature at which icing occurs indicate that not all of these hours provide suitable conditions for seeding. Note during the water years 1991 and 1993, critically dry years, the liquid water contents are small at  $0.05 \text{ g m}^{-3}$ . Also, the average temperature at which icing occurred during 1991 and 1993 was warmer than  $-2 \text{ }^\circ\text{C}$ . In fact, for the 7-yr record, these 2 yr are the warmest and have the least liquid water of the 7. Unfortunately, these 2 yr make up two-thirds of the LOREP seeding experiment. When seeding is conducted at these relatively warm supercooled temperatures and with relatively low liquid water amounts, seeded crystals will take much longer to grow to sufficient mass to be considered meaningful precipitation particles.

The upper histogram on figure 5.1a shows the ratio of icing hours to hours of precipitation measured at Plumas Eureka State Park. In every year, more hours of precipitation occurred than hours of icing. On average, this ratio is about 0.70, or 70 pct of the hours of precipitation have icing. This ratio indicates that Red Hill, at 1936 m (6400 ft), can be at or above freezing during 30 pct of the precipitation events.

Table 5.1. - Mt. Hough icing data for 1993-94.

Date	Icing (h)	No. of Trips	Trips per h	Precip. PLS (in)	Storm (h)	Precip. JCC (in)	Storm (h)	Avg. Temp (°C)	Wind Speed (m s <sup>-1</sup> )	Wind Direction (°True)	Avg. LWC (g m <sup>-3</sup> )
11/22	16	59	3.7	0.6	14	0.34	14	-3.1	16	208	0.03
11/28-29	12	59	4.9			0.47	20.5	-0.5	12	185	0.05
11/29	5	30	6.0	3.29	41	1.32	15.5	0	9	189	0.07
12/4	3.5	16	4.6	0.07	1	0.07	0.75	-2.2	9	223	0.05
12/6	3	4	1.3	0	0	0	0	-3.3	7	190	0.02
12/7-9	56	276	4.9	3.83	39.75	2.07	31.5	-1.3	14	175	0.04
12/11	10	30	3.0	0.79	9.75	0.43	6.15	-4.1	10	205	0.03
12/14	17	44	2.6	1.98	17.65	1.07	16.25	-5.1	8	198	0.04
12/27	4	8	2.0	0.12	5.15	0.02	2.5	-2.8	4	193	0.05
12/30	6	15	2.5	0.01	0.15	0	0	-1.6	11	206	0.02
1/1	3.5	15	4.3	0.09	1.75	0.04	1	-1.9	11	193	0.04
1/4-5	21	119	5.7	0.82	19.75	0.18	7.25	-1.6	7	208	0.09
1/8	11.5	36	3.1	0	0	0	0	-3.9	8	205	0.04
1/23-25	46.5	84	1.8	1.96	27.9	1.63	26	-3.5	11	180	0.02
2/6	7	12	1.7					-2.8	8	178	0.02
2/7	10	44	4.4	1.65	19.1	1.34	28	-2.7	9	205	0.05
2/10	18	82	4.6	1.78	19.5	1.48	19.5	-4.1	13	211	0.04
2/16-18	40.5	148	3.7	2.96	36.25	2.87	33.75	-6.2	8	200	0.05
2/18	3	7	2.3	0	0	0	0	-7.9	7	205	0.04
2/20-21	38.5	136	3.5	3.13	52.75	2.06	53	-6	10	211	0.04
2/26-27	29.5	194	6.6	0.75	22.45	0.14	6.75	-1.5	10	208	0.07
3/19	5	26	5.2	0	0	0	0	-2.7	7	211	0.08
3/23	6	20	3.3	0	0	0.03	1	-8.4	9	210	0.04
4/6	15.5	33	2.1	0.62	17	0.52	14	-2.5	9	205	0.03
4/8-9	21	85	4.0	0.57	25	0.09	6	-3	14	204	0.03
4/23-24	7	10	1.4			0.06	8	-3	7	181	0.02
4/25-26	27	82	3.0			0.48	18	-3.9	11	199	0.03
Mean	16.41	62	3.57	1.04	15.41	0.64	12.67	-3	10	199	0.04
STD	14.27	64	1.42	1.20	15.30	0.80	13.15	2	3	12	0.02
Total	443.00	1674		25.02	369.90	16.71	329.40				

Table 5.2. - Red Hill icing data for 1993-94.

Date	Icing (h)	No. of Trips	Trips per h	Precip. PLS (in)	Storm (h)	Precip. JCC (in)	Storm (h)	Avg. Temp (°C)	Wind Speed (m s <sup>-1</sup> )	Wind Direction (°True)	Avg. LWC (g m <sup>-3</sup> )
11/22	10	18	1.8	0.6	14	0.34	0.14	-1	9	225	0.02
11/28	4.5	6	1.3			0.47	20.5	0	4	200	0.04
11/29	8.25	39	4.7	3.29	41	1.32	15.5	0	5	244	0.11
12/7	14	35	2.5					-1	6	225	0.04
12/8	8.5	17	2.0					0	8	223	0.03
12/9	7	10	1.4	3.83	39.75	2.07	31.5	0		250	
12/11	9	43	4.8	0.79	9.75	0.43	6.15	-1		230	
12/14	2.5	3	1.2					-3		190	
12/14	3	4	1.3	1.98	17.65	1.07	16.25	-4		278	
1/1	1	9	9.0	0.09	1.75	0.04	1	-1		202	
1/4-5	6	9	1.5	0.82	19.75	0.18	7.25	-1		290	
1/8	13	20	1.5	0	0	0	0	-2		248	
1/22-23	12	33	2.8					0	8	215	0.04
1/24	14.5	29	2.0	1.96	27.9	1.63	26	-3	4	200	0.05
2/7	4.5	16	3.6	1.65	19.1	1.34	28	-2	1	151	0.52
2/10	9.5	24	2.5	1.78	19.5	1.48	19.5	-2	5	252	0.05
2/17	13	36	2.8					-2	8	187	0.04
2/18	14.5	25	1.7	2.96	36.25	2.87	33.75	-5	4	237	0.05
2/20	10	17	1.7					-4	4	260	0.05
2/20-21	24	40	1.7	3.13	52.75	2.06	53	-3	7	245	0.03
2/26-27	14	27	1.9	0.75	22.45	0.14	6.75	0	7	290	0.03
Mean	9.65	21.90	2.56	1.69	22.97	1.03	17.69	-1	6	220	
STD	5.19	12.26	1.75	1.20	14.62	0.86	14.49	2	2	59	
Total	202.75	460.00		23.63	321.60	15.44	265.29				

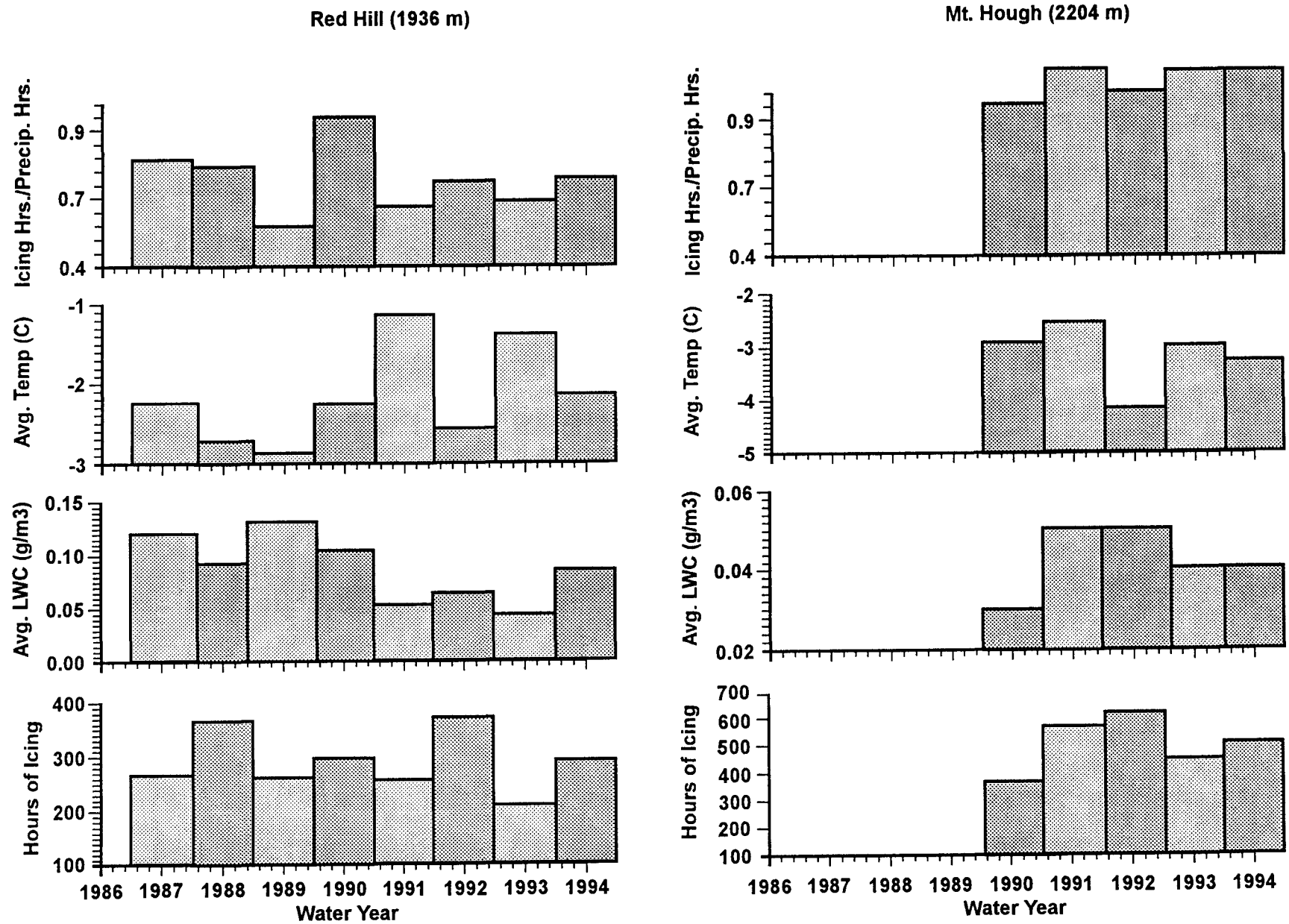


Figure 5.1. - a) Water year (Oct. 1 to Sept. 30) averages derived from the Red Hill mountaintop icing station. From top to bottom; ratio of icing hours to hours with precipitation; average temperature per storm when icing occurred; average storm liquid water content; number of hours of icing per water year. b) same as a) but for Mt. Hough. Note differences in vertical scales.

Figure 5.1b shows yearly statistics from Mt. Hough for the 4 yr of record. Mt. Hough is about 300 m (1000 ft) higher than Red Hill, and thus experiences sub-freezing temperatures more often. This elevation contributes to Mt. Hough averaging about 500 hours of icing per winter. The upper histogram on figure 5.1b shows that Mt. Hough also averages slightly more hours of icing than hours of precipitation recorded at Plumas Eureka State Park. Average liquid water contents are low, as was observed at Red Hill. Icing temperature averages just under  $-3\text{ }^{\circ}\text{C}$ , or about a degree cooler than Red Hill.

The importance of the results from Red Hill and Mt. Hough can be better appreciated by understanding ice crystal growth rate. Figure 5.2 shows mass growth rate of ice crystals as a function of temperature and time. This plot only includes ice crystal growth by conversion of water vapor to ice (diffusional growth), not collection of supercooled droplets by ice particles (riming). Given the liquid water contents observed during icing events, riming would only be significant during more limited periods when liquid water is greater than about  $0.1\text{ g m}^{-3}$ . Note that for temperatures warmer than  $-3\text{ }^{\circ}\text{C}$ , crystal mass even after 30 min is three orders of magnitude lower than a crystal growing at  $-5\text{ }^{\circ}\text{C}$ . Thus, unless seeded crystals can attain temperatures near  $-5\text{ }^{\circ}\text{C}$ , the crystals would require nearly 2 h to equal the mass of a crystal growing at  $-5\text{ }^{\circ}\text{C}$ .

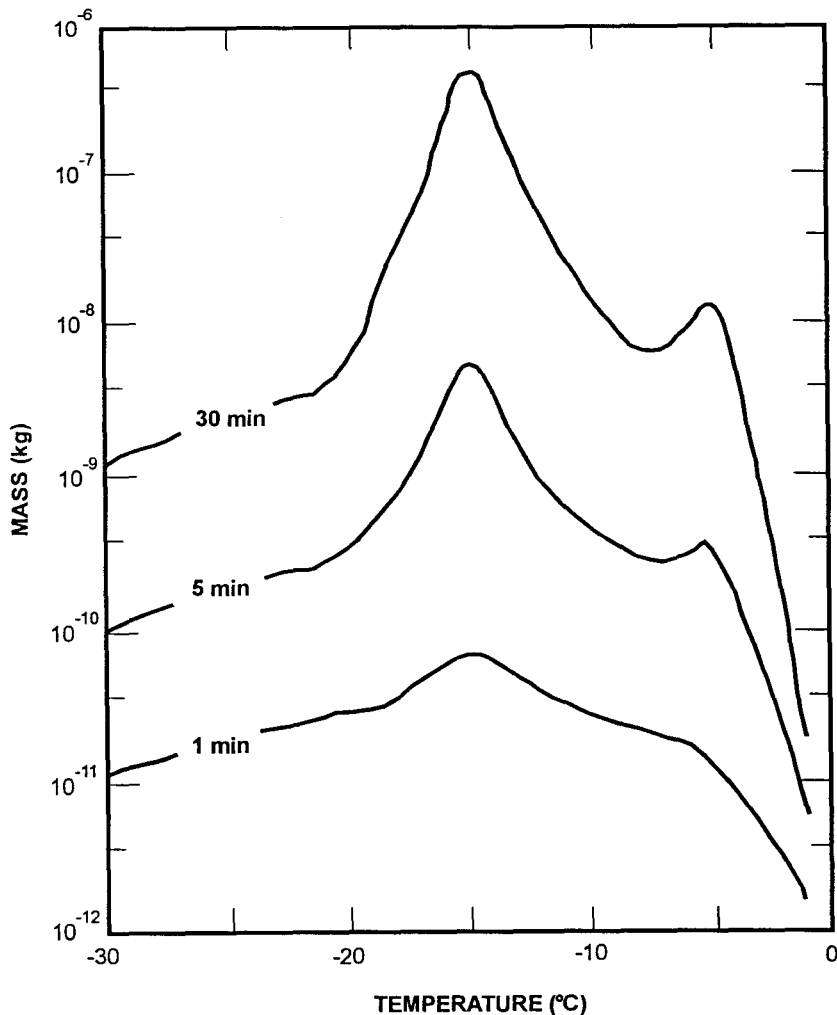


Figure 5.2. - Masses of growing ice crystals at various times as a function of temperature (After E.E. Hindman II and D.B. Johnson [1972]. *J. Atmos. Sci.* 29, 1313, by permission of American Meteorological Society and senior author).

Figure 5.3 shows the terminal velocities of unrimed needles, the type of crystals that would grow at  $-5\text{ }^{\circ}\text{C}$  (UN in diagram). The crystals have the lowest fall speed of any crystal observed up to a dimension of 1 mm. Terminal velocities of less than  $0.5\text{ m s}^{-1}$  make these crystals susceptible to the strong upward and downward motions observed to the lee of the main Sierra crest. The diagram shows that columns (C) or plates (P), the type of crystals expected to grow between  $-1$  and  $-4\text{ }^{\circ}\text{C}$ , have a faster fall speed at smaller sizes, mainly because they are more compact and have less drag. However, the mass of the crystals may be relatively small at these particle sizes. This type of information is programmed into the GUIDE model and allows calculation of particle trajectories.

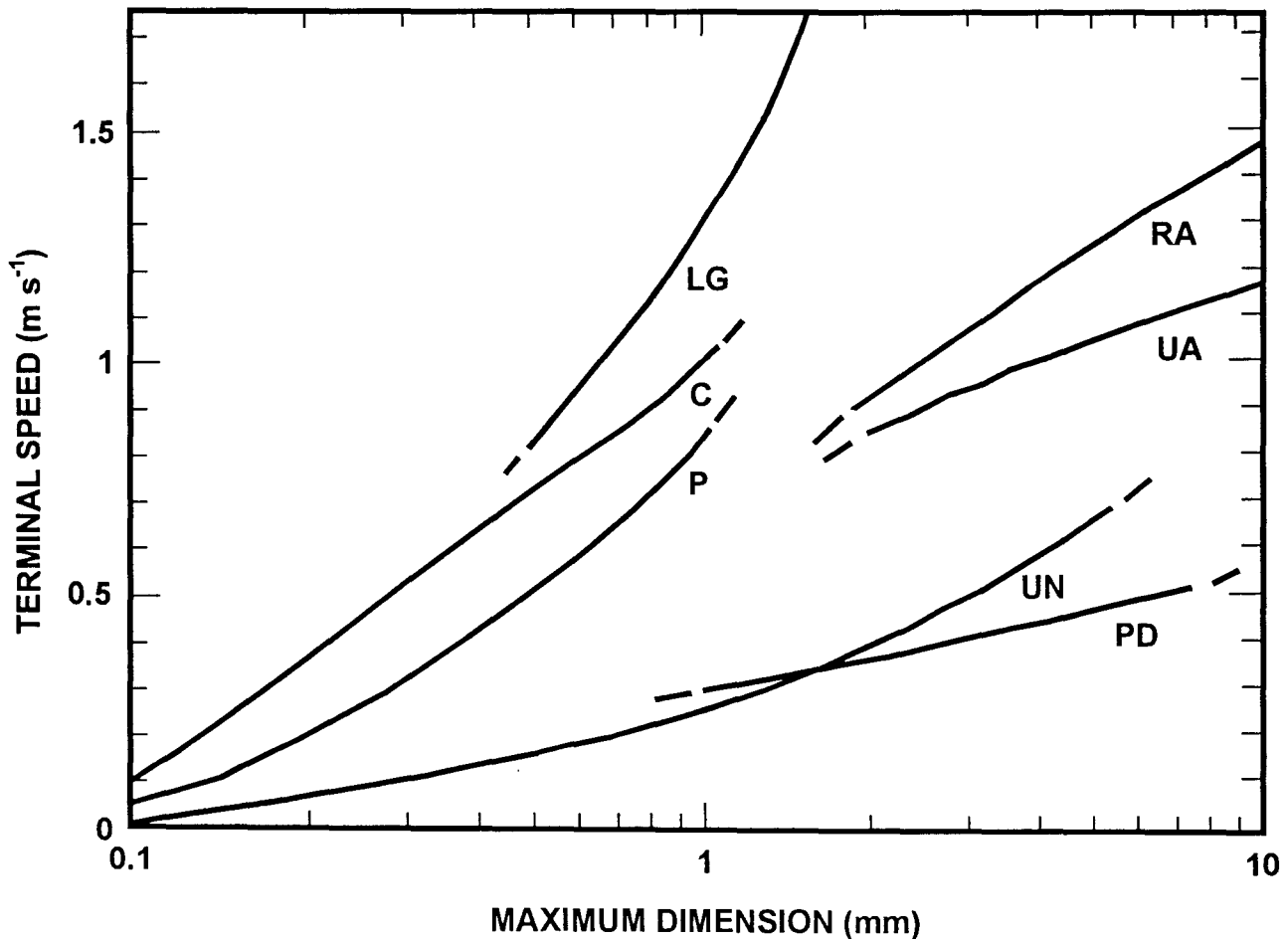


Figure 5.3. - Terminal speeds of ice crystals and snowflakes. Hydrometeor types and sources of information are as follows: LG—lump graupel of density  $0.1$  to  $0.2\text{ Mg m}^{-3}$  at the ground (Locatelli and Hobbs, 1974). C—columns at  $40\text{ kPa}$ ,  $-20\text{ }^{\circ}\text{C}$  (Heymsfield, 1972). P—plates at  $40\text{ kPa}$  (Heymsfield, 1972). RA—rimed aggregates at the ground (Locatelli and Hobbs, 1974). UA—unrimed aggregates at the ground (Locatelli and Hobbs, 1974). UN—unrimed needles at  $40\text{ kPa}$  (Heymsfield, 1972). PD—plane dendrites at  $85\text{ kPa}$  (Heymsfield, 1972).

## 6. APPLICATION OF A RADAR WIND PROFILER

The radar wind profiler was installed and operated near Blairsdene (BLN), which is located about 6 km northeast of Johnsville (fig 2.6) during the 1993-94 winter, in the hope of obtaining near continuous vertical velocities over the valley between the dispensers and the target ridge. This continuous data collection would help document the wave cloud activity and how the frequency and magnitude of this wave affect crystal transport. At the time of installation, no "clean" site existed anywhere in the valley to install the radar. Random noise can overwhelm the incoming signal to the profiler and essentially contaminate its wind finding capability. Noise is generated by wind blowing through the trees nearby or by moving telephone or power lines. The vertical velocities measured by the profiler are much more sensitive to this noise than are the horizontal velocities. Unfortunately, almost all the vertical velocity data measured by the profiler were contaminated during non-precipitating events.

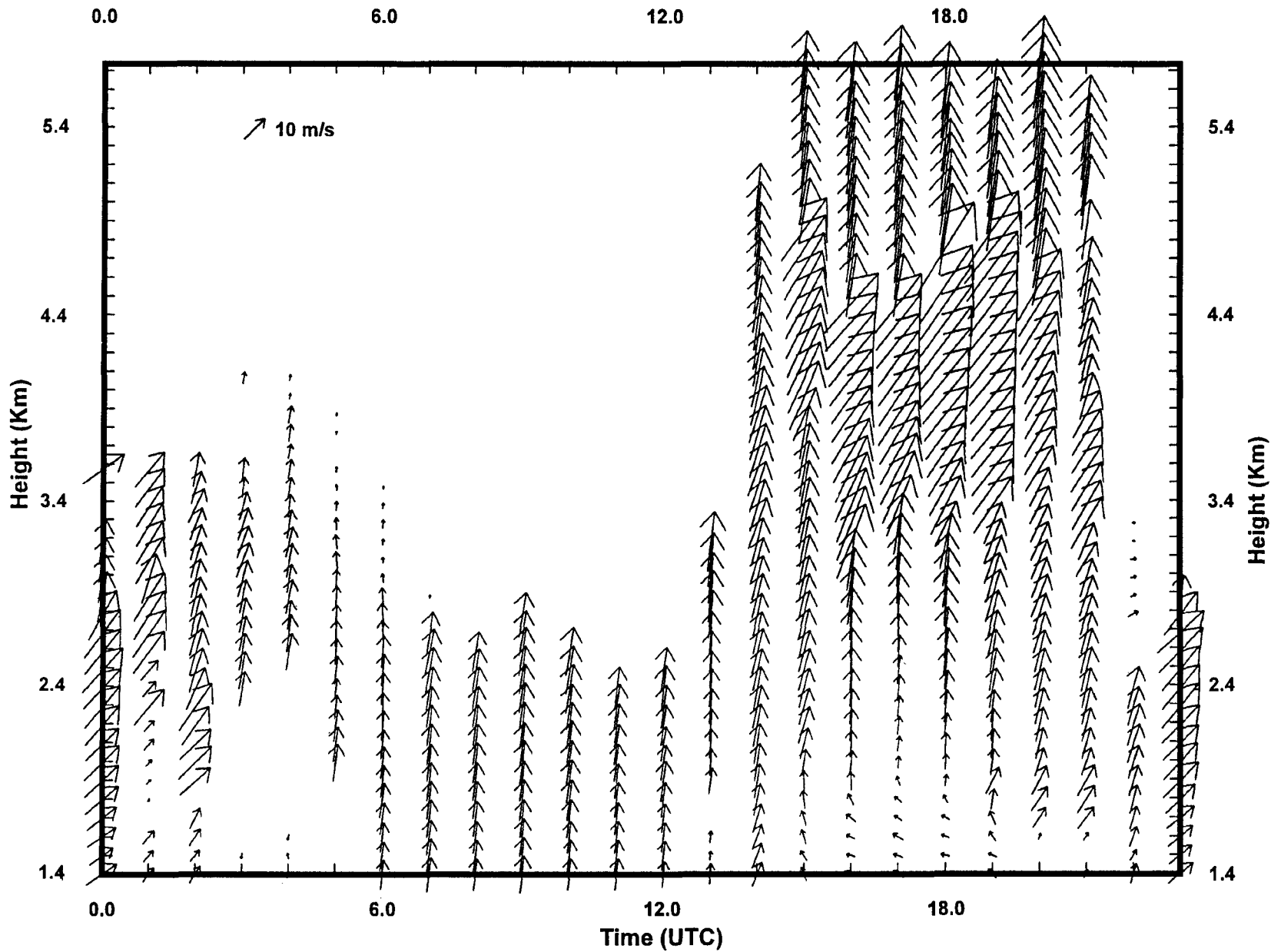
During rain or snow, the signal backscattered from the precipitation to the radar is generally much larger than the background noise. The radar at this point is simply measuring the fall speed of the ice crystals, which is the combination of the terminal velocity of the particle and the influence of the free air vertical motions. Because the Doppler spectra were recorded, it was hoped that a bimodal spectra would allow differentiation of the clear air vertical motions versus the snowflake terminal velocity. However, even in these situations, the turbulence associated with the air passing over the Sierra broadened the spectral width and eliminated the possibility of resolving vertical motions.

Even with the noise problems, much information was gained by looking at horizontal winds at high time resolution during seeding events. Three separate days will be examined. On these days, 50 pct of the randomized seeding cases that were predicted to have affected the target area occurred. A discussion of the randomized cases for 1993-94 is given in section 7.1.

Figure 6.1 shows the hourly horizontal winds for January 24, 1994, as measured by the profiler. All heights are above m.s.l. (mean sea level) unless otherwise noted. Each hour, 52 wind samples were collected at 100-m vertical intervals. For a given layer to have an hourly wind computed, at least 50 pct of the 52 samples from each horizontal wind component must have a mean wind within  $2 \text{ m s}^{-1}$  of each other. The figure shows that between 0000 UTC and 0600 UTC, periods of missing data were caused by ground clutter decreasing the signal to noise ratio. From 0600 to 1300, the antenna looking west is contaminated by clutter and only a southerly wind component is observed. Precipitation begins at 1400 UTC (0600 P.s.t.) as seen on figure 6.2. Station BON is the closest gauge to the profiler. The precipitation increases the depth over which winds can be calculated and increases the signal to noise ratio, allowing accurate winds to be computed. The westerly wind component is affected by clutter above about 5 km, and is obvious from the discontinuity in wind direction. Horizontal velocities are corrected for vertical velocity contamination. This procedure basically subtracts the horizontal component of a particle's terminal velocity from the  $U$  and  $V$  components.

Figure 6.3 compares the hourly profiler winds with the rawinsonde winds for 1700 UTC (0900 P.s.t.). It must be remembered in looking at this comparison that the rawinsonde is looking at the instantaneous winds, but the profiler is averaging over 1 h. In general, the comparison in speed and direction is fairly good. The main differences are in the lowest 500 m and in the layer from 3000 to 4500 m. The differences are most likely caused by the mountain lee wave. The profiler, located on the east side of the valley, is seeing a return flow in the lowest

BLAIRSDEN WIND PROFILER 24 JAN 94



33

Figure. 6.1. - Time-height plot of Blairسدn hourly profiler consensus wind vectors for January 24, 1994. Scale appears in upper left corner.

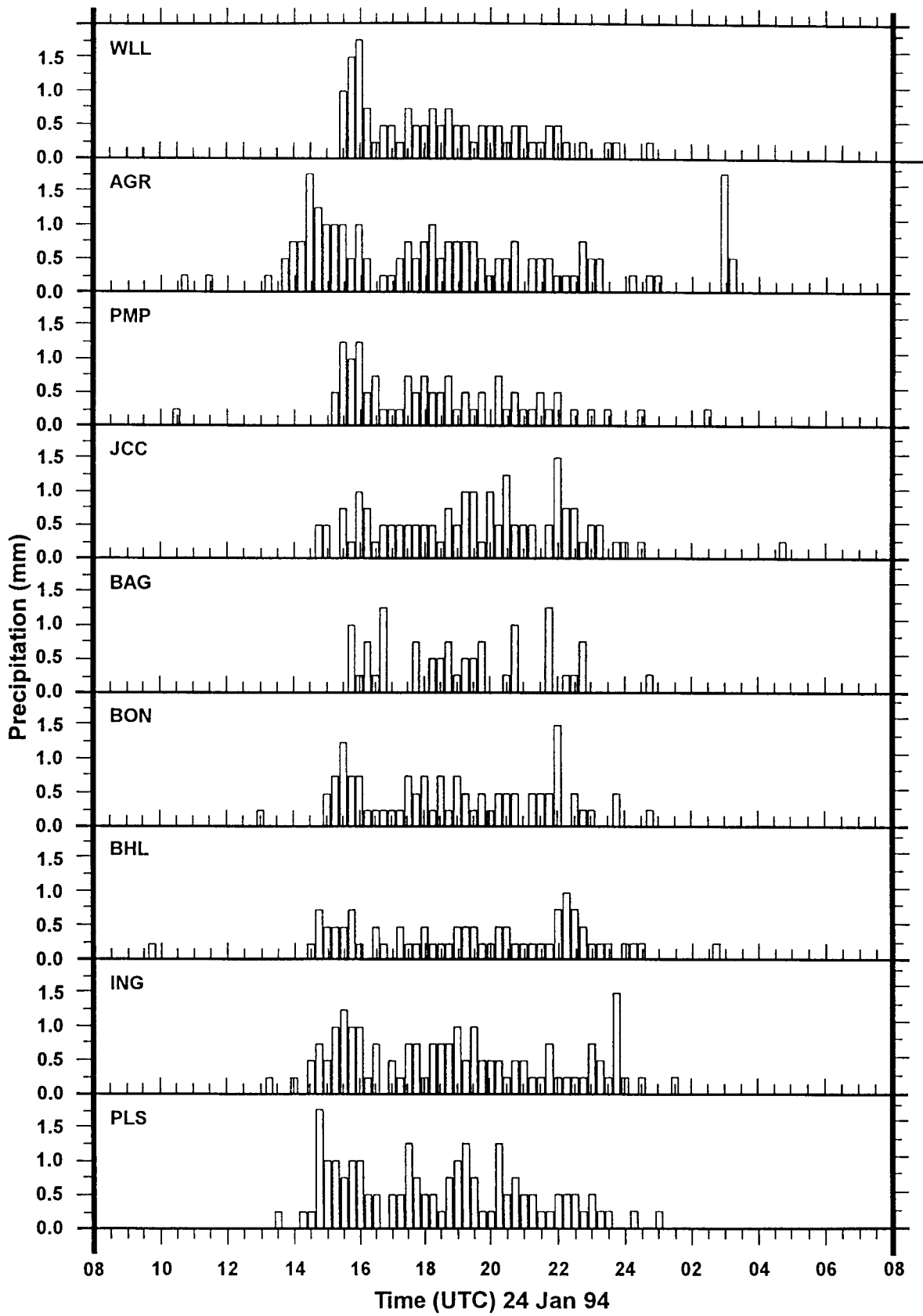


Figure. 6.2. - Precipitation measured in the gauge network for January 24, 1994. Gauge locations can be found on figure 2.6.

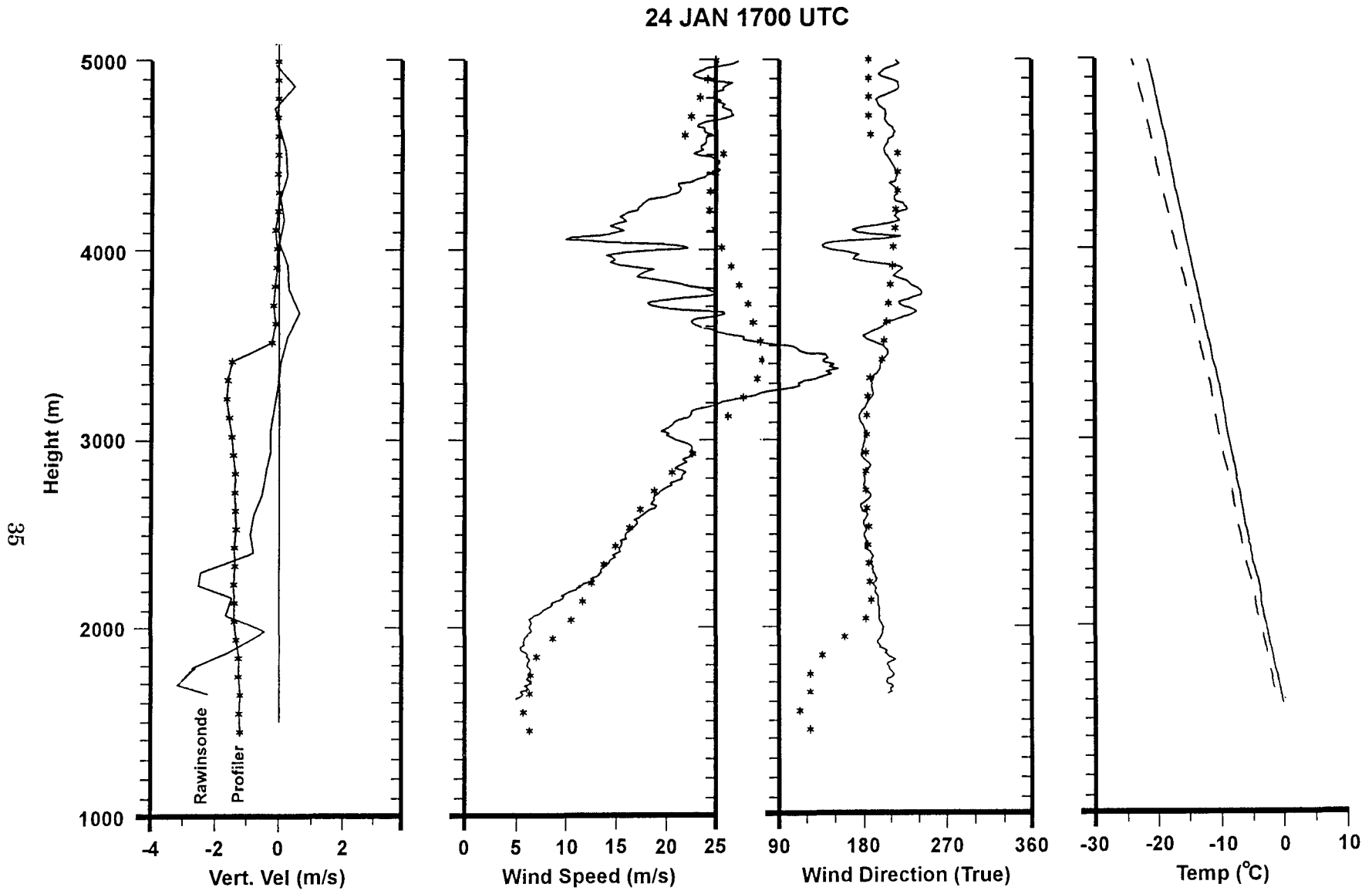


Figure. 6.3. - Comparison of the hourly profiler winds (\*) with the rawinsonde winds (solid) for 1700 UTC (0900 P.s.t) on January 24, 1994.

500 m out of the east underneath the crest of the lee wave. This return flow is better shown on figure 6.4, where a hand analysis of the streamlines has been done to match the balloon vertical motion field.

Both the profiler and the rawinsonde see an acceleration of the winds at about 3500 m (fig. 6.3). This acceleration occurs near the trough axis where the vertical motion field goes from negative to positive. The winds also converge near the trough, causing a strong acceleration of the horizontal winds. Note that this transition zone is positioned directly over the profiler. The profiler tends to time average the winds in this region, and probably produces a more representative mean wind profile than the rawinsonde.

The vertical velocities shown by the arrows on figure 6.4 simply indicate precipitation is falling. Velocities shown near the surface are too large for the types of snowflakes that were observed and are indicative of the spectral broadening taking place because of turbulence.

This day is representative of the results obtained from the profiler during precipitation. Unfortunately, as seen on figure 6.1, the winds determined by the profiler can change dramatically in less than a 6-h period as seen just after 1900 UTC. This wind speed and direction change is associated with a frontal passage. These changes occurring between rawinsonde launches dramatically affect targeting predictions from the GUIDE model. Three randomized seeding cases were conducted on this day; one began at 1700 UTC and ended at 2300 UTC, coexistent with this wind change. The profiler is the only instrument capable of detecting these types of changes other than expensive hourly rawinsonde launches.

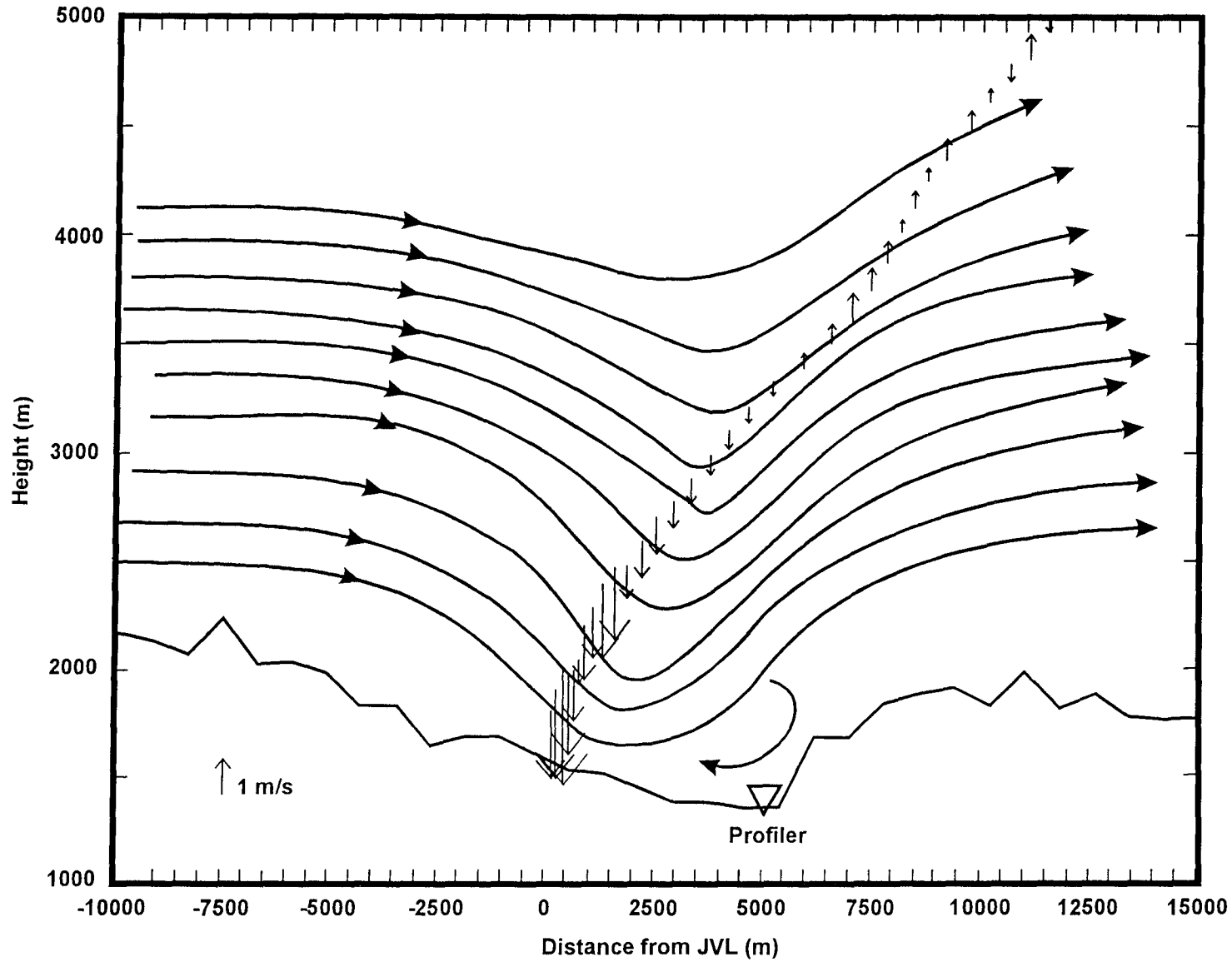
Figure 6.5 shows the 24-h wind profile from the profiler along with observed precipitation in the gauge network for February 7, 1994. The main precipitation event begins about 0400 UTC on February 7 (2000 P.s.t. on February 6), which corresponds to the increase in vertical range of the profiler. Maximum precipitation begins to fall just after 0800 UTC (0000 P.s.t. February 7) and corresponds to the onset of the low level easterly flow as seen by the profiler.

This period resembles the January 24, 1994, case, especially compared to rawinsonde data taken during easterly flow (fig. 6.6). During low level easterly flow (0700 to 1300 UTC), both 0600 and 1100 UTC soundings show significant downward motion; little or no indication of upward motion exists through 5 km. Both also show winds approaching 25 to 30 m s<sup>-1</sup> near 4000 m; the rapid variation in wind direction and speed through this region denotes strong turbulence.

A cold frontal passage was noted between 1500 and 1600 UTC (0700 to 0800 P.s.t.) on February 7, 1994. This frontal passage was associated with a significant period of precipitation observed in the gauge network (fig. 6.5). By 1800 UTC (1000 P.s.t.), precipitation ended at the profiler but continued near Johnsville. The clean and well mixed air mass advected in after the cold front passed provided no scatterers for the profiler to measure winds above 2500 m. A power failure at the profiler site occurred shortly before 1800 UTC (1000 P.s.t.). Power was restored shortly after 2000 UTC (1200 P.s.t.).

The final case analyzed was February 18, 1994. The time height profile of winds and observed precipitation for February 18 is shown on figure 6.7. This case was concentrated on the post-frontal air mass in that temperatures were at or below -5 °C at the dispensers. During this time, the GUIDE model predicted good targeting of the gauge network using rawinsonde data.

24 JAN 94 1700 UTC



37

Figure 6.4. - Rawinsonde derived vertical velocity vectors along path of ascending balloon for 1700 UTC (0900 P.s.t.) on January 24, 1994. Hand analysis of the streamlines done to match the balloon vertical motion field.

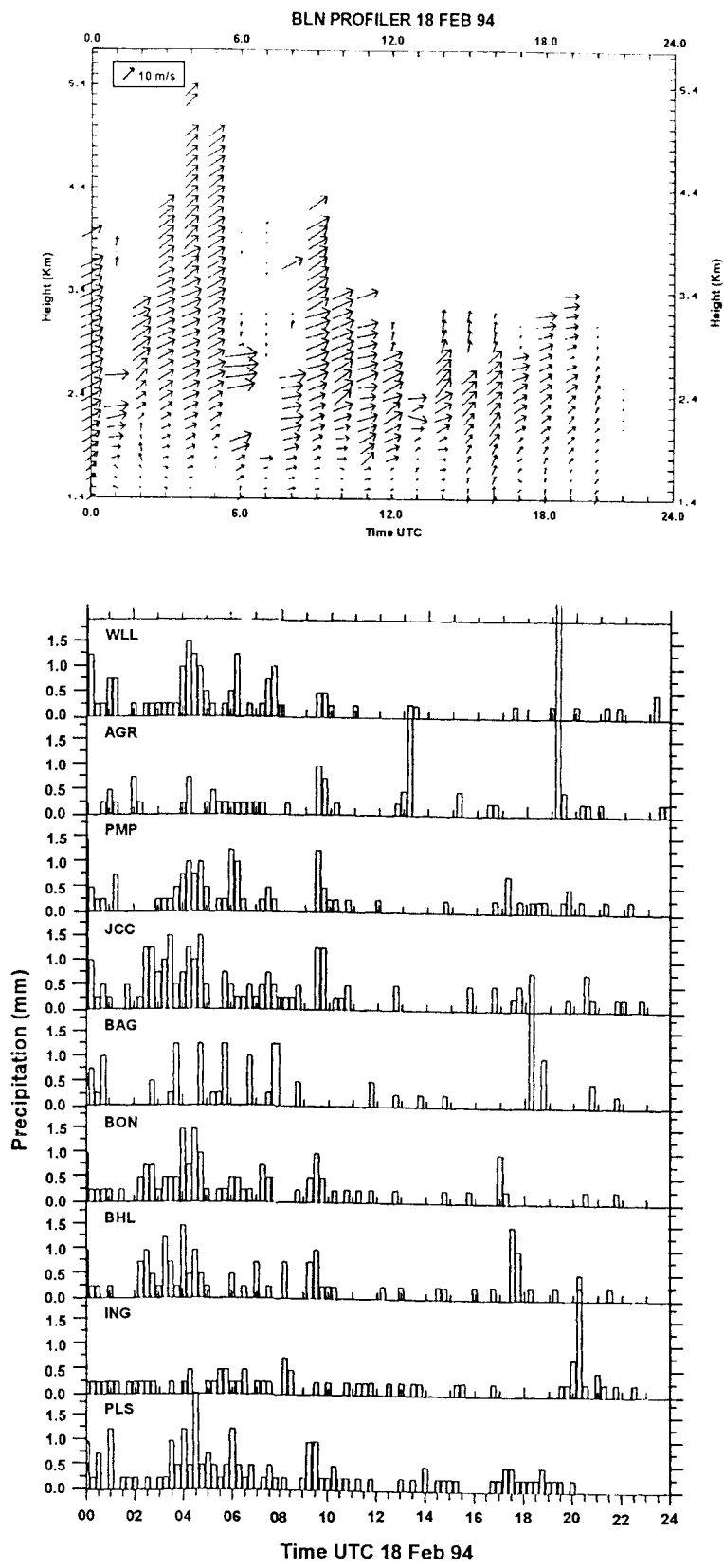


Figure 6.5. - The 24-h wind profile from the profiler (top) along with the observed precipitation in the gauge network (bottom) for February 7, 1994 (UTC).

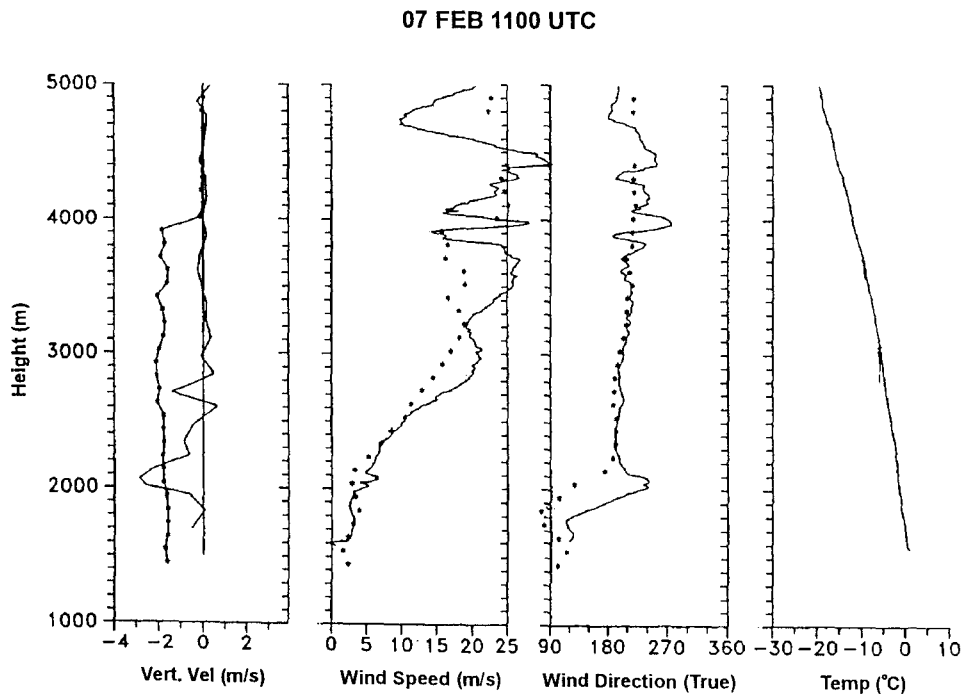
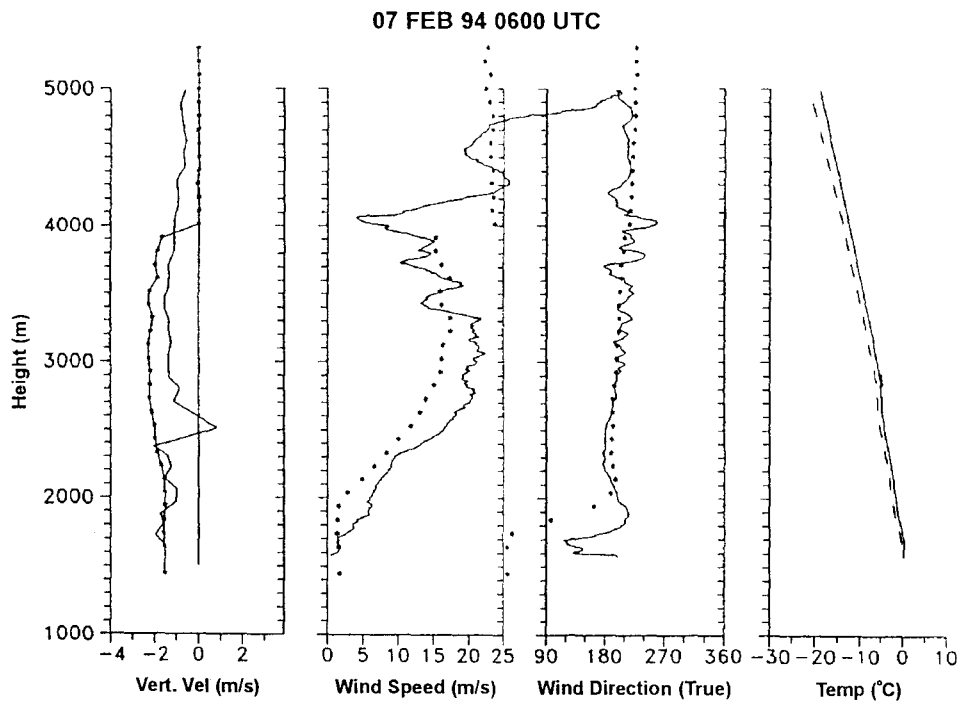


Figure 6.6. - Comparison of the hourly profiler winds (\*) with the rawinsonde winds (solid) for 0600 and 1100 UTC on February 7, 1994.

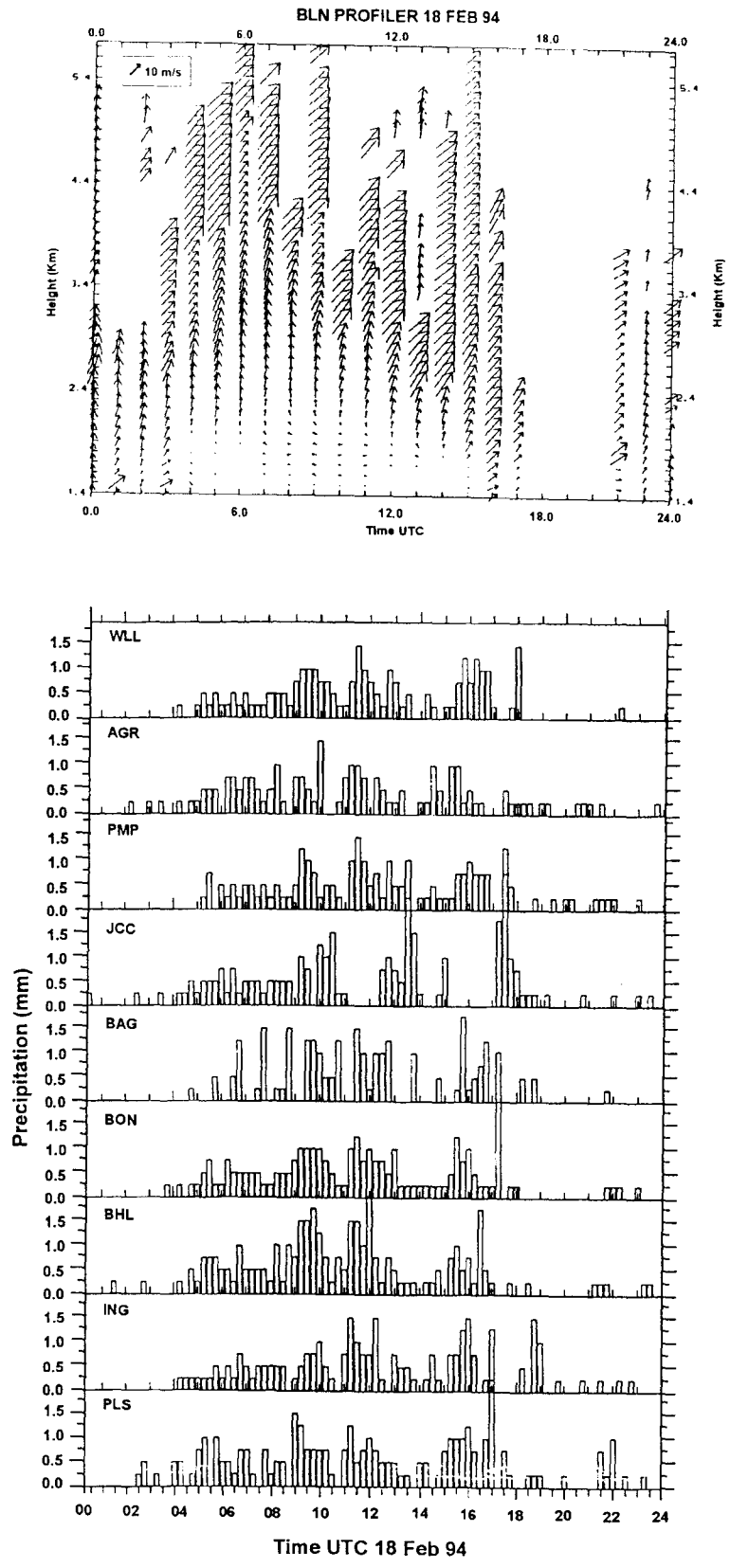


Figure 6.7. - The 24-h wind profile from the profiler (top) along with the observed precipitation in the gauge network (bottom) for February 18, 1994 (UTC).

Frontal passage was indicated to occur around 0600 UTC on February 18 (2200 P.s.t. on February 17). An extensive period of precipitation occurred all day on February 17 and continued through frontal passage on February 18; three randomized seeding cases occurred.

Only a brief period of low level easterly flow occurred prior to frontal passage. The 3-h period from 0000 to 0300 UTC exhibited rapidly changing wind speed and direction near dispenser elevations. Between 0600 and 0700 UTC (2200 to 2300 P.s.t. on February 17), winds became unreliable because precipitation became showery and ground clutter effects became significant. A major post-frontal precipitation band passed over the area at 0900 UTC (0100 P.s.t.), and southwesterly winds increased just above crest height both before and after the band passage.

The period after 1100 UTC represents the dissipating stage of the storm, with a shallow orographic cloud located over the Sierra and sporadic snow showers moving off the crest over the gauge network. Seeding ended at 2300 UTC (1500 P.s.t.). Ground clutter seriously affected the profiler winds after 2000 UTC.

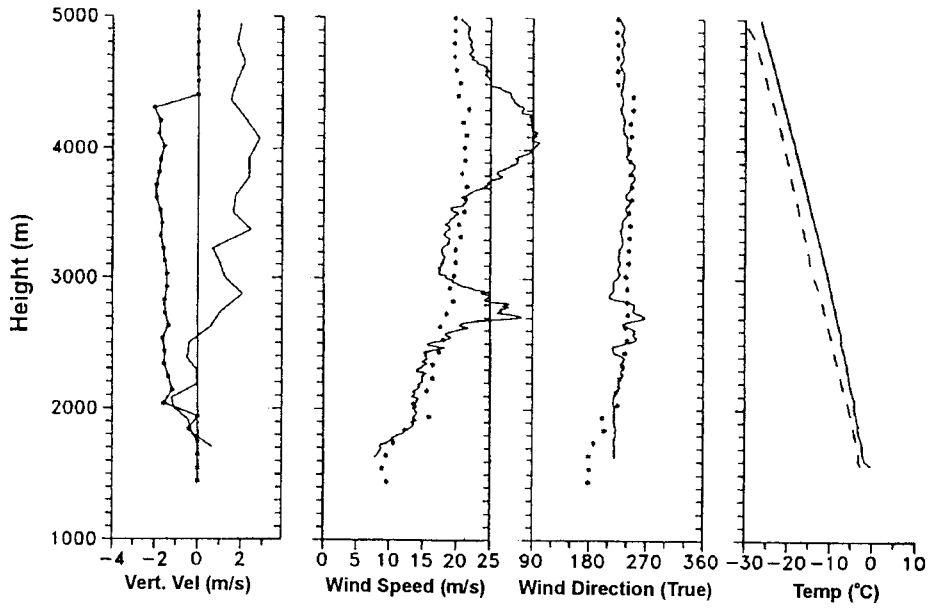
Figure 6.8 compares the profiler and rawinsonde data for 0000 and 0500 UTC (1600 and 2100 P.s.t. on February 17). The 0000 UTC comparison is quite good, except near 3000 m and 4000 m, where the lee wave may have accelerated wind speeds that are averaged out by the profiler. At the altitude of the dispensers, the two data sets compare quite well.

At 0500 UTC, the comparison was good except in the lowest 600 to 700 m. This comparison occurred very near frontal passage, and the profiler winds were very light below 2000 m. The discrepancy was about  $12.5 \text{ m s}^{-1}$  at 1800 m, and the rawinsonde winds were much higher. By 2200 m, the discrepancy was only a few meters per second, and the directions were less than  $5^\circ$  off. The air descending down the mountain near Johnsville in the low levels did not appear to penetrate out into the valley, but rose up and over the valley.

In the absence of ground clutter, a 915-MHz wind profiler appears to be capable of providing accurate hourly wind speed and direction measurements. These types of measurements are vital in accurately determining the targeting effectiveness of ground-based seeding. For the site used this winter, accurate vertical motions could not be derived by the profiler. In fact, because of turbulence and broadening of the spectra from the vertical beam, accurate terminal velocities could not be derived. Because of portability, the vertical antenna has a lower signal to noise ratio than the two horizontal antennas. A bigger vertical antenna might overcome the clutter and resolve the free air vertical motions.

Although the main objective for installing the profiler could not be met, the horizontal wind data have demonstrated that significant wind changes can occur between 6-h rawinsonde launches that, without a wind profiler, would be missed. The data also demonstrate that even within 6 km, the distance between Johnsville and Blairsden, low level flow in complex terrain can be very different because of mountain lee wave activity.

18 FEB 94 0000 UTC



18 FEB 0500 UTC

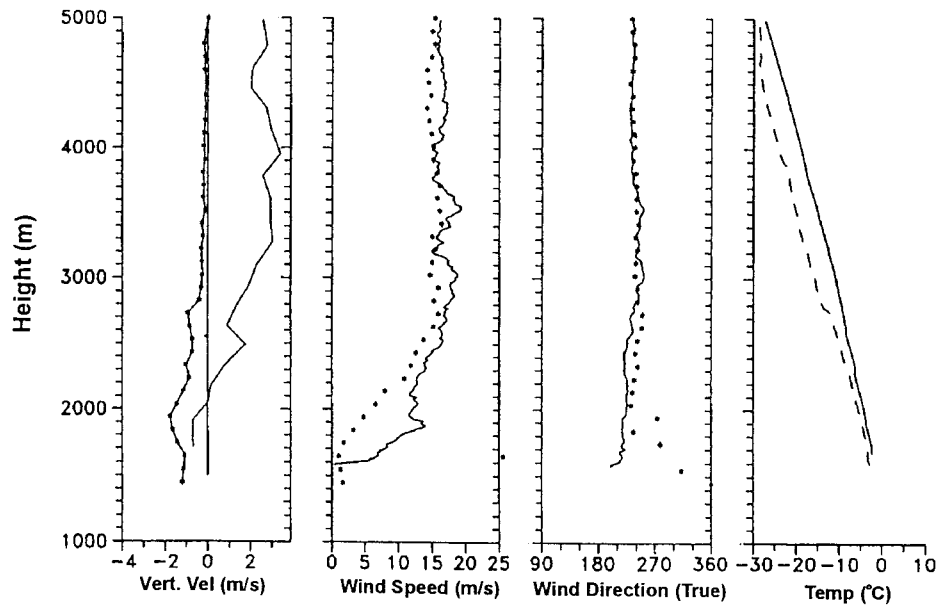


Figure 6.8. - Comparison of the hourly profiler winds (\*) with the rawinsonde winds (solid) for 0000 and 0500 UTC on February 18, 1994.

## 7. STATISTICAL ANALYSIS OF RANDOMIZED SEEDING

As has been mentioned, the LOREP was an exploratory experiment. That is, it was a guided search for substantial evidence or indication of a treatment effect. Its objective was to "stake a claim" for a treatment effect based on a conceptual model with model plausibility and some statistical credibility. The conceptual model in this experiment was the GUIDE model, which attempts to predict the area of effect from seeding for any given seeding experiment. Much of this report is focused on the "targeting" problem and the difficulty in attempting to estimate where the seeding effects, if any, might be located. The GUIDE model has been shown to have directional accuracy, but lacks the sophistication to handle the complex vertical motion field that has been observed over the target area. The model should be modified to account for a variable liquid water field as the crystal translates across the target area. At present, the model assumes a continuous liquid water field. Even with these changes, variations in wind speed and direction, along with lee wave fluctuations, will still have a significant impact on particle fallout between rawinsonde launch times. Given these limitations, a preliminary analysis has been made of the 90 randomized experiments conducted during the three LOREP winter seasons.

As mentioned in section 4, the experimental unit length was 6 h. The randomization scheme used was 3 seeds to 1 no-seed for the first winter, then 3 seeds to 2 no-seeds for the second and third winters. This change was made to even out the statistics because only half as many cases as expected were obtained during the first winter.

This analysis is based on a target-control comparison (for further information on this subject see Dennis, 1980). Prior to the start of the randomized seeding, a 2-yr comparison was made of 6-h precipitation using the average of the target gauges and the control gauge, LaPorte (fig. 2.1). LaPorte is located about 30 km upwind from the target. It is climatologically in a much wetter location, receiving more than double the amount of precipitation that falls in the target area.

To be considered, a 6-h period required at least the first 2 h of the 6-h period to have measurable precipitation in the target area. No precipitation was required at the control site. A 1-h gap between 6-h periods was used to simulate experimental conditions. Seventy-two 6-h periods were obtained for the period of record January through March for the winters of 1989-90 and 1990-91. The linear correlation was 0.85. This number of cases increased to 132 6-h periods using the non-randomized periods for 1991-92. The linear correlation was 0.86 between the target and control. This correlation helps explain nearly 75 pct of the variance between the target and control.

Of the 90 randomized cases, 3 were eliminated. The target precipitation data were missing for one case, and no precipitation was observed either in the target or control area for the other 2 cases.

The first method of analysis was to simply take the average from all the target gauges and compare to the control gauge for all 87 cases. A time lag was built into when to begin use of a particular target gauge. Time lags varied from 15 min up to 1 h. The lag time was a direct function of the distance downwind from the dispensers and was a constant for a particular gauge throughout all experiments. Figure 7.1 shows the gauge network and the time lag used for each gauge.

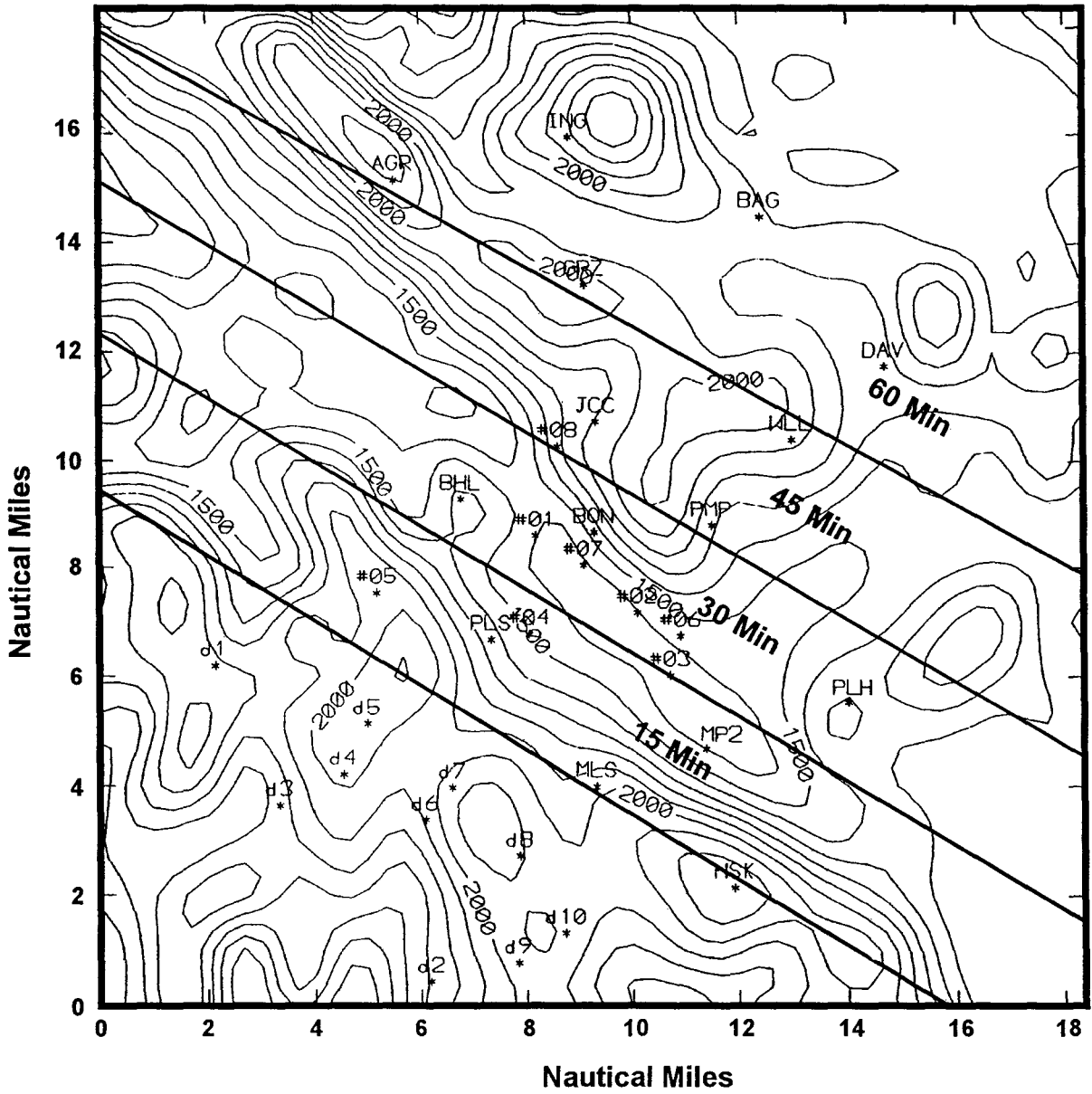


Figure 7.1. - Gauge network and time lag used for each gauge in the analysis of seeded and nonseeded periods.

No attempt was made to extrapolate data for missing target gauges. Periods of time occurred when target gauges were out of service. Also, no attempt was made to correct for snow drops in the target gauges, which occur when an accumulation of snow suddenly breaks loose from the side walls of the gauge and is recorded as snow. A problem was encountered with the control gauge on December 28 and 29, 1992. The gauge at LaPorte began to "cap" with snow on December 28, affecting precipitation measurements. The capping and subsequent snow drop required the precipitation data to be interpolated through a 15-h period, affecting 3 randomized cases (2 seed and 1 no-seed). Early on December 29, the gauge failed because of a lack of antifreeze. Four randomized cases were affected (2 seed and 2 no-seed). For these cases, the average of 3 gauges located on the west side of the Feather drainage (Strawberry, Bucks Lake, and Four Trees) was used in the analysis. A correlation was performed between LaPorte and Strawberry using 316 6-h periods. The correlation was 0.87. For Bucks Lake, 307 6-h periods were available, yielding a correlation of 0.77. A correlation coefficient for Four Trees was not calculated.

For the 1993-94 season, two additional days experienced gauge snow drops or communications problems at the LaPorte control site. Experiments 5 and 14 used the mean from the gauges at Strawberry and Bucks Lake for these two cases.

Figure 7.2 shows the results of this first analysis. The regression lines indicate almost no significant difference between the seeded and non-seeded randomized populations. The double ratio using the target and control means ( $T_s/C_s$ )/( $T_{ns}/C_{ns}$ ) is 0.97.  $T_s$  is the mean precipitation falling in the target area using all 56 seeded cases.  $C_s$  is the same, only using the LaPorte (control) gauge.  $T_{ns}$  is the non-seeded mean using all 31 non-seeded cases, and  $C_{ns}$  is the non-seeded control mean. This value also indicates little difference. A probability or  $P$  value was calculated using residuals. Residuals were calculated using the difference between the observed target mean and the predicted target mean using the regression calculated using the entire 87 target\control pairs. The method used for determining significance was the MRPP (Multiresponse Permutation Procedure) developed by Mielke et al. (1981). The MRPP is a nonparametric statistical procedure which yields inferential results about two samples in multivariate space. The  $P$  value for this sample was 0.82. This result means that an 82-pct probability exists that any difference in the populations is by chance alone.

The second method of analysis was to determine which gauges to use in the target depending on GUIDE model output. Those gauges located within the boundaries of the predicted plumes and downwind from the fastest falling crystal were included in the calculation of the mean target precipitation. The same time lags were used as in the previous method. The GUIDE model was run using the model-predicted vertical motion field, dividing the downward motion by 10 and the upward motions by 2. This procedure essentially smooths the lee wave across the target area and minimizes those cases where the crystal is forced out in the valley with little or no mass. In essence, it keeps the crystal growing longer at the colder temperatures, which allows the best possible seeding effects to occur. These crystals would be most likely to produce a seeding effect.

Even with this optimized approach, 21 seed and 6 no-seed cases showed seeding effects passing completely over the gauge network. In almost all these cases, the model indicated the fastest falling crystal fell beyond the gauge network because the temperature was too warm for adequate crystal growth to occur in the time available.

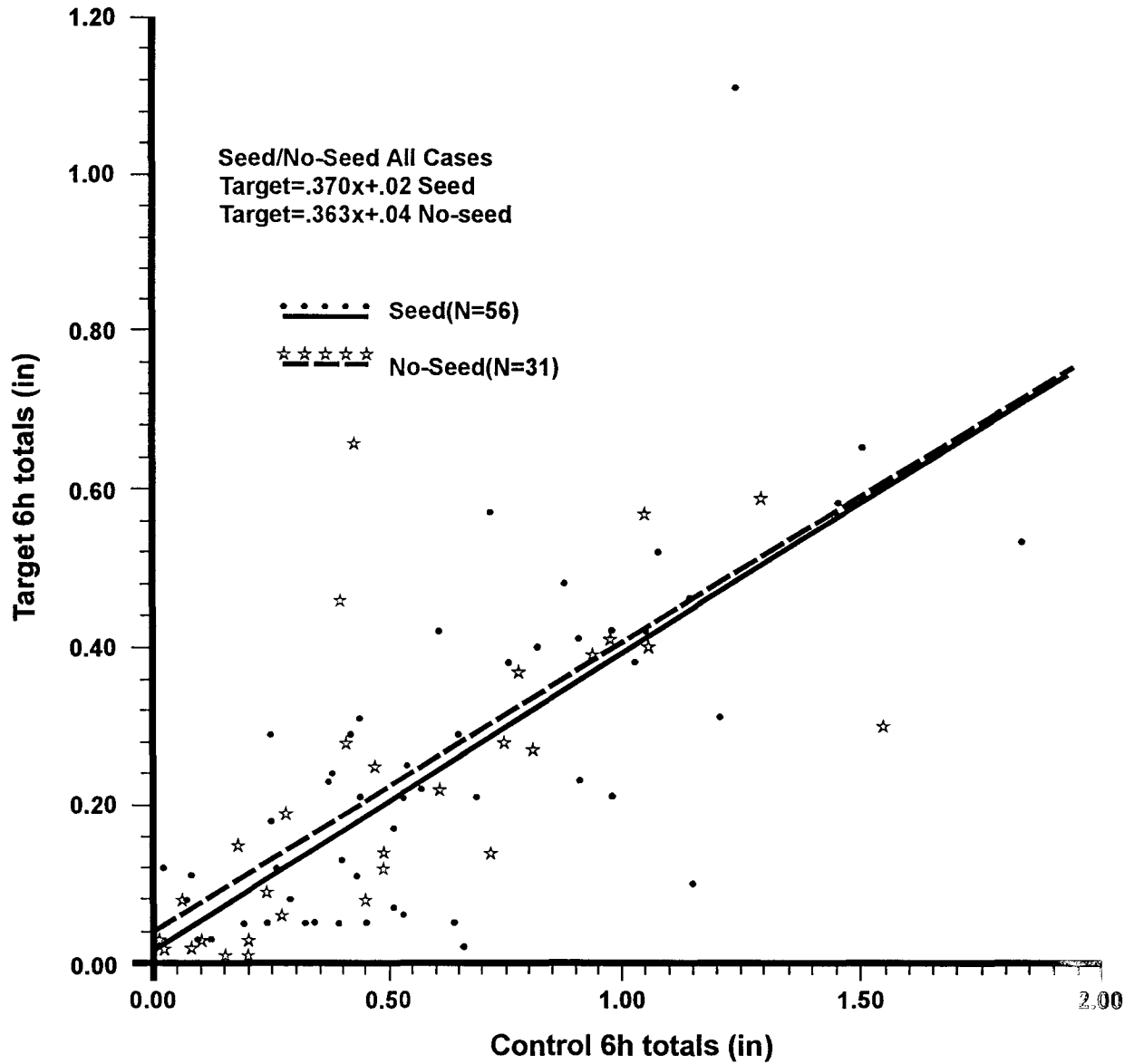


Figure 7.2. - Results of target versus control mean precipitation regression analysis for all 87 randomized cases.

The results of this analysis are shown on figure 7.3. The same regression lines are plotted as on figure 7.2. The populations are more distinct, and the seeded population is indicating more precipitation when the control gauge receives more than 0.5 in. of precipitation in a 6-h period. The double ratio, however, is 0.99, or no difference in the population means over what the control gauge would have predicted. The *P* value is 0.58, or a 58-pct probability that any difference in the seed and no-seed population is by chance alone.

These results are preliminary. With such a small sample size, stating that seeding had no effect on precipitation would be premature. As mentioned at the beginning of the LOREP, as many as 300 randomized cases would be needed to observe a 10-pct increase in precipitation in the target. Therefore, although results would appear disappointing, they are consistent with a small sample size and that any seeding effects are within a  $\pm 10$ -pct range.

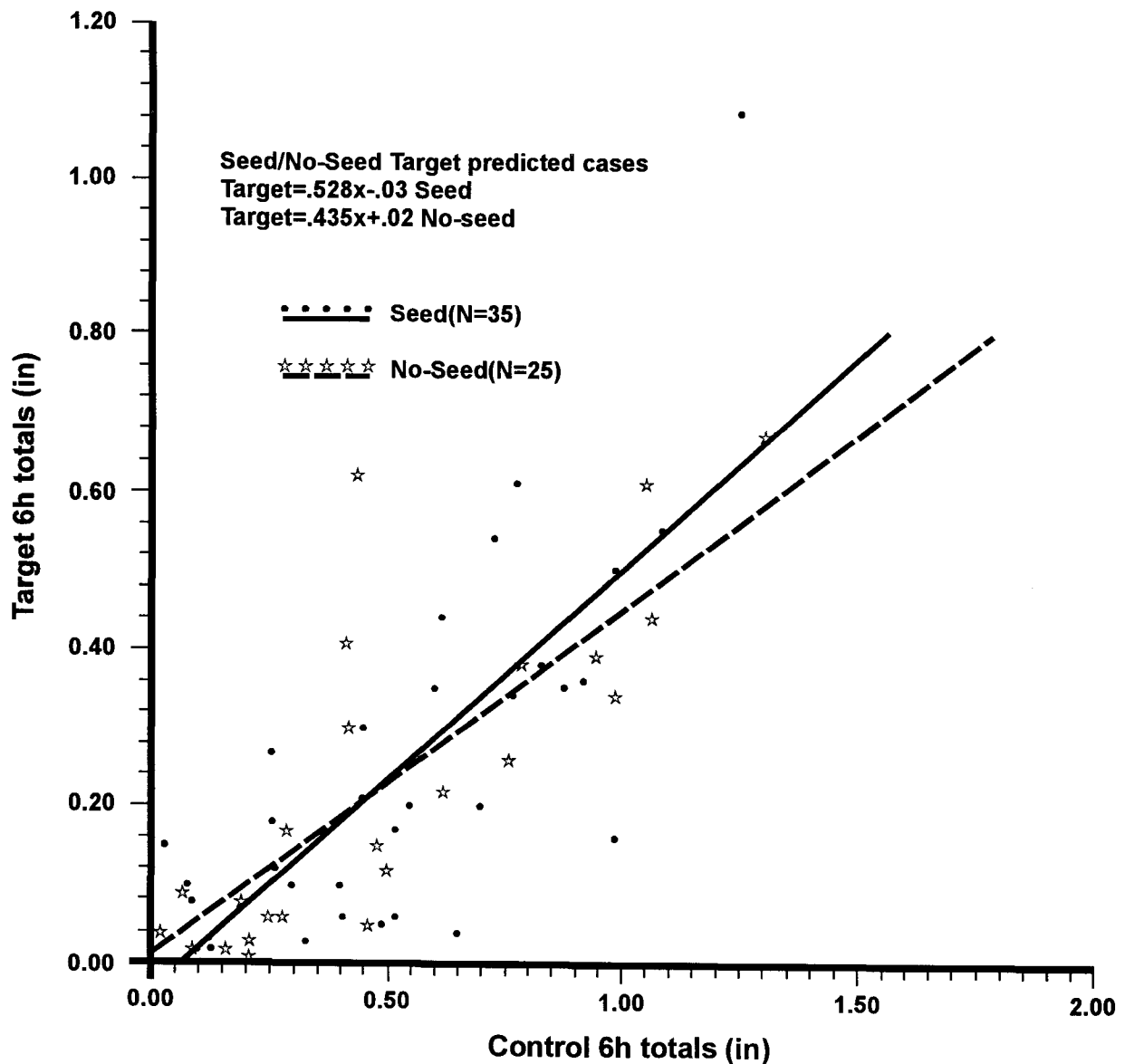


Figure 7.3. - Results of target versus control mean precipitation regression analysis for 60 randomized cases where GUIDE model predicted seeding effects in the target area.

## 8. THE EFFECTS OF MOUNTAIN LEE WAVES ON THE TRANSPORT OF LIQUID PROPANE GENERATED ICE CRYSTALS

### 8.1 Introduction to Lee Wave Effects Study

Results presented by Reynolds (1991, 1992a, 1993) have shown that when the tracer SF<sub>6</sub> is released from the Sierra crest, collocated with a propane dispenser site, the tracer is usually observed to descend into the Middle Fork Feather River valley within about 30 min. The physical mechanism for this transport was not well understood, nor was the magnitude of this downward motion. Aircraft data suggested that the tracer was at times also reaching 300 to 600 m above the release altitude about 12 to 20 km downwind from the release location. These data implied that a downward vertical motion field, followed by an upward vertical motion field, exists across the valley that is indicative of a mountain "lee wave."

Most results presented in this section were derived from a field program, conducted during mid-January to mid-March 1993, to study mountain lee waves in the LOREP area. Emphasis was placed on documenting transport and dispersion of tracer SF<sub>6</sub> or seeding induced ice crystals from propane dispensers to the downwind edge of the target area.

Four time-sequential syringe samplers (Krasnec et al., 1984) were used to collect 15-min air samples at specified locations within the valley to monitor SF<sub>6</sub> (table 2.4 and fig. 2.3). Each sampler had 9 30-cm<sup>3</sup> syringes, providing 2.25 h of sampling time. In addition, the NOAA research aircraft and the high-altitude site at Jackson Creek were equipped with continuous SF<sub>6</sub> analyzers (Benner and Lamb, 1985). The SF<sub>6</sub> analyzer used is capable of detecting SF<sub>6</sub> concentrations down to 5 p/t (parts per trillion).

### 8.2 Rawinsonde Observations of Mountain Lee Waves

Mountain lee waves downwind from the Sierra have been studied extensively (Holmboe and Klieforth, 1957). The studies concentrated on lee waves forming in the absence of major storm systems. However, lee waves can exist during major precipitation events because the air mass in winter is relatively stable (Brintjes et al., 1994). Earlier LOREP tracer studies during winter storms released SF<sub>6</sub> from the main Sierra ridge line and sampled for the tracer in the downwind valley using either a mobile SF<sub>6</sub> analyzer in a van or stationary time sequential samplers (Reynolds, 1992). Results showed that in 9 of 10 experiments, SF<sub>6</sub> was observed in the downwind valley at levels well above background (10 p/t). Results suggested that downward transport to the lee of the Sierra commonly occurred during most winter storms. It seems reasonable that lee waves may play an important role in this transport.

Ascent rates of rawinsonde balloons can be used to identify the presence of lee waves (Lalas and Einaudi, 1980; Reid, 1972; Shutts and Broad, 1993; Shutts et al., 1994). These authors showed that ascent rate can be measured to within 0.2 m s<sup>-1</sup> using change in pressure (altitude) transmitted by the rawinsonde every 2 s. Ascent rate was calculated from observed pressures at 20-s intervals. Using free lift (volume of helium-filled balloon) and the balloon payload, a nominal ascent rate of 5.2 m s<sup>-1</sup> was calculated. This nominal value of ascent rate was subtracted from the observed ascent rate to estimate free air vertical velocities experienced by the balloon. A schematic of the hypothetical path of the rawinsonde through a mountain lee wave for this project area is shown on figure 8.1. An example of how this methodology is applied in a real case is shown on figure 8.2 for 1500 UTC on February 10, 1994. All heights are above mean sea level unless otherwise noted.

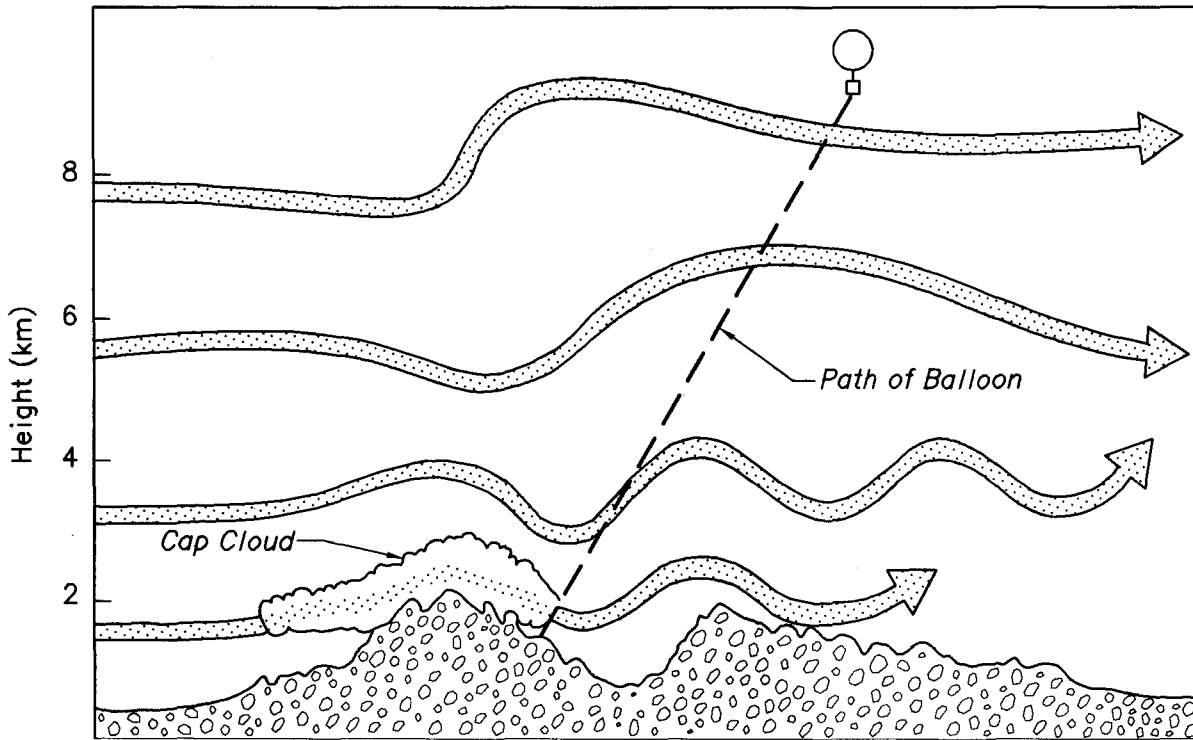


Figure 8.1. - Schematic illustration of mountain waves forming over and to the lee of the project area. Typical path of the ascending rawinsonde balloon through the lee wave is shown.

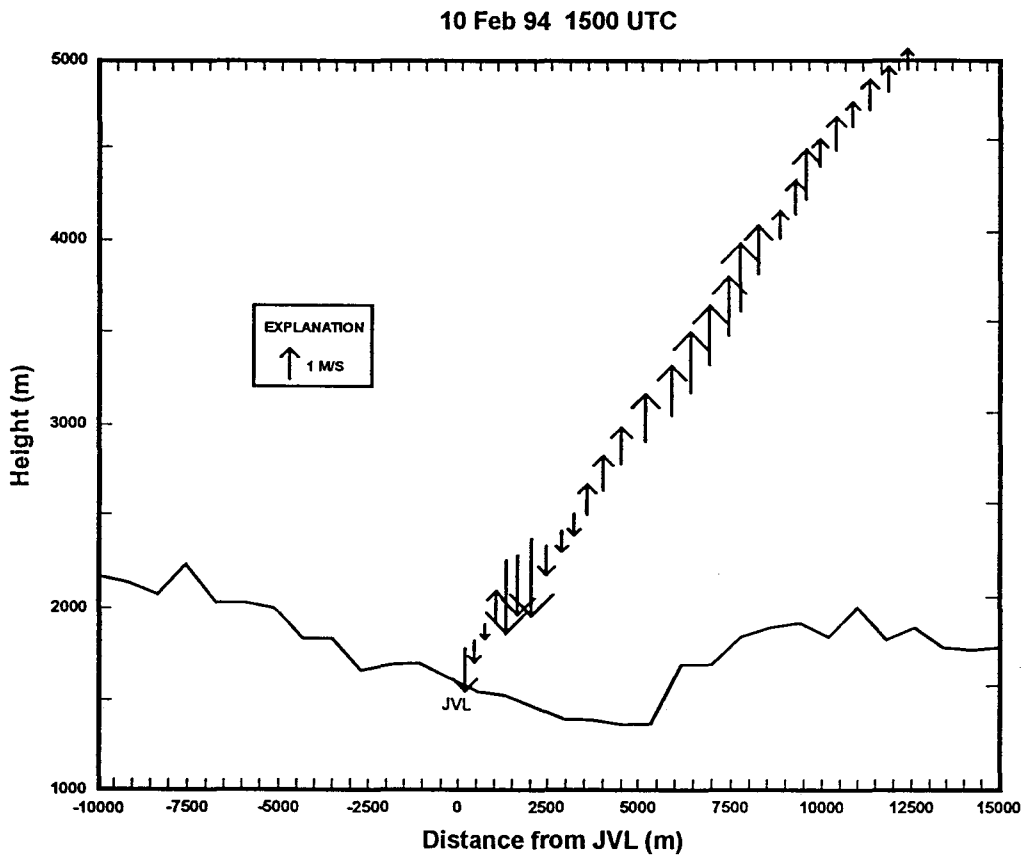
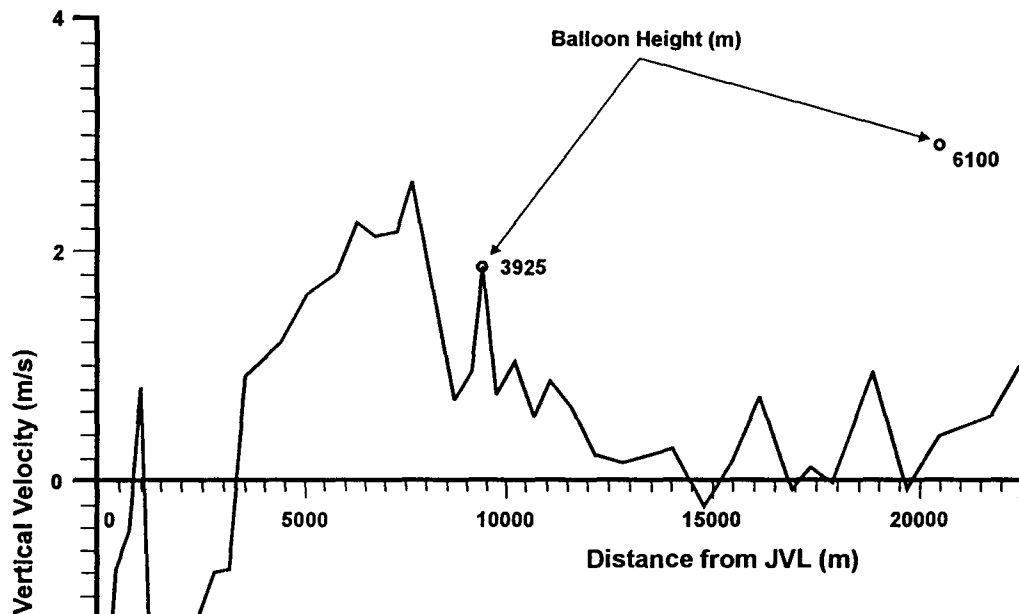


Figure 8.2. - Rawinsonde determined vertical velocities measured along the path of the ascending balloon for February 10, 1994. Magnitudes are scaled using the arrow shown in the insert.

What effect do these large upward and downward vertical motions have on the transport of seeded crystals across the target area? First, it must be emphasized that ground-based seeding experiments need only be concerned with the lowest kilometer above the dispensers. Past tracer studies reviewed by Reynolds (1988) and Super (1990) and the results to be presented here confirm this fact. Thus, it is a relatively narrow vertical region that the three-dimensional wind field is needed for determining the transport and dispersion of seeded crystals. Determining the three-dimensional wind field requires vertical extrapolation of the balloon-derived vertical velocities across the project area from this single vertical profile. Following Shutts and Broad (1993), the calculated rawinsonde vertical velocity versus downstream distance is shown on figure 8.3. An attempt is made to estimate the horizontal wavelength below 3 km over the project area from analysis of the distance between maxima and minima in the vertical velocities. From figure 8.3, the wavelength is about 12 km for February 10. The assumption will be made that the wave has near-vertical phase lines in the lowest 1000 m above the crest.



10 Feb 94 1500 UTC

Figure 8.3. - Balloon derived vertical velocities plotted with respect to distance from Johnsville for February 10, 1994. Number plotted near 10000 and 20000 m is the elevation of the balloon at that distance downwind. This technique allows an estimate of the horizontal wavelength of the lee wave by measuring the distance between peaks and valleys in the velocity data (after Shutts and Broad, 1993).

Figure 8.1 shows what is meant by vertical phase and how it is important to this study. Note the balloon trajectory shown in the figure. One can see that it is sampling a different portion of the wave at different altitudes. If the waves are vertically in phase (stacked vertically), the assumption is made that the wave has the same vertical velocities and position directly below the altitude it was sampled. This is much like what is shown on figure 8.1 for the first two streamlines above the mountain, between 2 and 4 km. At higher altitudes, the waves are no longer in phase but tilt upwind with height. However, remember that this study only concerns the lowest 1000 m above the crest; anything above 3.2 km can be disregarded.

However, the temporal stability of these lee wave characteristics must be determined to determine their effects on particle trajectories from storm to storm or within individual storms. Lee waves are known to change their wavelength and amplitude based on changing winds and atmospheric stability. To determine the magnitude of these changes, soundings were analyzed from the last several winter field seasons using the technique shown on figure 8.2. In analyzing these plots, two recurring patterns appeared. Pattern 1 is represented on figure 8.4. The two cases included from 1992 were days when  $SF_6$  was observed to descend rapidly into the valley as observed using an  $SF_6$  detector mounted in a van (Reynolds, 1992). Several hundred parts per trillion of  $SF_6$  was observed on March 5 in the valley. This was one of the largest concentrations observed during the several winter seasons in which tracer releases were made. In these situations, the strong downdraft is followed by a strong updraft as the balloon begins to pass over the downwind ridge.

The wave velocity pattern shown on figure 8.4 appears to occur most often prior to the passage of the surface cold front in moderate to strong southerly to southwesterly winds as determined from the three mountain-top weather stations. Brintjes et al. (1994) observed a similar relationships over the Mogollon Rim of Arizona. In fact, the stronger the winds near the ridge top (inferred by the rapid downwind displacement of the balloon just after launch), the more intense the downdraft as shown for February 17, 1994.

Pattern 2 is shown on figure 8.5. These days show the lack of the strong downdraft just after balloon launch. The crest of the lee wave appears to have moved toward the mountain with good updrafts where downdrafts were located in pattern 1. Pattern 2 is typical of the lighter wind cases which normally occur post-frontally or near upper level closed lows. In these situations, the atmospheric stability is less, which dampens the amplitude of the lee wave. Note that lighter winds are indicated by the fact that the balloon has translated only 6 or 7 km downwind by the time it reaches 5000 m, in contrast to the 15 km for pattern 1. The February 5, 1993, case shown, representative of this pattern, was a case when the aircraft observed the highest vertical transport of  $SF_6$  of the nine releases made in 1993.

Tracer studies and balloon vertical velocities indicate that the higher wind and more stable situations that normally occur prior to frontal passage are less conducive to ground-based seeding. The lighter wind and less stable environment which occur most often post-frontally are more conducive to seeding (targeting). These results compliment the results summarized by Reynolds (1988), which noted that post-frontal cloud conditions over the Sierra Nevada have the highest liquid water content and the coldest supercooled cloud temperatures, which would also be more conducive to glaciogenic seeding. The 1993 tracer studies will be examined in more detail to see if these results can be confirmed.

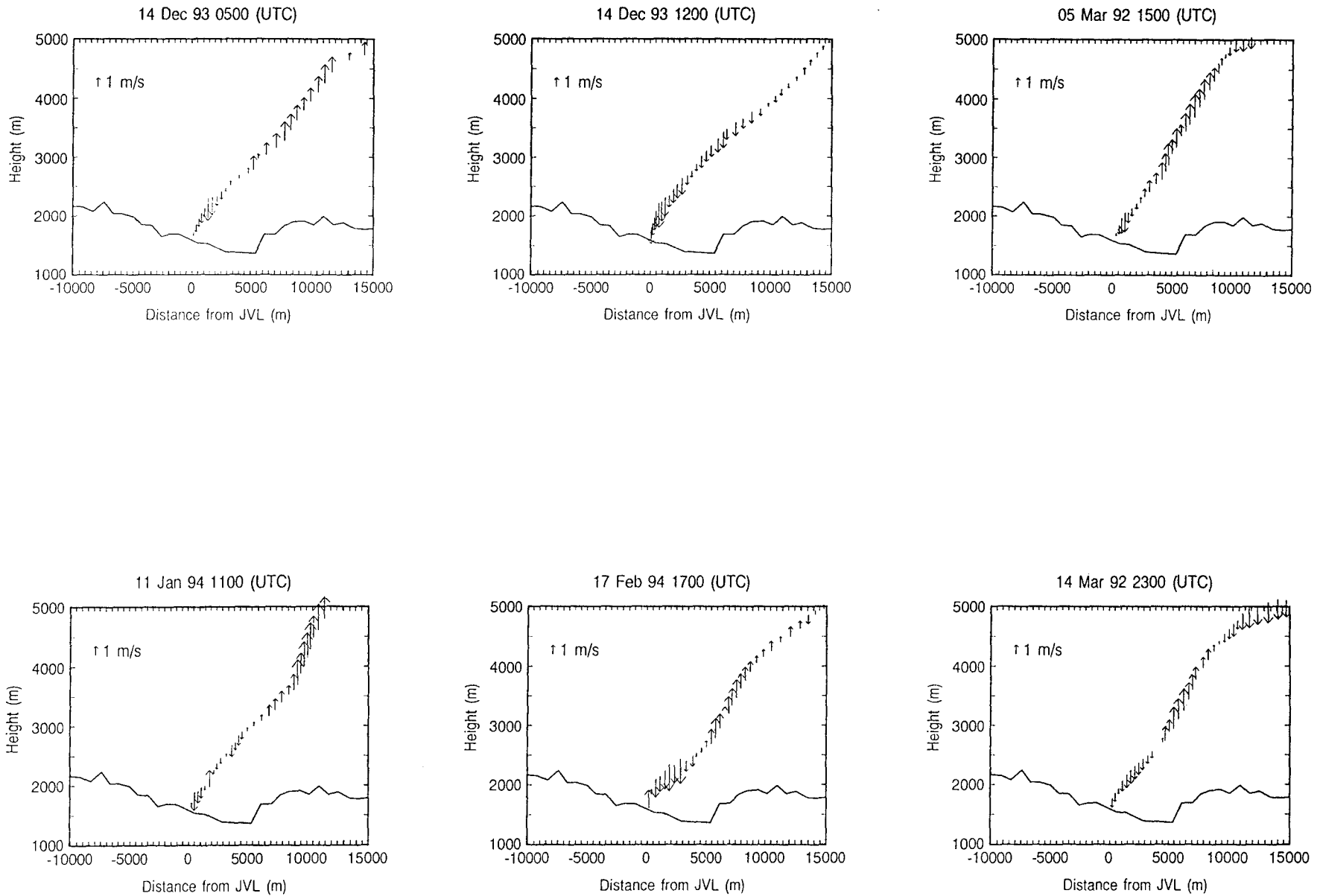


Figure 8.4. - Rawinsonde derived vertical velocities for soundings taken during storm events prior to the passage of the surface cold front. Note the very strong downdraft observed immediately after launch and the rapid horizontal displacement.

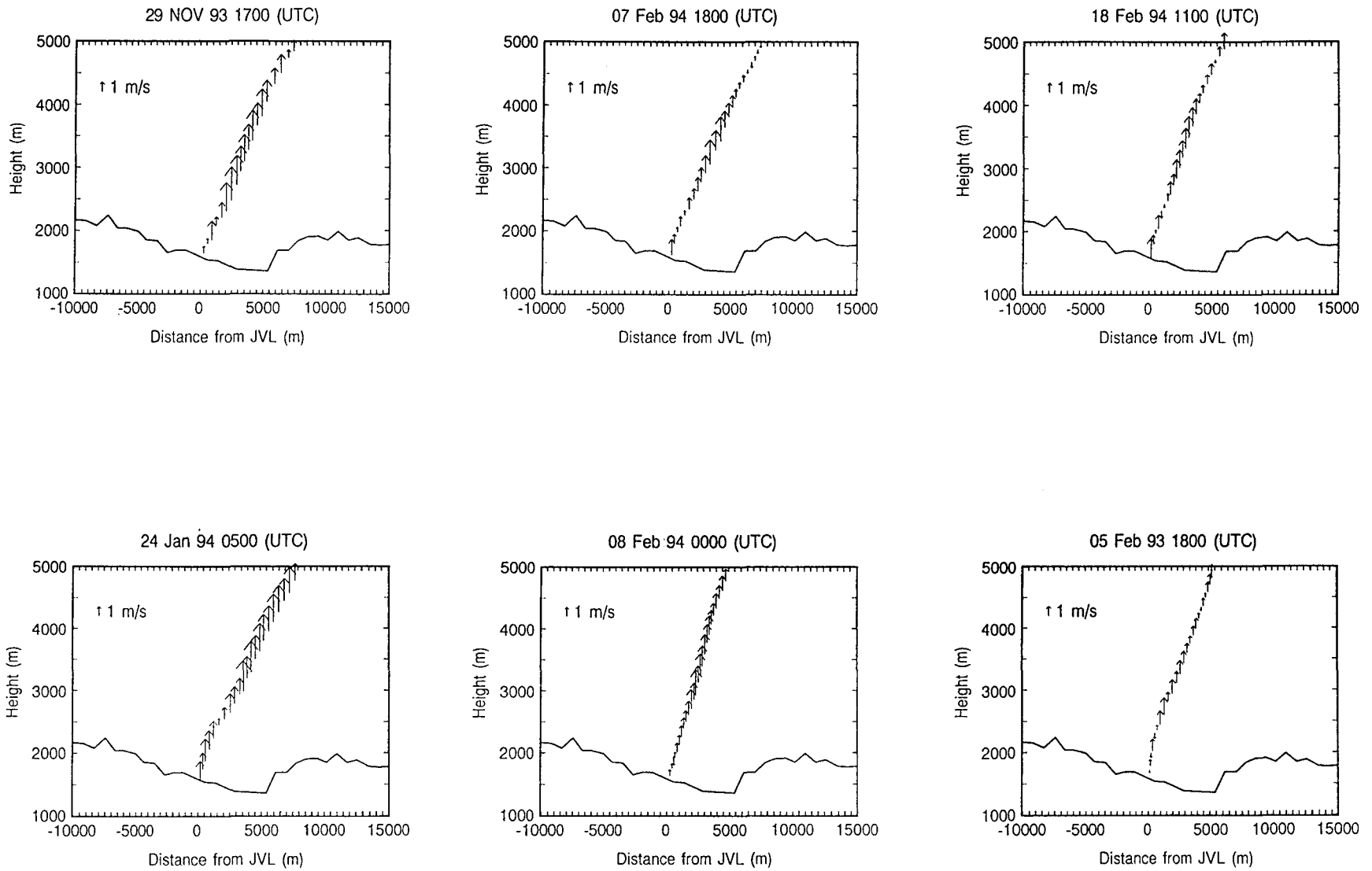


Figure 8.5. - Same as figure 8.4 but for soundings taken after surface frontal passage. Note the strong downdraft observed immediately after launch has been replaced with a general upward motion through 5000 m. Much less horizontal displacement occurs during these events, indicating much lighter winds.

## 8.3 Aircraft Tracer Studies

### 8.3.1 Experimental Procedures

The procedures followed were to remotely release the SF<sub>6</sub> at either dispenser site d7 or d9 or both. Release rates varied from 20 to 25 kg h<sup>-1</sup>. The transport and horizontal dispersion of the tracer gas was monitored by aircraft and ground-based samplers. The ground-based sampling procedures were similar to those used the previous two winters (1990-91 and 1991-92) except the ground-based continuous analyzer was operated at a fixed location (JCC) instead of a mobile van driven within the valley.

The NOAA aircraft flight pattern used during the early 1993 research missions is shown on figure 8.6. During IFR (instrument flight rules) conditions, the flight leg flown between P1 and P2 was the valley track flown at a nominal flight level of 2500 m. The flight leg between P3 and P4 was the ridge track flown at 2680 m. If SF<sub>6</sub> was observed at these nominal altitudes, the aircraft would fly the next set of flight legs 200 m higher. The flight altitudes would be incremented at 200 m intervals until no tracer above background was observed. During VFR (visual flight rules) flights (4 days), these same tracks were flown but at flight levels down to 2100 m. At an airspeed of 80 m s<sup>-1</sup>, completing one race track circuit would take about 15 min. About 8 complete circuits could be completed during a routine mission.

Nine separate aircraft experiments were conducted. Of these nine experiments, four had both SF<sub>6</sub> and propane released, and five had SF<sub>6</sub> only. Table 8.1 lists the dates and times of each experiment and other relevant information, including the location and amount of the maximum SF<sub>6</sub> observed by the network of sequential samplers. If the maximum SF<sub>6</sub> as observed by the aircraft was below the nominal flight altitudes, the actual altitude of interception is noted in column 9.

### 8.3.2 Plume Analyses

The SF<sub>6</sub> plume was defined as the time when the concentration moved above background to the time when the concentration fell at or below background levels. Background levels varied from flight to flight but were generally between 5 and 10 p/t. This methodology was patterned after the work of Stith et al. (1986) and Super et al. (1989). The 1993 experiments found an 11-s lag between the time of SF<sub>6</sub> ingest into the sampling port of the aircraft and registration of SF<sub>6</sub> on the analyzer. This lag was accounted for in the analysis of these data but was not in the figures of SF<sub>6</sub> plumes to be shown in this paper. Plume intercept times were compiled and identified as to whether the plume originated from site d7 or d9 if simultaneous releases were made. Statistics were compiled on each plume and parameters were tabularized as to the site of origin, and whether it was sampled on the valley, ridge, or downwind flight track. These results are discussed in the following subsections.

#### 8.3.2.1 Valley Track Plume Intersections

Table 8.2 lists a total of 31 valley interceptions of the SF<sub>6</sub> plume from site d7 made by the aircraft. The mean distance from site d7 to the valley intercept was 13 km. At this distance, the plume age varied depending on wind speed. On average, the plume was about 15 min downwind from the release point, but varied from 10 min on February 17 to 27 min on March 19.

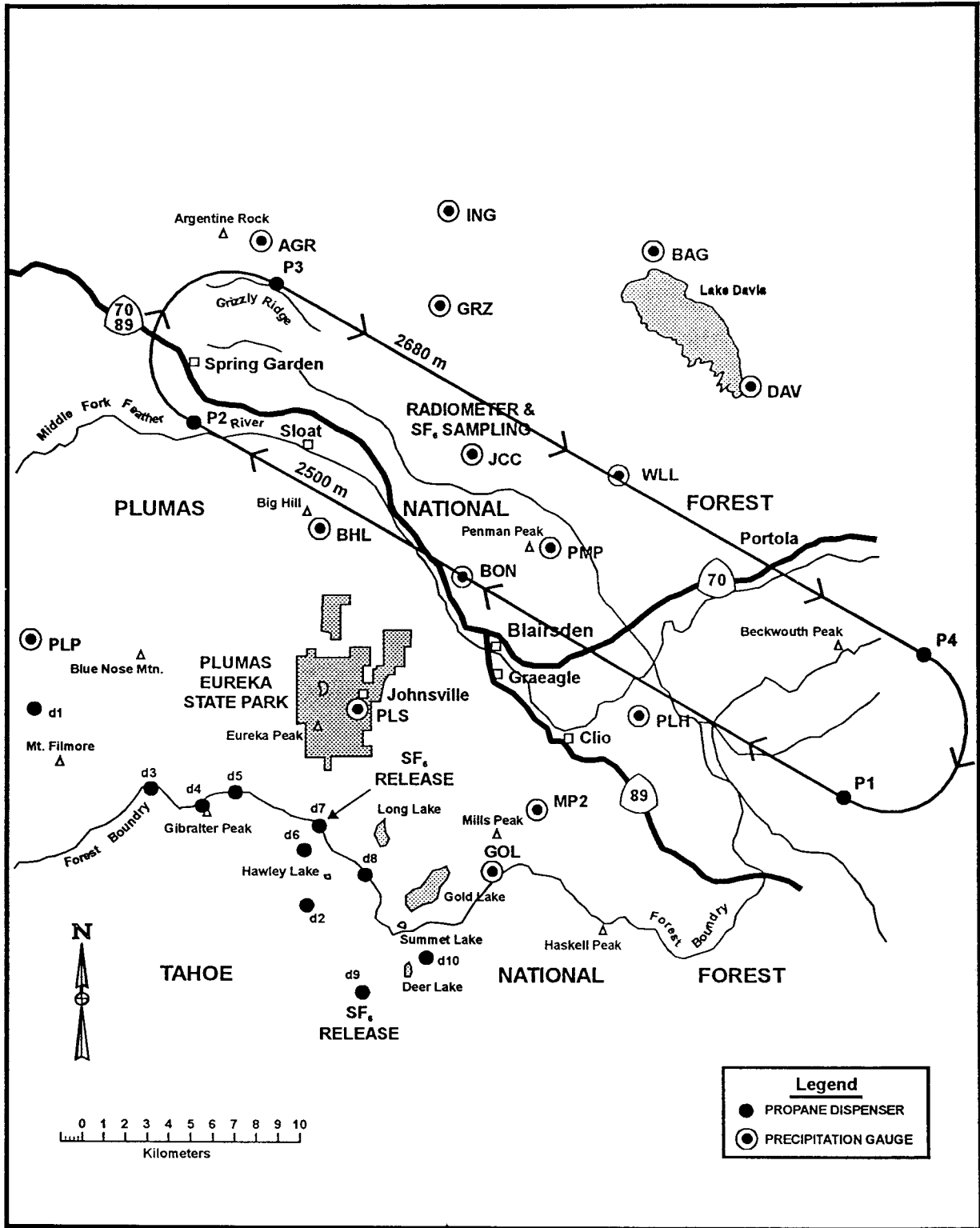


Figure 8.6. - Nominal flight tracks used by the NOAA research aircraft during the mid-January to mid-March 1993 tracer and seeding experiments superimposed over the project area.

Table 8.1. - SF<sub>6</sub> experiments conducted during early 1993.

Date	Release Site	Times (UTC)	Period (h)	SF <sub>6</sub> Rate (kg h <sup>-1</sup> )	Site Temp (°C)	Raob Winds 2200 m (m s <sup>-1</sup> /°True)	Sampling Times (UTC)	Max SF <sub>6</sub> Aircraft V=Valley R=Ridge (p/t)	Max SF <sub>6</sub> Sequential Sampler # (p/t)	Vertical Velocity Pattern
02/05/93	7	1700-1800	1.0	20.0	-0.6	7/205	1625-1850	137(V)	45-#4	2
02/08/93	7 <sup>1</sup>	2230-2330 0015-0115	2.0	22.0	1.6	7/205	2230-0110	78(V)	40-#4	1
02/09/93	7 <sup>1</sup>	1800-1900 1915-2015	2.0	20.0	-4.8	11/209	1815-2037	47(V)	91-#4	2
02/17/93	7 <sup>1</sup> 9 <sup>1</sup>	1630-1730 1730-1830	1.0 1.0	23.0 23.5	-4.4 -4.4	13/193 13/193	1625-1850 1625-1850	53(V) 89(V)	42-#8	2
03/02/93	9	2309-0009	1.0	21.7	3.7	5/197	2330-0130	140(V)	0	2
03/09/93	7-9 7-9	1635-1735 1635-1735	1.0	19.9 21.8	5.3	5/192	1637-1914	364 (2.2 km) 271 (2.2 km)	60-#8	1
03/16/93	7 <sup>1</sup> 9 <sup>1</sup>	1515-1615 1515-1615	1.0	19.9 22.1	3.1	14/219	1533-1815	48(V) 33(V)	80-#8	1
03/17/93	7 9	1515-1615 1515-1615	1.0	19.9 22.1	1.5	19/223	1530-1719	25(R) 15(R)	25-#3	1
03/19/93	7-9 7-9	2315-0015 0030-0130	2.0	19.9 22.1	4.7	11/204	2315-0200	227 (2.2 km) 50 (2.1 km)	110-#3	1

<sup>1</sup> Propane seeding conducted from this site.

Table 8.2. - SF<sub>6</sub> plume characteristics from site d7 observed by aircraft for valley track.

Date	Pass No.	Plume Width (°)	Plume Width (km)	Dist. Site d7 (km)	Max SF <sub>6</sub> (p/t)	Avg SF <sub>6</sub> (p/t)	Alt. (m)	Temp (°C)	Avg. LWC (g m <sup>-3</sup> )	Wind Speed (m s <sup>-1</sup> )	Wind Dir. (° True)
2/5	7	13	3.0	13.8	137	66	2526	-2.2	0.10	18	191
2/5	9	8	1.9	13.6	132	80	2528	-2.4	0.13	11	193
2/5	11	6	1.2	12.8	65	37	2653	-3.1	0.13	7	198
2/8	3	11	2.5	13.5	32	9	2523	-2.8	0.02	20	182
2/8	5	4	1.0	13.7	21	10	2511	-2.6	0.00	16	200
2/8	7	6	1.4	13.8	23	9	2520	-2.7	0.06	19	184
2/8	13	13	2.9	13.0	11	3	2518	-2.6	0.03	11	172
2/8	15	13	3.1	13.4	27	10	2522	-2.6	0.04	9	184
2/8	17	15	3.7	14.2	78	27	2523	-2.5	0.05	6	155
2/9	3	12	2.7	13.0	47	15	2525	-7.5	0.01	13	207
2/9	5	15	3.2	12.3	27	8	2529	-7.2	0.02	10	209
2/9	7	15	3.3	12.2	31	11	2524	-7.1	0.01	9	210
2/17	3	7	1.5	13.1	53	32	2483	-6.8	0.01	22	184
2/17	5	13	3.0	13.0	52	26	2481	-6.8	0.02	21	182
2/17	7	6	1.4	13.2	15	9	2492	-6.6	0.01	23	185
2/17	9	9	2.0	13.3	52	26	2477	-6.6	0.03	21	188
3/9	3	4	1.0	13.3	20	11	2161	5.8	0.00	13	209
3/9	5	16	3.4	12.2	313	118	2165	5.8	0.00	12	196
3/9	6	23	4.9	12.3	364	130	2231	5.3	0.00	9	204
3/9	7	17	3.5	12.0	276	119	2282	4.9	0.00	13	199
3/9	8	21	4.8	12.9	171	70	2367	4.1	0.00	11	204
3/9	9	14	3.0	12.5	195	76	2357	4.2	0.00	15	213
3/16	3	18	3.8	12.3	48	14	2544	0.5	0.17	17	217
3/16	5	38	9.2	13.3	14	6	2541	0.7	0.07	19	224
3/17	1	16	3.4	12.4	19	8	2507	0.9	0.01	26	215
3/19	4	18	3.9	12.3	71	29	2321	4.7	0.00	10	208
3/19	5	17	5.0	16.6	56	26	2307	4.6	0.00	10	238
3/19	7	14	3.0	12.5	39	13	2474	2.6	0.00	10	210
3/19	11	12	2.7	12.5	57	18	2176	4.7	0.00	7	214
3/19	12	9	1.9	12.1	227	88	2314	3.5	0.00	7	243
3/19	13	6	1.4	12.6	23	7	2467	2.8	0.00	8	225
Avg.		13	3.0	13.0	87	36	2437	-0.5	0.03	14	201

For flights made in IFR conditions, the highest concentrations of SF<sub>6</sub> at 2500 m and above were found on February 5. Unfortunately, temperatures were too warm at the release site to initiate seeding. This day, along with March 16, had the most liquid water at and above 2500 m. The fewest plume interceptions were on March 17. Only one plume intercept was observed on the valley track. Winds were near 25 m s<sup>-1</sup> on this day and may have caused the plume to move almost horizontally from the release altitude of 2200 m because very little SF<sub>6</sub> was found in the valley as well. It should be mentioned that aircraft operations were aborted when winds exceeded 25 m s<sup>-1</sup>.

If the average SF<sub>6</sub> concentration is plotted against SF<sub>6</sub> intercept altitude (fig. 8.7) for all plume interceptions on all experimental days, it is apparent that concentrations peak at the release altitude (2225 m) and fall off dramatically above and below this altitude. Fifty-five percent of the passes made along the valley track at 2500 m showed no SF<sub>6</sub>. Almost all passes made below 2400 m along the valley track showed SF<sub>6</sub> above background levels.

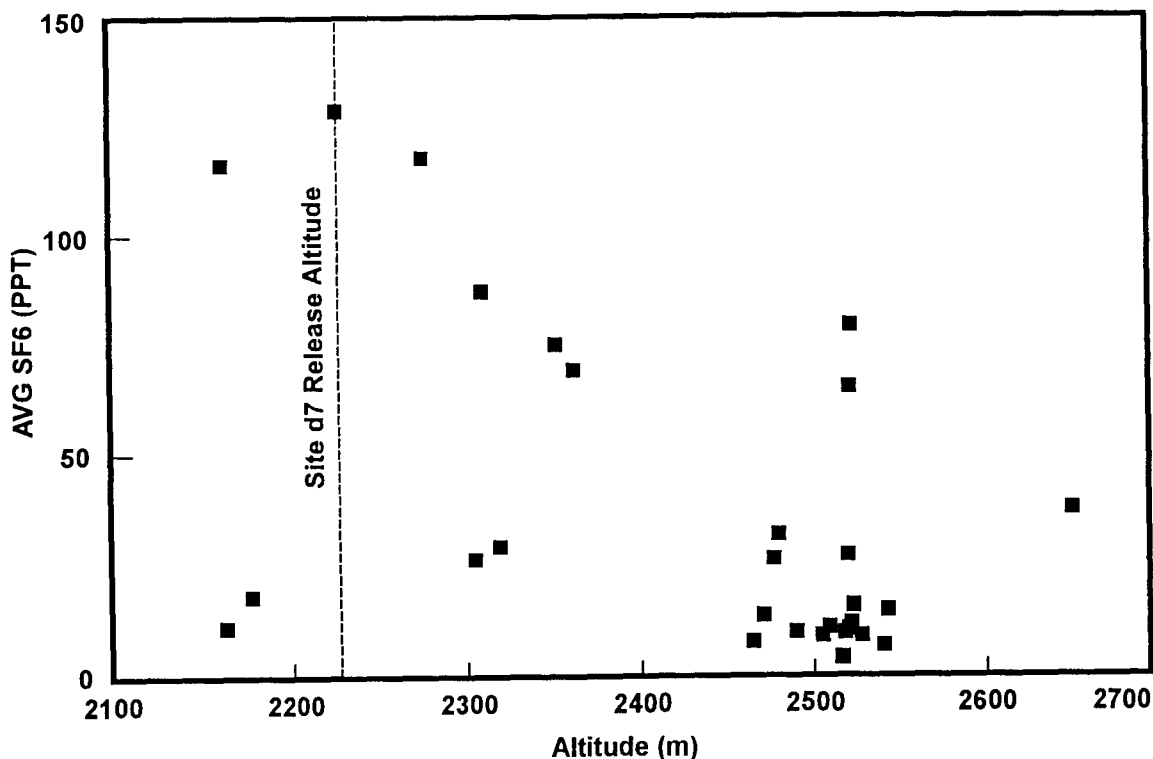


Figure 8.7. - Average SF<sub>6</sub> concentrations plotted with respect to altitude for all SF<sub>6</sub> plume penetrations from site d7 (EL 2225 m) along the valley track.

It is important to note the plume's horizontal dimensions to determine if dispenser density will cover the target area. The plume is about 13° (3 km) wide over the valley. This width is close to the dispersion rate used in the operational targeting model (section 8.4) and similar to average dispenser separation. The plume tends to be wider at plume interceptions made near release altitude. This tendency would indicate the plume centerline remains near the release altitude with the plume becoming narrower both above and below this elevation. Thus, at 2500 m, the aircraft is probably sampling near the top of the plume over the valley as the frequency of plume intersection drops off dramatically and the plume width narrows.

Table 8.3 summarizes valley plume interceptions from site d9. Site d9 SF<sub>6</sub> releases could not be made until February 17 because of equipment problems. Thus, many plume interceptions were made on VFR flights below 2500 m. The mean distance from site d9 to the plume intercept was almost 18 km. This 5-km difference compared to site d7 is a result of site d9 being 5 km farther southwest of the valley flight track. Thus, the plumes will have about 7 min additional dispersion time on average before being sampled along the valley track.

Table 8.3. - Site d9 plume characteristics observed by aircraft for valley track.

Date	Pass No.	Plume Width (°)	Plume Width (km)	Dist. Site d9 (km)	Max SF <sub>6</sub> (p/t)	Avg SF <sub>6</sub> (p/t)	Alt. (m)	Temp (°C)	Avg. LWC (g m <sup>-3</sup> )	Wind Speed (m s <sup>-1</sup> )	Wind Dir. (° True)
2/17	11	15	5.0	19.5	57	19	2472	-6.6	0.07	18	184
2/17	13	14	4.8	19.2	89	36	2479	-6.5	0.14	15	181
2/17	15	15	5.1	19.4	86	26	2478	-6.2	0.12	17	184
3/2	8	13	4.1	18.0	68	29	2273	2.9	0.00	8	228
3/2	9	22	6.6	17.2	133	58	2267	2.8	0.00	na	na
3/2	10	32	11.0	18.9	135	46	2145	4.0	0.00	8	217
3/2	11	38	11.0	16.0	140	44	2145	3.8	0.00	7	198
3/9	5	10	3.1	17.7	100	43	2163	6.0	0.00	10	200
3/9	6	19	5.6	17.1	271	70	2229	5.4	0.00	8	205
3/9	7	17	5.3	17.4	182	80	2285	5.0	0.00	11	212
3/9	8	19	6.0	17.7	130	64	2375	4.2	0.00	10	218
3/9	9	28	9.1	18.0	124	64	2346	4.5	0.00	9	217
3/9	11	19	6.0	17.5	92	40	2400	4.3	0.00	6	227
3/9	13	12	3.5	17.6	15	6	2484	3.1	0.00	8	222
3/16	5	13	3.9	17.4	33	12	2533	0.7	0.16	16	218
3/19	7	7	2.2	17.4	38	20	2480	3.7	0.00	13	209
3/19	11	11	3.4	17.4	50	28	2178	4.7	0.00	11	229
3/19	12	9	2.6	17.2	24	11	2317	3.6	0.00	10	204
3/19	13	5	1.4	17.3	24	11	2476	3.3	0.00	15	215
Avg.		17	5.2	17.6	93	36	2352	2.2	0.03	11	208

SF<sub>6</sub> releases were made from both site d7 and d9 on 5 days, allowing plume characteristics to be compared. February 17 did not have simultaneous releases, but releases were separated by 1 h. Site d9 plume dimensions averaged 5 km in width and site d7 plume dimensions averaged 3.3 km in width. SF<sub>6</sub> average plume concentrations were 35 p/t for site d9 and 43 p/t for site d7. Liquid water concentrations averaged 0.12 gm<sup>-3</sup> in site d9 plumes and only 0.05 gm<sup>-3</sup> in site d7 plumes. More on these findings will be discussed in section 8.4 discussing seeding effects. Because the average sampling distance downwind from the dispensers was 13 km for site d7 and almost 18 km for site d9, site d9, which is located farther back from the crest, would appear to be more effective in treating a larger cloud volume.

Two VFR flight days, March 9 and March 19, provided comparisons for sampling of site d7 and d9 plumes at altitudes comparable to release altitudes. Distinguishing between plumes along the valley track was easy because they were quite distinct. March 9 provided excellent documentation of SF<sub>6</sub> plumes over the valley from both sites. Six passes noted plumes from site d7 and seven passes for site d9. Five passes noted plumes from each site. Pass 8 on this day is shown on figure 8.8. It is typical of the averages computed from all plume intersections on this day. For site d7, the average plume width was 3.4 km. The average plume concentration was 87 p/t at an elevation of 2261 m. For site d9, the average plume width was 5.5 km with an average SF<sub>6</sub> concentration of 52 p/t at an elevation of 2326 m. Note that the plume from site d7 was detected at and below 2347 m; the plume from site d9 was detected to 2484 m.

For March 19, a day in which strong turbulence was observed, six plumes were intersected from site d7 and four from site d9. Average plume dimension for site d7 was 3 km with an average SF<sub>6</sub> concentration of 30 p/t. For site d9, the respective values were 2.4 km and 18 p/t. The average plume elevation was 2350 m for both sites. In this case, the site d7 plume was transported to higher elevations than occurred from site d9. Plume characteristics from site d9 were less than half the values observed on March 9.

Plotting the average plume SF<sub>6</sub> concentrations versus plume intercept altitude for all site d9 interceptions on experimental days (fig. 8.9), a similar pattern to site d7 (fig 8.7) is noted. On figure 8.9, concentrations peak near the release altitude (2207 m) but are about half of the site d7 peak values (fig. 8.7). Another difference is that the peak is about 100 m higher in altitude and not quite as sharp as for site d7 (plume more dispersed).

In general, the valley plume intersections would substantiate that a site located farther back from the crest allows more time for plume dispersion and better lift of the tracer/seeding material into cloud regions. However, this scenario is not always the case. Days such as March 16, 17, and 19, where strong turbulence was noted at aircraft altitudes, indicate that site d9 is not as effective as site d7, although neither are very effective in getting material to altitudes at or above 2500 m.

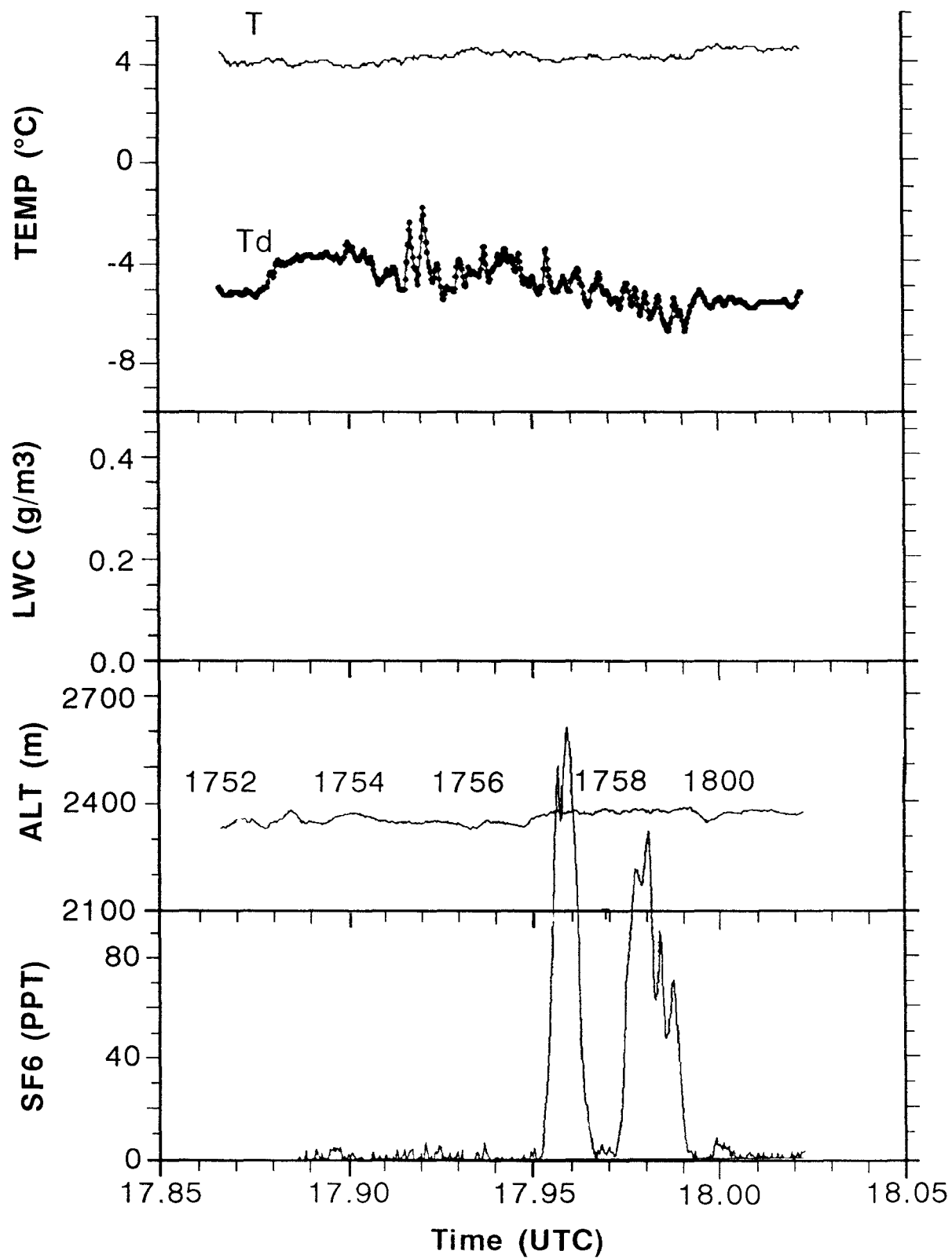


Figure 8.8. - Variables observed or calculated from aircraft observations made during plume tracing experiments during VFR conditions on March 9 along the valley track. From top to bottom; temperature and dew point, cloud liquid water, aircraft altitude (time in hours and minutes given with altitude), and SF<sub>6</sub> concentration. Distinct SF<sub>6</sub> plumes seen from site d7, then site d9.

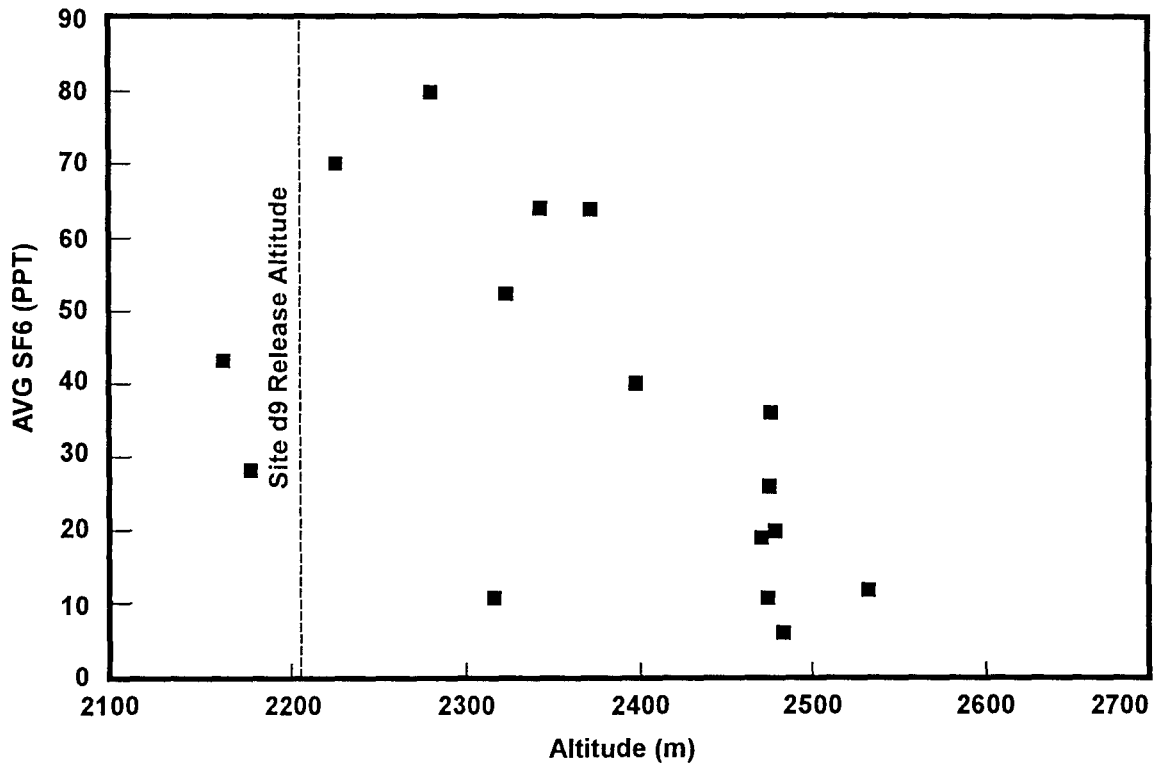


Figure 8.9. - Average SF<sub>6</sub> concentrations plotted with respect to altitude for all SF<sub>6</sub> plume penetrations from site d9 (EL 2146 m) along the valley track.

### 8.3.2.2 Ridge Track Plume Intersections

Table 8.4 summarizes SF<sub>6</sub> plume intersections from site d7 along the ridge track. A little over half the number of intersections were noted compared to the valley track. The average distance from site d7 to the ridge plume intersection was almost 22 km. Based on an average wind speed of 10 ms<sup>-1</sup>, the plume was about 36 min old. Although the plumes were more than twice the age as over the valley, the plumes' horizontal dimensions were only slightly wider—4 km to 3 km over valley, but the spread angle was less—10° versus 13° for the valley. February 5 still shows the best day of vertical transport of SF<sub>6</sub>.

Based on an average of five ridge passes per flight when SF<sub>6</sub> would have time to reach the ridge position, only 40 pct of the passes indicated plumes at flight altitude, which averaged 2562 m. In fact, 11 of 18 plume intersections came on three days, February 5, February 17, and March 9.

Table 8.5 summarizes the ridge plume intersections for site d9. These plumes were about 45 min old when sampled. For March 17, where no valley intercepts were noted, 3 separate plume intersections were noted over the ridge. This result would indicate that the downward portion of the wave transported the tracer below aircraft altitudes over the valley and the upward portion of the wave transported the tracer to higher altitudes over the ridge. This scenario seems to be confirmed on figure 8.10. On average, plume characteristics for the ridge versus valley interceptions for site d9 are respectively: plume width—6.6 versus 5.2 km; average SF<sub>6</sub> concentrations—24 versus 36 p/t. Again, at the nominal in cloud flight altitude of 2650 m, the aircraft would appear to be just skimming the top of the plumes.

Table 8.4. - SF<sub>6</sub> plume characteristics from site d7 as observed by aircraft for ridge pass.

Date	Pass No.	Plume Width (°)	Plume Width (km)	Dist. Site d7 (km)	Max SF <sub>6</sub> (p/t)	Avg SF <sub>6</sub> (p/t)	Alt. (m)	Temp (°C)	Avg. LWC (g m <sup>-3</sup> )	Wind Speed (m s <sup>-1</sup> )	Wind Dir. (° True)
2/5	8	8	3.3	23.0	75	29	2524	-2.0	0.05	8	173
2/5	10	7	2.6	23.0	119	63	2523	-2.2	0.08	3	180
2/5	12	6	2.5	23.0	107	66	2654	-3.0	0.12	1	250
2/5	14	8	2.9	22.0	20	8	2809	-3.9	0.03	9	190
2/8	6	6	2.4	24.0	16	6	2661	-3.7	0.11	11	176
2/9	4	6	2.1	22.0	12	8	2662	-8.0	0.08	8	239
2/9	10	4	1.5	21.0	19	7	2527	-7.1	0.01	14	221
2/17	4	1.4	0.5	21.8	13	11	2619	-8.6	0.01	14	215
2/17	6	13	5.0	22.3	24	7	2618	-8.5	0.02	15	185
2/17	8	12	4.4	22.4	16	8	2621	-8.5	0.01	17	190
2/17	10	7	2.8	22.2	14	6	2619	-8.3	0.03	16	182
3/9	10	20	7.1	19.8	124	44	2342	4.3	0.00	6	206
3/9	12	23	7.9	19.9	110	38	2404	3.9	0.00	7	194
3/9	14	7	2.6	20.1	27	13	2421	3.5	0.00	6	207
3/17	2	8	2.8	21.2	25	13	2664	-0.7	0.07	22	222
3/17	6	30	11.8	22.3	25	8	2650	-1.4	0.11	21	227
3/19	6	6	2.2	20.2	22	11	2313	5.0	0.00	9	208
3/19	8	12	4.6	21.4	37	18	2487	3.2	0.00	11	218
Avg.		10	3.8	21.7	45	20	2562	-2.5	0.04	11	205

Table 8.5. - SF<sub>6</sub> plume characteristics from site d9 as observed by aircraft for ridge pass.

Date	Pass No.	Plume Width (°)	Plume Width (km)	Dist. Site d9 (km)	Max SF <sub>6</sub> (p/t)	Avg SF <sub>6</sub> (p/t)	Alt. (m)	Temp (°C)	Avg. LWC (g m <sup>-3</sup> )	Wind Speed (m s <sup>-1</sup> )	Wind Dir. (° True)
2/17	12	9	4.5	28.0	17	8	2614	-6.6	0.02	20	191
2/17	14	7	3.5	28.5	11	6	2616	-6.7	0.02	20	193
2/17	16	1	0.7	29.4	13	8	2622	-6.5	0.02	19	183
3/2	12	18	7.9	25.0	107	43	2146	3.8	0.00	7	240
3/2	13	30	11.8	21.7	120	49	2134	3.7	0.00	4	208
3/2	14	17	7.2	24.2	58	26	2135	3.7	0.00	9	232
3/2	15	30	13.6	25.1	136	40	2144	3.5	0.00	8	208
3/9	10	15	6.7	24.9	77	42	2359	4.3	0.00	9	211
3/9	12	15	6.7	24.8	144	73	2419	3.9	0.00	10	216
3/9	14	13	5.7	24.7	87	20	2477	3.3	0.00	10	217
3/16	6	30	14.3	27.1	28	9	2689	-0.4	0.20	17	241
3/17	2	5	2.4	26.2	15	5	2671	-0.7	0.17	23	225
3/17	6	8	3.5	26.4	15	7	2658	-1.2	0.09	23	231
3/19	8	10	4.4	26.4	15	5	2480	3.5	0.00	7	228
Avg.		15	6.6	25.9	60	24	2440	0.54	0.04	13	216

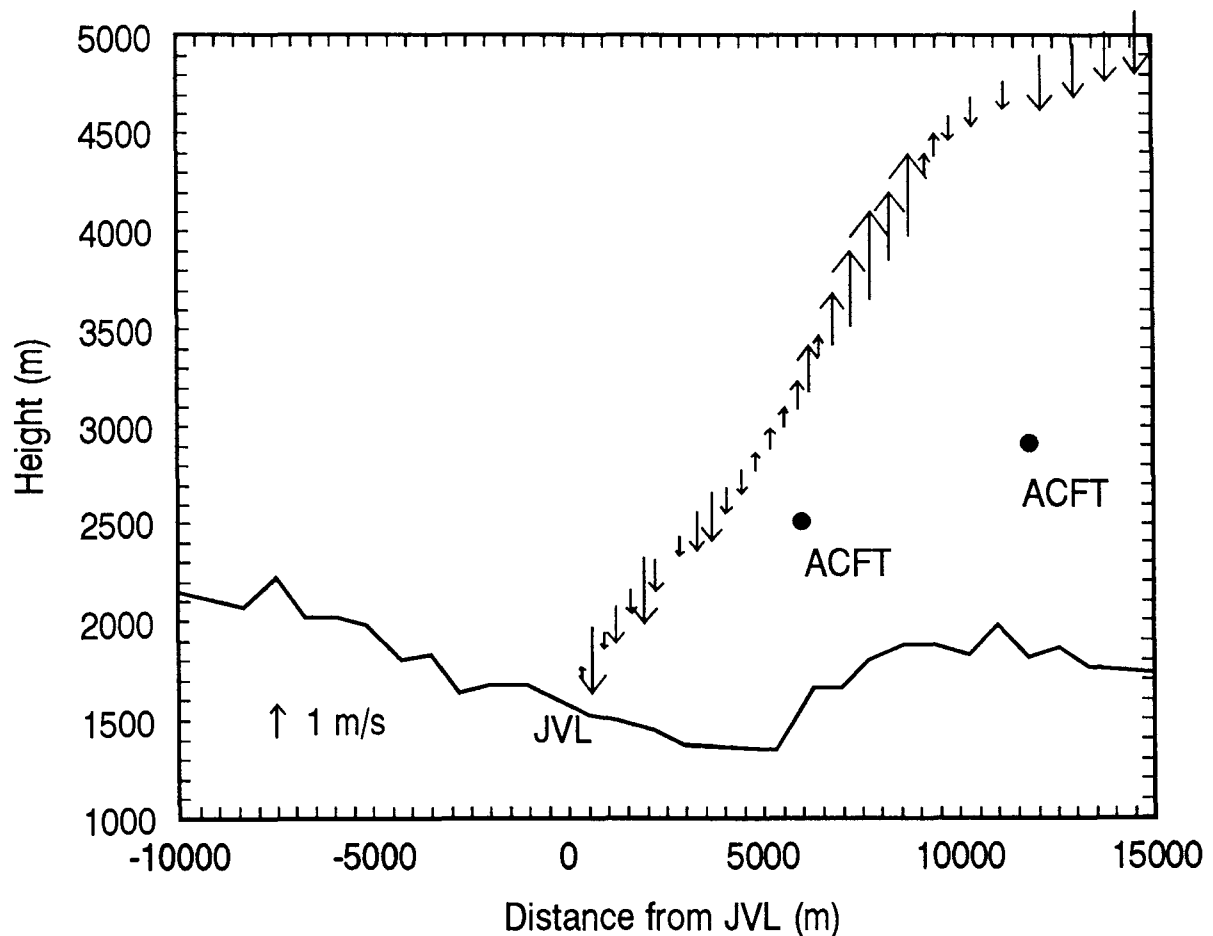


Figure 8.10. - Rawinsonde derived vertical velocities for March 17 showing well defined lee wave pattern which influenced the transport of SF<sub>6</sub> on this day. Locations of aircraft sampling altitudes over the valley and ridge passes are annotated.

Comparing site d7 and d9 SF<sub>6</sub> intercepts along the ridge pass for the same days (February 17, March 9, March 17, and March 19), the following plume characteristics are found for d7 and d9 respectively: plume width—4.7 to 4.2 km; average SF<sub>6</sub> concentrations—16 versus 19 p/t; and average LWC—0.02 versus 0.04 gm<sup>-3</sup>. These results indicate little difference in tracer transport over the target ridge from these two sites.

### 8.3.2.3 Downwind Plume Intersections

On a few days, the aircraft flew along flight segments about 10 km downwind (northeast) from the flight pattern shown on figure 8.6. Results for site d7 and site d9 are shown in tables 8.6 and 8.7, respectively. The best documented case is for March 9, where plume dimensions were rather consistent for both sites. The average distances downwind were 34 and 38 km for sites d7 and d9 respectively. Thus, for a 10-m s<sup>-1</sup> wind, the plume would be about 1 h downwind. For this day, plume characteristics showed widths of 15 and 14 km and average SF<sub>6</sub> concentrations of 23 and 25 p/t for sites d7 and d9, respectively. Aircraft altitude at plume intercept was 2475 m, or 275 m above the release altitude. Figure 8.11 shows plume interceptions for one downwind leg on March 9. The plumes cover a horizontal distance of over 31 km, having merged at this downwind distance. A plan view of all SF<sub>6</sub>

intercepts for this day is shown on figure 8.12. Predicted locations of these intercepts by the operational targeting model (see section 8.4) for sites d7 and d9 are annotated. Results for March 16 are much more erratic, indicating that the plumes may be sporadically rising to aircraft altitudes during these downwind passes.

Table 8.6. - SF<sub>6</sub> plume characteristics from site d7 as observed by aircraft for downwind track.

Date	Pass No.	Plume Width (°)	Plume Width (km)	Dist. Site d7 (km)	Max SF <sub>6</sub> (p/t)	Avg SF <sub>6</sub> (p/t)	Alt. (m)	Temp (°C)	Avg. LWC (g m <sup>-3</sup> )	Wind Speed (m s <sup>-1</sup> )	Wind Dir. (° True)
3/9	15	26	15	31	58	25	2471	3.1	0.00	10	197
3/9	16	28	15	30	45	21	2475	2.9	0.00	5	215
3/16	11	1	1	38	14	8	2606	0.0	0.25	na	na
3/16	16	7	5	36	23	11	2597	-0.3	0.33	6	196
3/16	18	16	10	33	23	9	2598	0.4	0.20	13	227
Avg.		16	9	34	33	15	2549	1.2	0.16	8	209

Table 8.7. - SF<sub>6</sub> plume characteristics from site d9 as observed by aircraft for downwind track.

Date	Pass No.	Plume Width (°)	Plume Width (km)	Dist. Site d9 (km)	Max SF <sub>6</sub> (p/t)	Avg SF <sub>6</sub> (p/t)	Alt. (m)	Temp (°C)	Avg. LWC (g m <sup>-3</sup> )	Wind Speed (m s <sup>-1</sup> )	Wind Dir. (° True)
3/9	16	21	14.2	39.0	62	27	2475	3.3	0.00	10	213
3/9	17	20	13.8	38.5	43	23	2470	3.1	0.00	8	227
3/9	18	20	13.7	39.9	64	30	2480	3.1	0.00	9	228
3/16	18	11	6.7	33.9	14	8	2604	0.5	0.03	17	242
3/19	10	4	2.4	38.0	13	7	2619	2.6	0.00	15	228
Avg.		15	10.2	37.9	39	19	2530	2.5	0.01	12	228

## 8.4 Seeding Studies and Targeting Model Verification

### 8.4.1 February 17, 1993, Seeding Studies

The February 17, 1993, case will be described by example because it represents a day typical of conditions in which seeding would normally be performed, although temperatures were slightly colder than normal. Of the 4 days having both SF<sub>6</sub> and propane releases, February 17 provided the best documented case of seeding effects. On February 17, seeding was conducted (13 L h<sup>-1</sup> propane) from site d7 from 1630 to 1730 UTC and from site d9 from 1730 to 1830 UTC. Temperatures at the dispensers were near -5 °C. Radiometric liquid water averaged 0.1 mm. This is shown with other meteorological data collected at the JCC observatory on figure 8.13. Mountaintop icing data from Mt. Hough showed liquid water contents of 0.1 g m<sup>-3</sup> as shown on figure 8.14.

Of the eight aircraft intersections of the site d7 SF<sub>6</sub> plume (refer to tables 8.2 and 8.4), no definitive seeding effects were observed. Data from both aircraft liquid water probes indicated liquid water contents averaged less than 0.02 g m<sup>-3</sup>; cloud droplet concentrations averaged less than 25 per cubic centimeter within the eight plumes. Results presented in the next section indicate predicted particle trajectories may be below the aircraft sampling level.

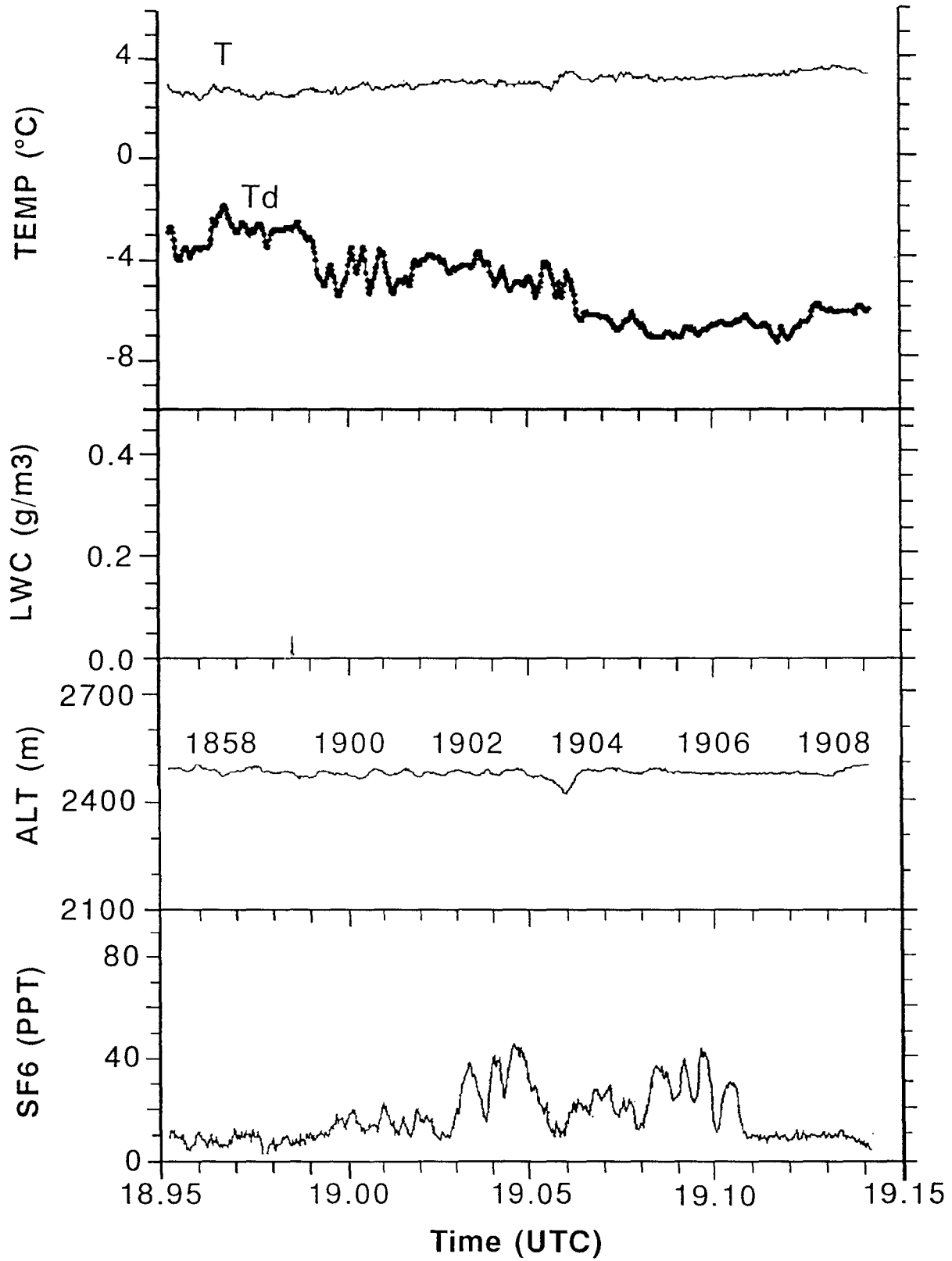


Figure 8.11. - Same as figure 8.8 but for March 9 downwind (northeast) from the flight track shown on figure 8.6. Plumes from sites d7 and d9 have merged at this downwind location.

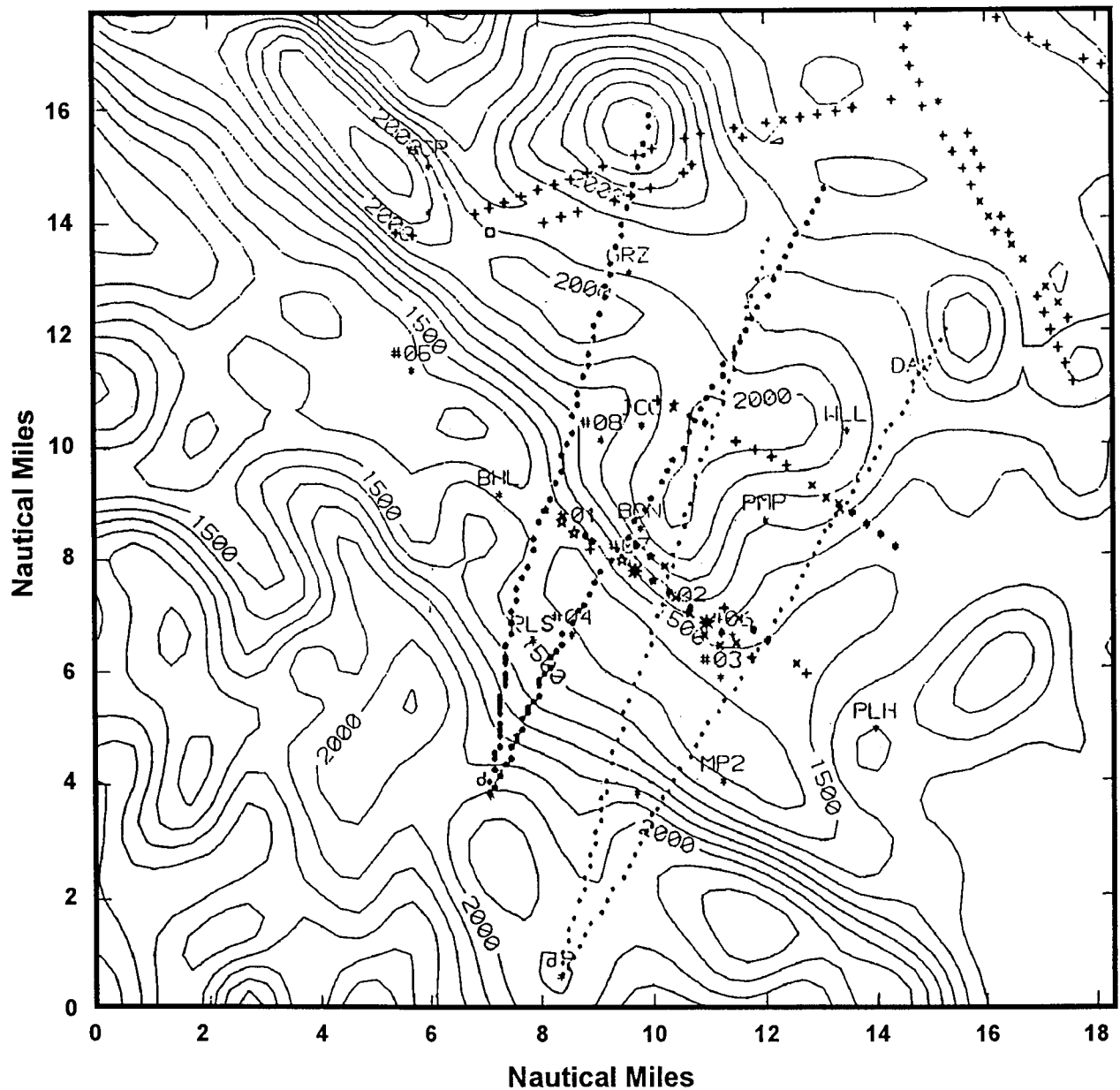


Figure 8.12. - Aircraft-observed SF<sub>6</sub> concentrations above 10 p/t plotted over target area terrain contours for March 9, 1993. GUIDE model predicted plumes from site d7 and d9 are annotated. Symbols used for SF<sub>6</sub> concentrations are: box—10 to 15 p/t, +—15 to 50 p/t, x—50 to 100 p/t, \*—100 to 150 p/t, shaded star—150 to 200 p/t, sun—200 to 250 p/t, open star—> 250 p/t. Scale along outer boundary is in nautical miles.

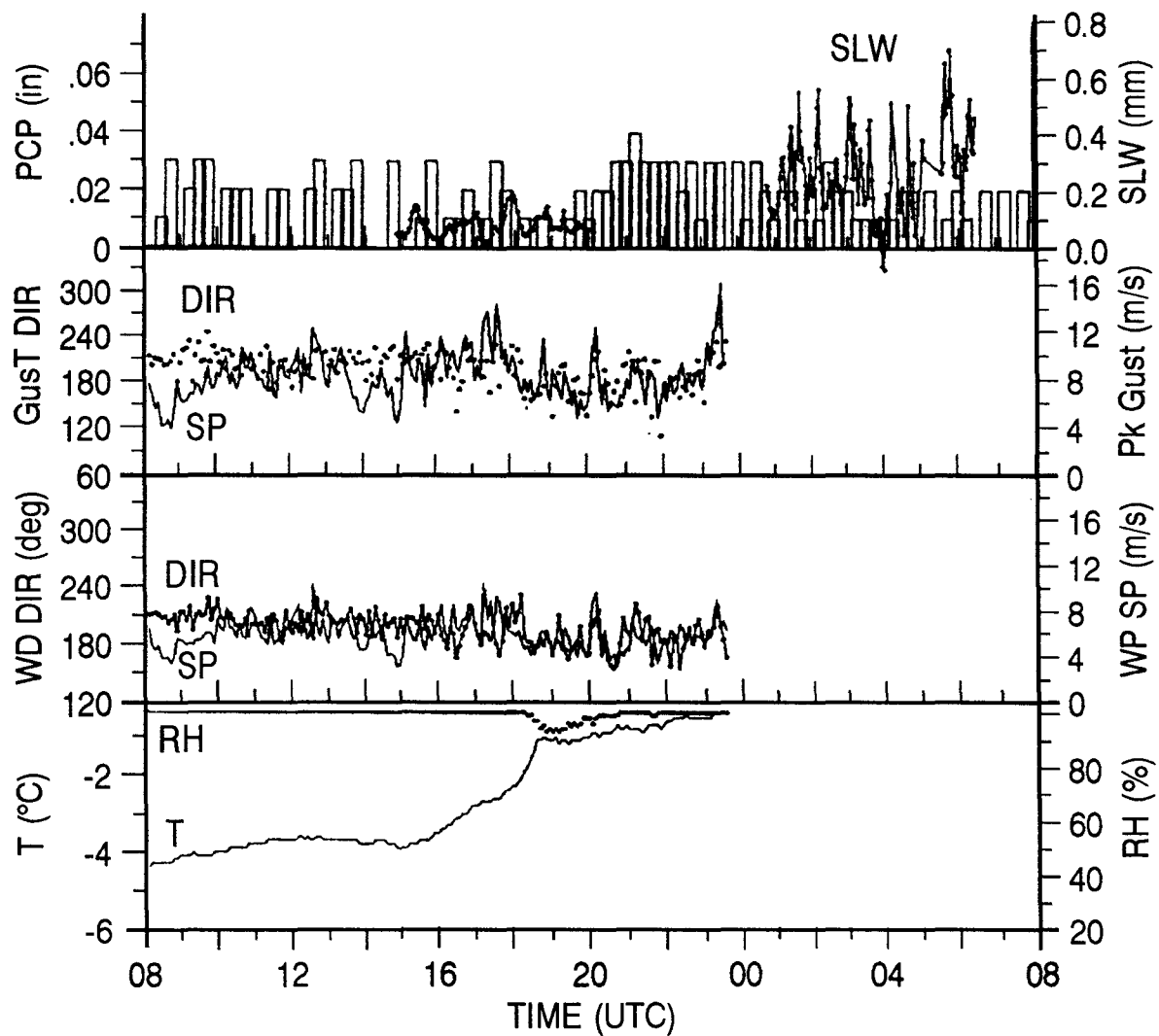


Figure 8.13. - Various parameters observed at the Jackson Creek Observatory for February 17, 1993. Parameters from top to bottom: precipitation (bar) and cloud integrated liquid water from radiometer (dotted line); peak gust direction (dotted line) and speed; average wind direction (dotted line) and speed; relative humidity (heavy); and temperature. Radiometer data deleted when contaminated. Temperature and wind data missing after 0000 UTC.

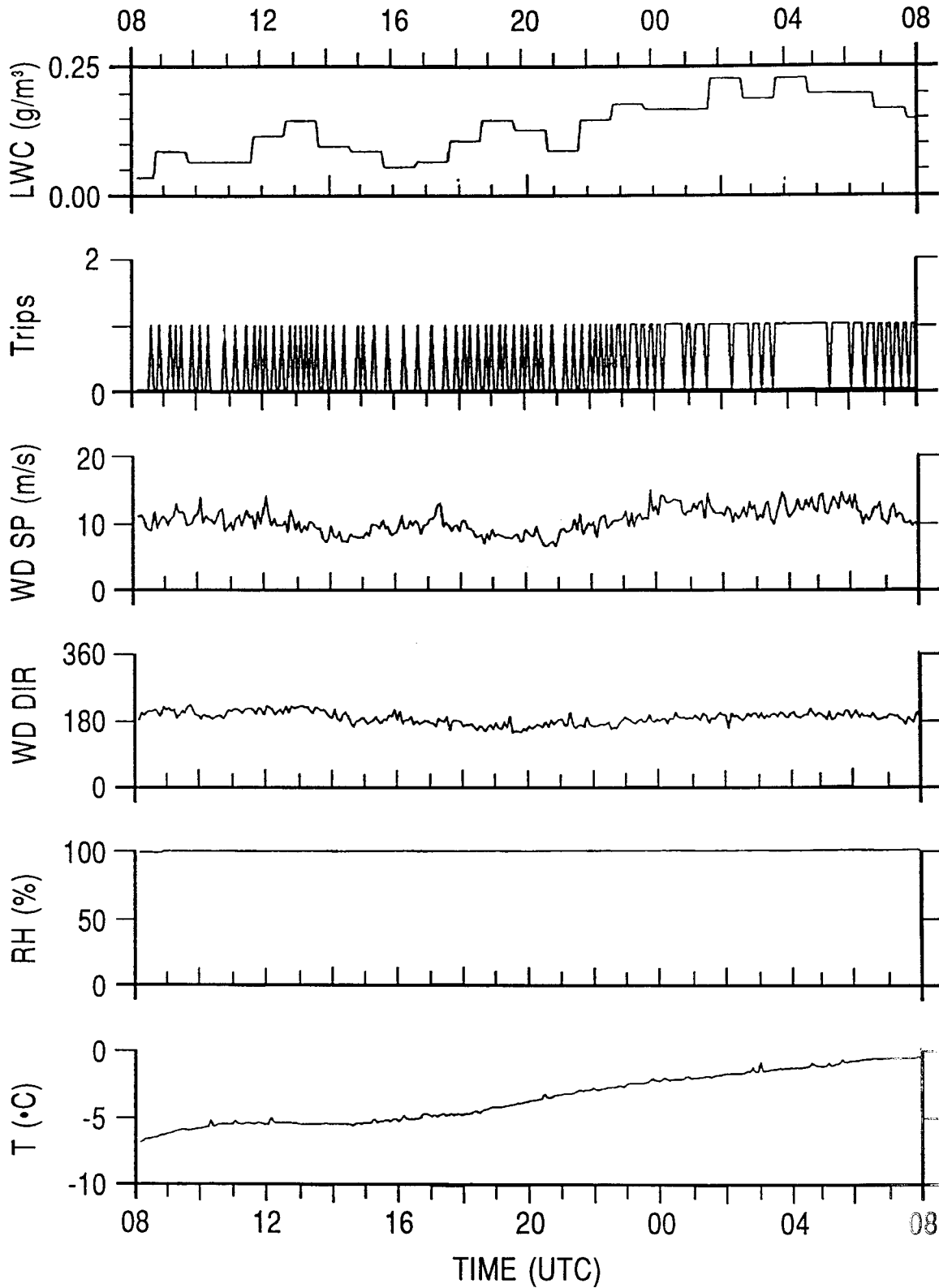


Figure 8.14. - Temporal plot of meteorological variables measured at Mt. Hough for February 17, 1993. Variables from the top down are derived hourly averaged liquid water content from ice detector trips and wind speed; ice detector trips; 1-min average wind speed; 1-min average wind direction; relative humidity; temperature.

The plume from site d9 was intersected six times (refer back to tables 8.3 and 8.5). Four had apparent seeding signatures. Liquid water contents in site d9 plumes averaged  $0.11 \text{ g m}^{-3}$ . Pass 13, along the valley, shows the most distinct seeding signature observed.

Figure 8.15 shows a well defined  $\text{SF}_6$  plume (vertical lines denote the true position of the  $\text{SF}_6$  plume) centered on a region of enhanced, but rather small ice crystals (dashed line in 2D panel are crystals  $< 250 \text{ }\mu\text{m}$ ). A distinct habit change from hexagonal to needle crystals occurred at this location. The liquid water at this location is also the highest observed on this flight.

This finding is contradictory to the glaciogenic seeding hypothesis in that seeding should reduce cloud water by growth of the enhanced ice crystals. An explanation is that seeding rates with propane are much higher than normally used for silver iodide,  $6000 \text{ g h}^{-1}$  versus  $30 \text{ g h}^{-1}$ , respectively. Because of homogenous nucleation, propane produces very rapid condensation and subsequent freezing of billions of ice crystals, releasing latent heat which can increase the cloud's buoyancy by several tenths of a degree centigrade. This additional buoyancy is realized as increased updraft in the seeded parcel of air leading to the production of additional liquid water. These results are consistent with numerical model results simulating seeding of orographic clouds with glaciogenic seeding material (Orville et al., 1984). Similar but not as impressive signatures were seen on the other three passes. This enhanced updraft may have brought seeded crystals up to the aircraft sampling level in contrast to site d7. One pass on February 9 indicated very similar results to this case as shown on figure 8.16. Although the  $\text{SF}_6$  plume is weak, the location of this seeding signature, indicated by plus (+) signs, is within the projected plume as predicted by the targeting model (fig. 8.17).

The question arises as to whether these enhanced regions of liquid water may be associated with the updraft portion of the lee wave and the enhanced ice a result of ice multiplication because both days indicated needle crystals in these regions. The purpose of releasing the tracer  $\text{SF}_6$  was to avoid any confusion between natural and artificial ice production. The signature shown for February 17 has a distinct  $\text{SF}_6$  tag. It is highly unlikely that at just this location a distinct lee wave updraft would occur and not appear anywhere else along the flight track. The signature shown for February 9 is not as definitive because the  $\text{SF}_6$  signature is not as distinct. The similarities of the two seeding effects on two different days, however, suggest that a dynamic seeding effect may be occurring.

Following Super and Boe (1988), 1-min averages (about 4.8 km of flight time) of crystal concentrations and calculated precipitation rates were made for the February 17 site d9 seeded plumes. These averages were made beginning the minute prior to entering the  $\text{SF}_6$  plume (non-seeded), the minute centered on the plume (seeded), and the minute following the plume (non-seeded), for all six plumes sampled from site d9. The mean of the six 1-min averages centered on the seeding plume showed a 33-pct increase in ice crystal concentration and an 18-pct increase in calculated precipitation rate compared to the mean of the six 1-min averages on either side.

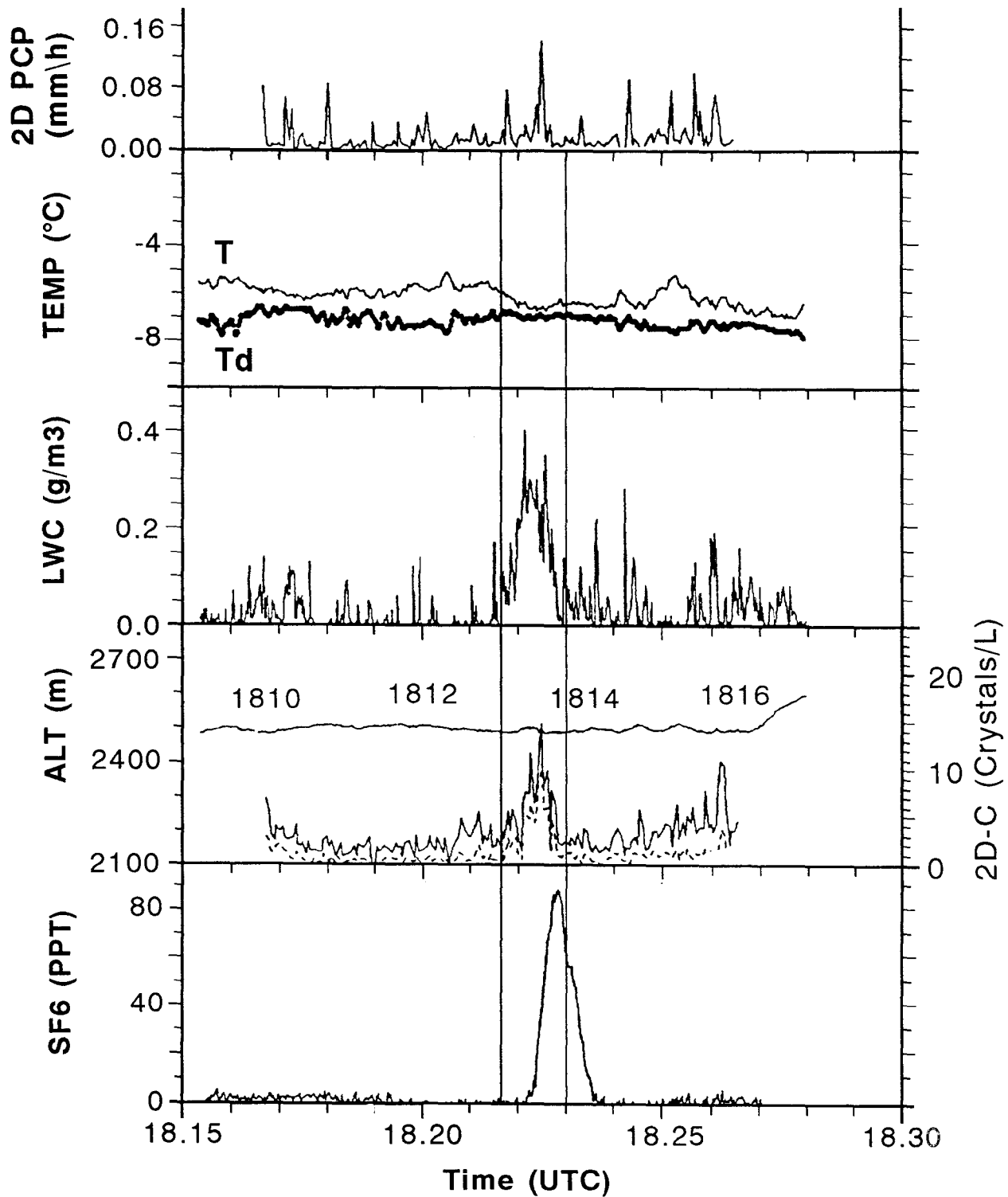


Figure 8.15. - Temporal plots of measurements made by the NOAA aircraft on pass 13 for February 17, 1993. Panels from top to bottom are: calculated precipitation rate from the ice particle probe, temperature and dew point, cloud liquid water, aircraft altitude and ice particle concentrations (total ice-solid, particles <250  $\mu\text{m}$  dashed), and SF<sub>6</sub> concentration. SF<sub>6</sub> analyzer has 11-s lag. Vertical lines denote the true position of SF<sub>6</sub>.

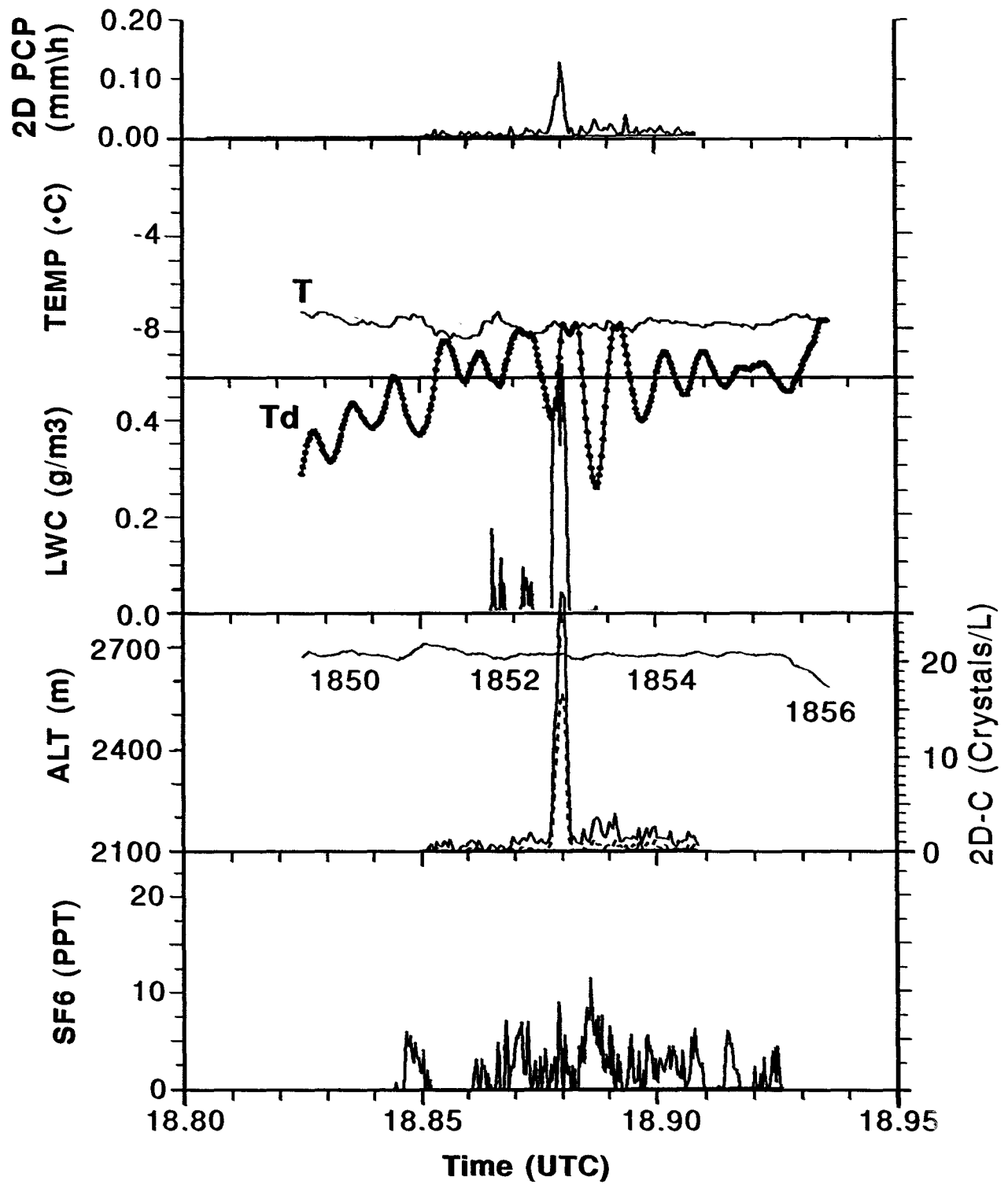


Figure 8.16. - Same as figure 8.15 but for February 9, 1993 along ridge pass for seeded plume initiated from site d7. The 11-s lag shown on figure 8.15 should be applied to the SF<sub>6</sub> trace.

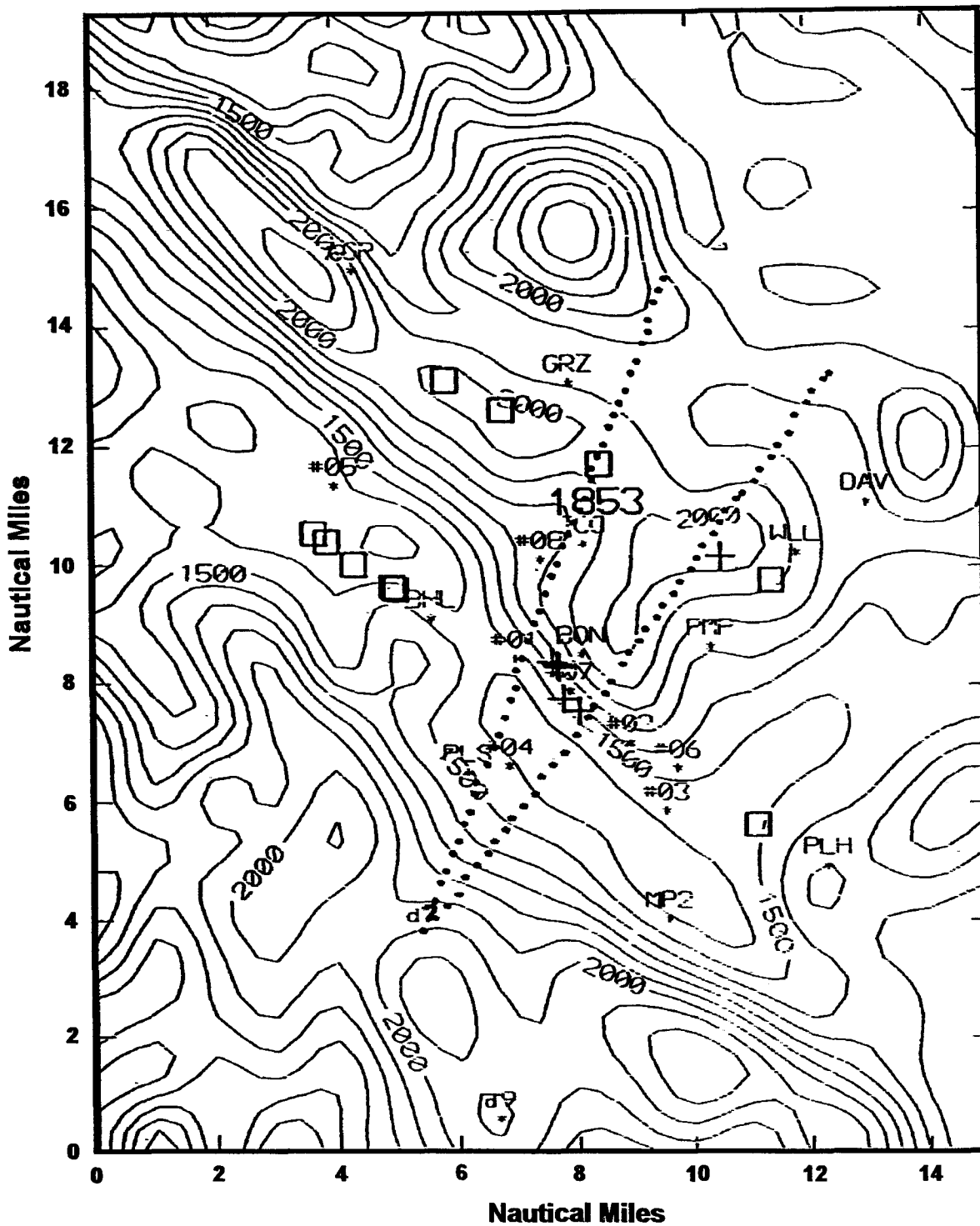


Figure 8.17. - Guide predicted plume from site d7 overlaid onto terrain contours for February 9, 1993. Aircraft observed SF<sub>6</sub> concentrations above 10 p/t noted by symbols. Seeding plume noted on figure 8.16 is annotated with the time of 1853 along the ridge pass. Boxes well outside seeding plume are noise associated with aircraft beginning or ending a turn. [box—10 to 15 p/t, +—15 to 50 p/t]. Scale along outer boundary is in nautical miles.

## 8.4.2 GUIDE Model Plume and Crystal Trajectory Simulations for February 17, 1993

The GUIDE is a simple two-dimensional kinematic model incorporating Gaussian plume dispersion (Rauber et al., 1988). The model is used operationally to predict the area of effect from seeding. The model has 5-km horizontal resolution and 100-m vertical resolution. In contrast to the method used by Rauber et al., the horizontal winds are derived by simply extrapolating the winds measured from the Johnsville rawinsonde across the model domain. Flow channels are not used. Cloud liquid water is a user input and is held constant over the model domain. Crystal growth rates and fall-speed calculations are identical to those described in Rauber et al. Vertical motions are crudely modeled by multiplying the component of the wind normal to the model terrain by the slope of the terrain between model grid points. This method of calculating vertical velocities may only be valid within a few hundred meters of the terrain. Based on the results presented in section 8.2, it may be possible to better simulate vertical motions at elevations above a few hundred meters of the terrain as will be described below.

GUIDE model predicted crystal trajectories for ice initiated from sites d7 and d9 using the 1800 UTC sounding and for site d7 only using the 2100 UTC rawinsonde data for February 17, 1993, are shown on figures 8.18a (top) and 8.18b (bottom) respectively. To account for the effects of the lee wave, the vertical velocities as shown by the up or down arrows on figure 8.18a were input to the GUIDE as shown on figure 8.19 for 1800 UTC. The balloon-observed ascent rates are held constant in the vertical over the grid box observed under the assumption that the waves are vertically in phase. Vertical motion values upwind from the crest and in the lowest 200 to 300 m above the model terrain are the model calculated values. It is important to stress that we only need to be concerned about the layer below 3200 m and, in fact, we might restrict this concern to elevations below 2500 m. Thus, to a first approximation, the simple approach of extrapolating the balloon vertical velocities for such a shallow layer seems reasonable. For the 1800 UTC data, the crystal is initiated and grows at a temperature near  $-5^{\circ}\text{C}$  in a liquid water cloud of  $0.2\text{ g m}^{-3}$ . This is the magnitude of liquid water observed by the research aircraft during sampling of the site d9 plumes. Earlier studies found very little difference in particle growth and fall speeds in the model when liquid waters vary between  $0.1$  and  $0.3\text{ g m}^{-3}$ . Below  $0.1\text{ g m}^{-3}$ , the lack of riming will extend particle trajectories several kilometers. The site d7 particle is shown to fall out about 20 km downwind in 28 min (dashed line on fig. 8.18a), at a size of just over 1 mm (needle crystal) with a maximum fall speed of  $0.75\text{ m s}^{-1}$ . The site d9 crystal also falls out at about 20 km from the dispenser in 31 min (dotted line on fig 8.18a) at a size of 1.2 mm. For 2100 UTC, the large negative vertical motions just downwind from the ridge cause the seeded crystals to fall out just 5.5 km from the site d7 dispenser (dashed line on fig. 8.18b) with very little growth having taken place ( $71\text{ }\mu\text{m}$  in 18 min).

Figures 8.20 and 8.21 reproduce the aircraft  $\text{SF}_6$  plume intersections ( $\text{SF}_6$  concentrations above 10 p/t are noted by symbols: box—10 to 15 p/t; +—15 to 50 p/t) in plan view, along with the predicted plumes from the GUIDE model, the crystal fallout locations, and the precipitation observed from 1800 UTC to 1900 UTC for sites d7 and d9 respectively. The figures show that the actual plumes are narrower than predicted and are to the left of the predicted plume track, but line up very well with the location of gauges showing higher precipitation values. The crystal fallout locations predicted by the model have been shifted to the northwest a few kilometers to match the observed plume positions.



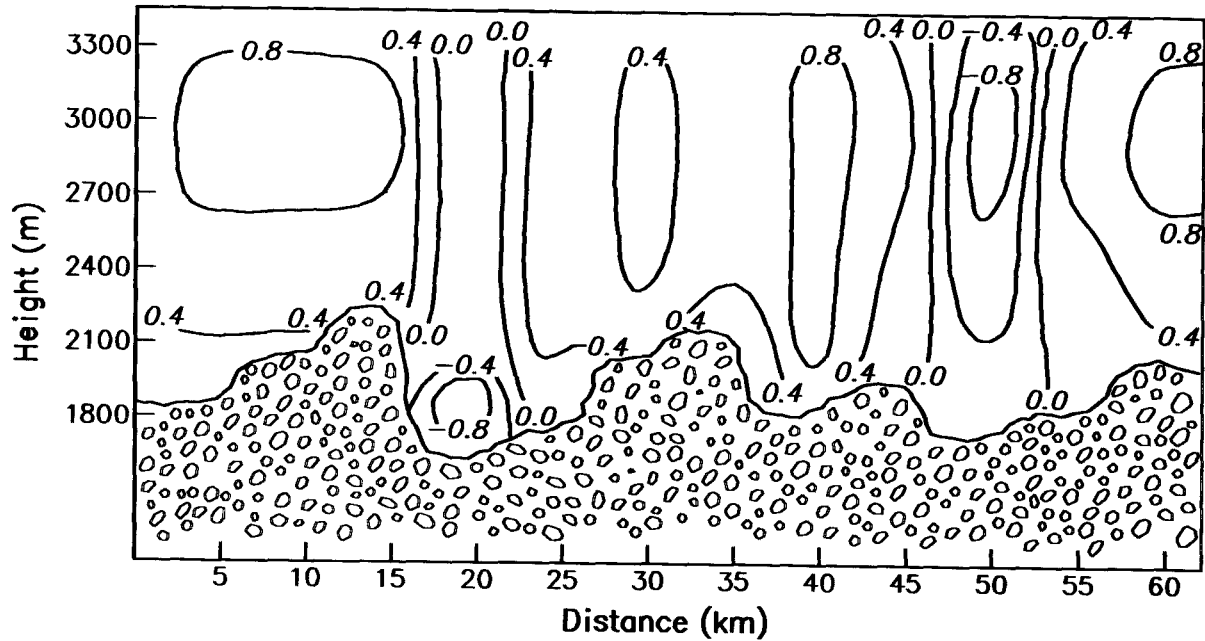


Figure 8.19. - GUIDE model contoured vertical velocities ( $\text{m s}^{-1}$ ) across the project area for 1800 UTC, February 17, 1993. Horizontal grid spacing is every 5 km. Rawinsonde derived vertical velocities are substituted from 20 to 40 km downwind except in the lowest 300 m.

This result should be considered fairly encouraging. It says that by using the rawinsonde horizontal and vertical motion fields, and with a reasonable estimate of the cloud liquid water, a relatively good estimate of crystal fallout can be achieved. This conclusion is predicated on the fact that one believes the enhanced precipitation is a direct result of seeding.

As shown, the  $\text{SF}_6$  from site d9 was on a trajectory passing over the Jackson Creek Observatory. Figure 8.22 shows that the  $\text{SF}_6$  sequential sampler (No. 8), about a kilometer west of JCC, indicated  $\text{SF}_6$  from both site d7 (1730 to 1800 UTC) and site d9 releases (1815 to 1845 UTC). However, no  $\text{SF}_6$  above background levels was observed with the continuous analyzer at the JCC Observatory. There were indications of ice crystal concentration increases on the 2-D probe at JCC during the period from 1700 to 1815 UTC of up to  $30 \text{ L}^{-1}$  above a background of  $15 \text{ L}^{-1}$ . However, these data were compromised by wind blown snow into the 2-D aspirator, thus making it difficult to quantify the magnitude of seeding effects (Deshler, 1988).

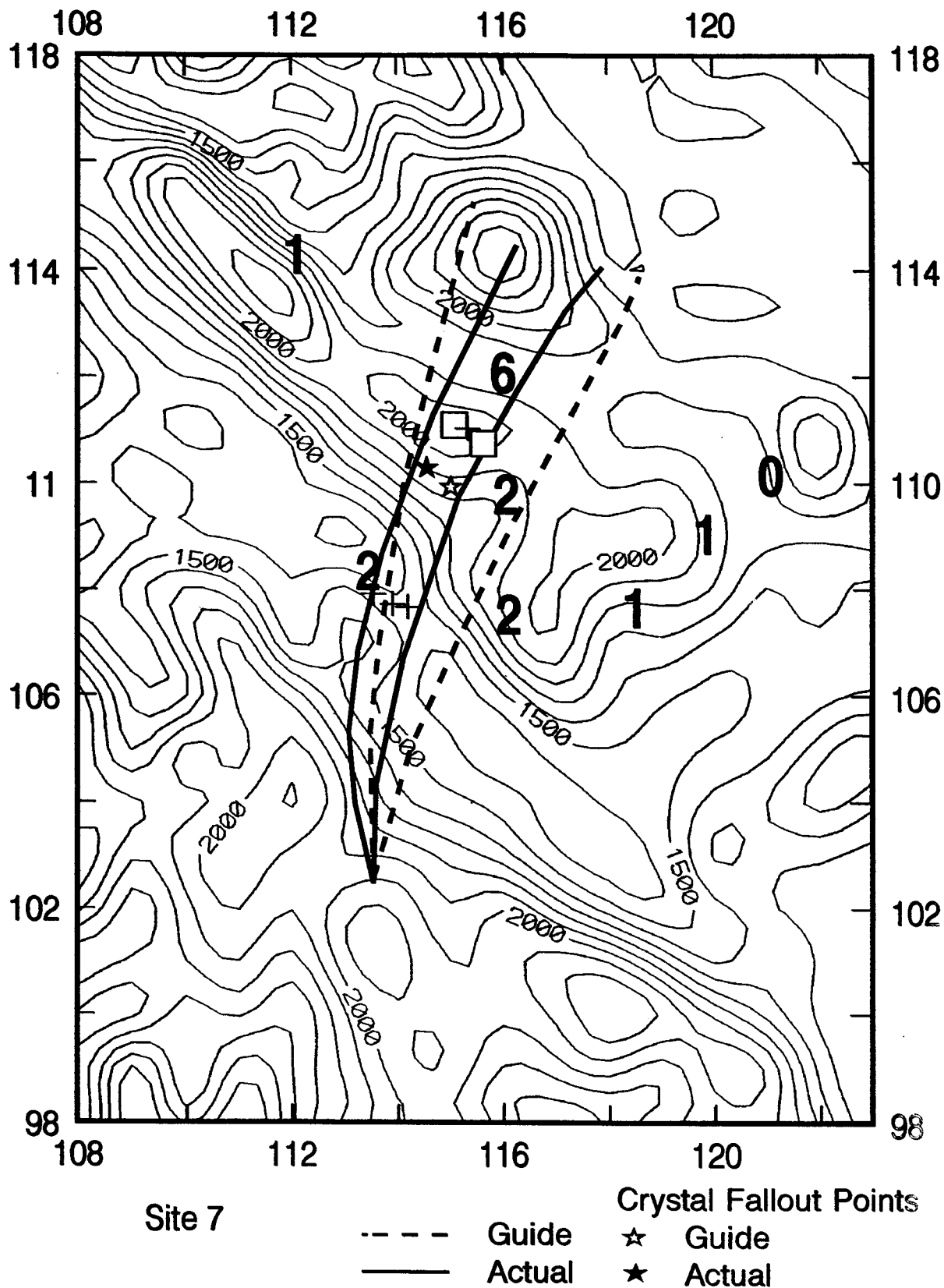


Figure 8.20. - GUIDE model predicted plume from site d7 along with actual aircraft observed SF<sub>6</sub> plume. Observed precipitation in hundredths of inches is shown for the period 1800 to 1900 UTC as large bold numbers. Model predicted crystal fallout shown by open star and corrected fallout based on aircraft plume as solid star.

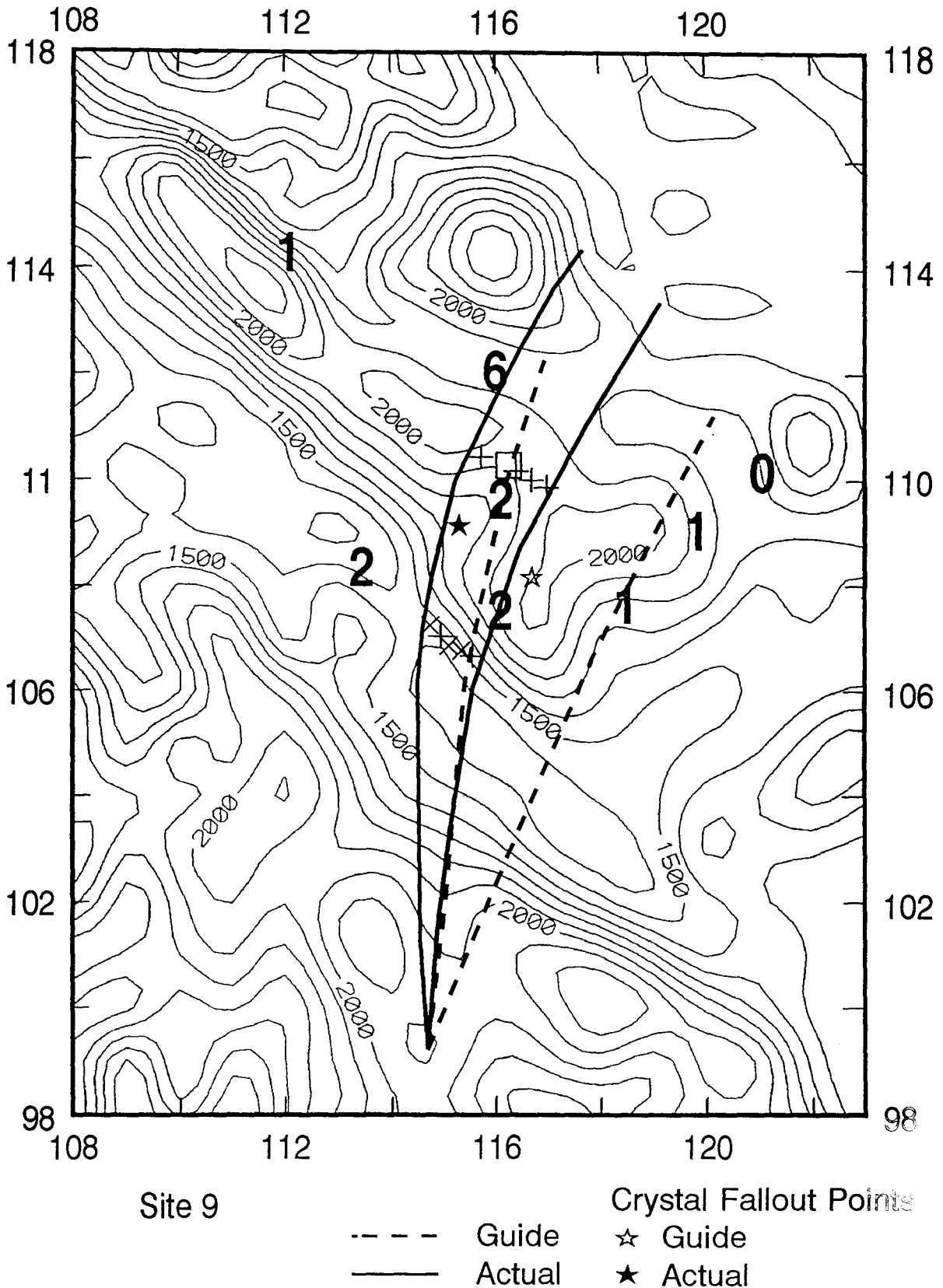


Figure 8.21. - GUIDE model predicted plume from site d9 along with actual aircraft observed SF<sub>6</sub> plume. Observed precipitation in hundredths of inches is shown for the period 1800 to 1900 UTC as large bold numbers. Model predicted fallout location for fastest falling crystal shown by open star and corrected fallout based on aircraft plume as solid star. Scale along outer boundary is in nautical miles.

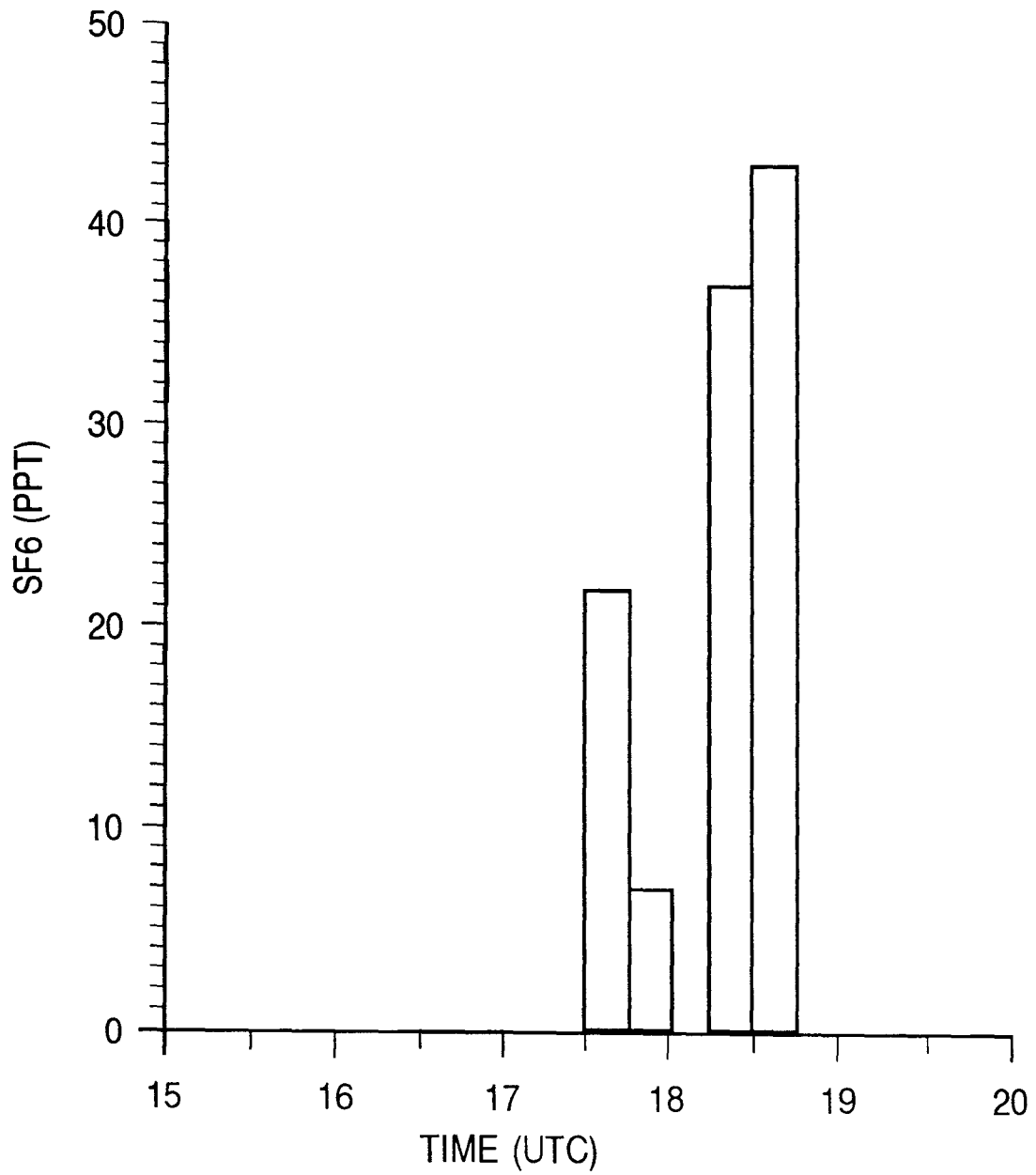


Figure 8.22. - SF<sub>6</sub> measured by sequential sampler located at site No. 8 on figure 2.3 (near JCC). First rise in SF<sub>6</sub> is from the plume from site d7 and the second rise is from the plume from site d9.

## 8.5 Summary of Lee Wave Effects Study Results

Rawinsonde balloon ascent rates and aircraft and ground-based tracer studies indicate that lee (gravity) waves are a common phenomena during winter storms to the lee of the Sierra Nevada. These data along with simple modeling studies indicate these lee waves have a significant impact on the trajectory of ice crystals produced from liquid propane seeding atop the Sierra Nevada.

The tracer SF<sub>6</sub> was released from two separate high-altitude propane dispenser sites during many winter storms over several consecutive winter seasons. SF<sub>6</sub> sampling from ground-based measurements taken 600 to 700 m below the release altitudes in a downwind valley indicate that the tracer is often observed within 30 min after start of the tracer release. Aircraft sampling of the tracer indicates the plumes rarely rose above 2700 m, or 500 m above the release altitude.

Rawinsonde balloon ascent rates have been used to calculate the magnitude of the vertical velocities within these lee gravity waves. A technique has been presented that subtracts the nominal balloon ascent rate from the observed ascent rate to infer atmospheric vertical motions across the target area. Given that the SF<sub>6</sub> and thus the ice crystals are confined to within 1000 m of the ridge top, a simple extrapolation of the balloon-derived vertical motions within this layer seems appropriate. This three-dimensional wind field is then input into a simple two-dimensional gaussian plume model (GUIDE) with empirical microphysics to infer plume dimensions and ice crystal trajectories.

On February 17, 1993, distinct seeding effects were noted by the research aircraft on five of six plumes intersected from one of the dispenser sites. This allowed comparison of GUIDE model predictions of crystal trajectories with these aircraft observations. Model predicted fallout of seeded crystals correlated well with projected fallout from aircraft observations and gauge observed precipitation increases. Precipitation at several gauges directly in line with the aircraft observed seeding plume showed a factor of two to five increase in precipitation over surrounding gauges. Apparent dynamic seeding effects were noted on several aircraft passes on this day and one other. These effects were unexpected but consistent with seeding rates used and numerical model simulations done in stratiform clouds using glaciogenic seeding agents.

This study points out the complexities associated with the transport and the successful targeting of seeding-induced ice crystals initiated over complex terrain. It shows that nearly continuous horizontal and vertical wind fields along with a vertical profile of temperature are needed to accurately predict crystal growth and fallout.

## 9. SUMMARY AND CONCLUSIONS

The LOREP was designed to be an exploratory 5-yr experiment to determine the feasibility of enhancing the winter snowpack in the Feather River basin and subsequent runoff into Oroville Reservoir. The experiment began with a feasibility study completed in 1986, which indicated that a 10- to 15-pct increase in the snowpack would lead to an economically viable amount of additional runoff. In 1987, DWR management determined that a prototype seeding program should be conducted prior to initiating a fully operational seeding program.

Based on an extensive 10-yr study carried out by the Bureau of Reclamation concerning the potential for cloud seeding in the American River Basin, the Reclamation scientist in charge of this research was asked to design and implement the LOREP. A design was completed in 1988. This design emphasized the use of ground-based seeding with an agent capable of producing ice crystals at temperatures warmer than  $-5^{\circ}\text{C}$ . The LOREP became the first wintertime cloud seeding program to use liquid propane as a seeding agent. After 2 yr of testing and evaluation of a remote liquid propane dispenser, the 5-yr program began during the winter of 1991-92.

This report has attempted to summarize the main results from the 3 yr (1991-92 through 1993-94 winter) of both in-situ physical studies and statistical analysis of precipitation data collected during 87 randomized seeding cases. The major findings from these studies are summarized in the following paragraphs.

Liquid propane released from high elevation sites has proven to be a very viable and reliable method of seeding wintertime clouds in the Sierra Nevada. Because mountain-top icing data collected over 7 yr suggest the bulk of the liquid water present in these clouds is warmer than  $-5^{\circ}\text{C}$ , liquid propane was certainly the right choice for this project. Refinement of the remote-controlled dispenser has now produced a system that required no servicing during this last winter season of operation. Appendix C provides a summary of the design and operation of this latest version of the dispenser.

Targeting of the seeded crystals produced from the propane dispenser has proven to be quite difficult. Complicating factors include the almost continuous presence of a mountain lee wave. Using the ascent rate of the project rawinsonde balloon, free air vertical velocities and thus, the presence of this lee wave, can be calculated. This wave can force crystals produced at the crest of the Sierra to rapidly descend the east side of the barrier, inhibiting the growth of the crystals to precipitation-size particles. Several years of tracer studies confirm this downward transport to the lee of the crest. This strong downward motion is most often present prior to the passage of the cold front. The pre-frontal air mass is relatively warm, and thus seeding is conducted at temperatures at or above  $-3^{\circ}\text{C}$  where crystal growth rates are very slow. Therefore, either tiny crystals are forced out of the cloud in the valley, or these crystals can be blown over the gauge network in the rising portion of the mountain lee wave.

The post-frontal air-mass appears to be much more conducive to seeding. The lighter winds and less stable, colder environment reduce the amplitude of the lee wave, allowing more growth time for the seeded crystals and thus the opportunity to produce precipitation-size particles that can fall out within the prescribed target area. Unfortunately, suitable post-frontal conditions are short lived—about 3 to 6 h—reducing the number of hours seeding might be conducted with the current configuration of dispensers and gauges.

Additional complicating factors are the wind-speed and direction variations that can take place between 6-h rawinsonde launches. Radar wind profiler data collected in the valley downwind from the dispensers has proven to be a viable method of monitoring these changing wind conditions during precipitation. Unfortunately, the profiler could not resolve vertical motions within the cloud to help refine rawinsonde vertical motion data. However, the horizontal winds produced by the profiler indicate that almost hourly monitoring of the low level winds is necessary if accurate predictions of targeting are to be produced from a model such as GUIDE. The GUIDE model does a very good job of predicting the location of seeding plumes downwind from the dispensers if the proper wind information can be input.

Based on these findings, project suspension is appropriate after 3 yr. A redesign of the project is necessary. Further field testing of various dispenser locations south and west of their current locations would be needed. This testing would include the release of the tracer SF<sub>6</sub>. Restrictions placed on the project by the Forest Service would require modification of the EIR/EIS and a possible lengthy delay.

Statistical analyses of the randomized seeding experiments have shown almost no difference in the seeded and non-seeded precipitation. Because of the small sample size, this result is not surprising, but stating that seeding had no effect on precipitation would be premature. An additional 5 yr of randomized seeding may be needed to observe a 5- to 10-pct increase in the target area precipitation. This work seems unwarranted unless the above design changes are made.

The LOREP should be considered a successful program because of its exploratory nature. Indications of positive propane seeding effects were observed, but ice crystal growth processes were relatively slow when the temperature at the dispenser sites was warmer than -5 °C. If ground-based seeding is to succeed, adequate separation of the dispensers and target gauges is necessary.

Related observations of microphysical effects of liquid propane seeding on Utah's Wasatch Plateau during early 1995 (appendix E) indicate that higher propane release rates may be appropriate for slightly supercooled temperatures, i.e., above -5 °C. Propane seeding can increase snowfall at such temperatures when excess SLW is available. The questions yet to be answered are: what release rate is required to produce significant snowfall, and is such a release rate economical? The potential importance of being able to seed slightly supercooled cloud, which is found in abundance, especially in California but throughout the intermountain West as well, is too great to ignore these questions.

If the LOREP is to be continued at some future date, detailed tracer studies from potential seeding sites should be completed prior to randomized seeding. Studies using higher propane release rates are also recommended. These studies would require both ground-based and aerial sampling to determine the vertical dispersion of the tracer and ice crystals. Sampling very close to the lee of the barrier by an aircraft equipped with an accelerometer for measuring vertical motions would be highly desirable. A modified radar wind profiler with a larger vertical beam antenna would also be beneficial. The technology to do these types of studies exists today.

## 10. BIBLIOGRAPHY

- Benner, R.L. and R. Lamb, 1985: "A fast response continuous analyzer for halogenated atmospheric tracers." *J. Atmos. and Ocean. Tech.*, 2, 582-589.
- Bruintjes, R.T., T.L. Clark, and W.D. Hall, 1994: "Interactions between topographic airflow and cloud/precipitation development during the passage of a winter storm in Arizona." *J. Atmos. Sci.*, 51, 48-67.
- Dennis, A.S., 1980: *Weather Modification by Cloud Seeding*, Academic Press, New York, 267pp.
- Deshler, T. 1988: "Corrections of surface particle probe measurements for the effects of aspiration." *J. Atmos. and Oceanic. Tech.*, 5, 547-560.
- Hall, W. 1994: personal communication.
- Hicks, J.R. and G. Vali, 1973: "Ice nucleation in clouds by liquified propane spray." *J. Appl. Meteor.*, 12, 1025-1034.
- Hindman, E.E., 1986: "Characteristics of supercooled liquid water clouds at mountaintop sites in the Colorado Rockies." *J. Clim. Appl. Meteor.*, 25, 1271-1279.
- Hogg, D.C., F.O. Guiraud, J.B. Snider, M.T. Decker, and E.R. Westwater, 1983: "A steerable dual-channel microwave radiometer for measurement of water vapor and liquid in the troposphere." *J. Climate Appl. Meteor.*, 22, 789-806.
- Hogg, D.C., M.T. Decker, F.O. Guiraud, K.B. Earnshaw, D.A. Merritt, K.P. Moran, W.B. Sweezy, R.G. Strauch, E.R. Westwater, and C.G. Little, 1983: "An automatic profiler of the temperature, wind, and humidity in the troposphere." *J. Climate Appl. Meteor.*, 22, 807-831.
- Holmboe, J. and H. Klieforth, 1957: Investigations of mountain lee waves and the air flow over the Sierra Nevada. Final Report, Contract No. AF19(604)-728, Dept. of Meteor., UCLA, 299 pp.
- Krasnec, J.P., D.E. DeMaray, B.Lamb, and R.Benner, 1984: "An automatic sequential syringe sampler for atmospheric tracer studies." *J. Atmos. Oceanic Tech.*, 1, 372-378.
- Lalas, D.P. and F. Einaudi, 1980: "Tropospheric gravity waves: their detection by and influence on rawinsonde balloon data." *Quart. J. R. Met. Soc.*, 106, 885-864.
- May, P.T., R.G. Strauch, K.P. Moran, and W.L. Eckhard, 1992: "Temperature sounding by RASS with wind profiler radars: a preliminary study." *IEEE Transactions, Geoscience Remote Sensing*, 28, pp. 19-28.
- Mielke, P.W., K.J. Berry, and G. W. Brier, 1981: "Application of Multi-Response Permutation Procedures for Examining Seasonal Changes in monthly mean sea-level pressure patterns." *Mon. Wea. Rev.*, 109, 120-126.

- Orville, H.D., R.D. Farley, and J.H. Hirsch, 1984: "Some surprising results from simulated seeding of stratiform-type clouds." *J. Climate Appl. Meteor.*, 23, 1585-1600.
- Rauber, R.M., R.D. Elliott, J.O. Rhea, A.W. Huggins, and D.W. Reynolds, 1988: "A diagnostic technique for targeting during airborne seeding experiments in wintertime storms over the Sierra Nevada." *J. Appl. Meteor.*, 27, 811-828.
- Reid, S.J., 1972: "An observational study of lee waves using radiosonde data." *Tellus*, 24, 93-596.
- Reynolds, D.W., 1988: "A report on winter snowpack augmentation." *Bull. Amer. Meteor. Soc.*, 69, 1290-1300.
- Reynolds, D.W., 1989: "Design of a ground based snowpack enhancement program using liquid propane." *J. Wea. Mod.*, 21, 29-34.
- Reynolds, D.W., 1991: "Design and field testing of a remote liquid propane dispenser." *J. Wea. Mod.*, 23, 49-53.
- Reynolds, D.W., 1992a: A snowpack augmentation program using liquid propane. Preprints, AMS Symposium on Planned and Inadvertent Weather Modification. Atlanta, GA. 88-95.
- Reynolds, D. W., 1992b: Lake Oroville Runoff Enhancement Project Annual Report of Field Activities, 1991-92. California Dept. of Water Resources, Sacramento, CA, 43pp.
- Reynolds, D. W., 1993: Lake Oroville Runoff Enhancement Project Annual Report of Field Activities, 1992-93. California Dept. of Water Resources, Sacramento, CA, 92pp.
- Reynolds, D.W., 1994: "Further analysis of a snowpack augmentation program using liquid propane." *J. Wea. Mod.*, 26, 12-18.
- Rodgers, R.R., W.L. Ecklund, D.A. Carter, K.S. Gage, and S.A. Ethier, 1993: "Research applications of a boundary-layer wind profiler." *Bull. Amer. Meteor. Soc.*, 74, 567-580.
- Shutts, G.J. and A. Broad, 1993: "A case study of lee waves over the Lake District in northern England." *Quart. J. Roy. Meteor. Soc.*, 119, 377-407.
- Shutts, G.J., P. Healy, and S.D. Mobbs, 1994: "A multiple sounding technique for the study of gravity waves." *Quart. J. R. Met. Soc.*, 120, 59-77.
- Stith, J.L., D.A. Griffith, R.L. Rose, J.A. Flueck, J.R. Miller and P.L. Smith, 1986: "Aircraft observations of transport and dispersion in cumulus clouds." *J. Climate Appl. Meteor.*, 25, 1959-1970.
- Super A.B., E.W. Holyrod III, and J.T. McPartland, 1989: Winter cloud seeding potential on the Mogollon Rim. Final Report, Arizona Department of Water Resources Intergovernmental Agreement No. IGA-88-6189-000-0051, Research and Laboratory Services Division, Bureau of Reclamation, Denver, CO, 173 pp.

- Super, A.B. and B.A. Boe, 1988: "Microphysical effects of wintertime cloud seeding with silver iodide over the Rocky Mountains. Part III: observations over the Grand Mesa, Colorado." *J. Appl. Meteor.*, 27, 1166-1182.
- Super, A.B., 1990: "Winter orographic cloud seeding status in the intermountain west." *J. Wea. Mod.*, 22, 106-116.
- Sward, S, 1991: "New Propane Experiment in Sierra Cloud Seeding," *San Francisco Chronicle*, December 6, 1991.
- Swart, H.R., D.A. Griffith, G.W. Wilkerson, E.B. Jones, and C.F. Lear, 1986: Feather River Basin Cloud Seeding Feasibility Study, NAWC Report WM-86-5 for California Department of Water Resources.



## **APPENDIX A**

### **LOREP Cost Estimates for FY94 Field Program and FY95 Report**



Part 1 Field operations and analysis

SECTION 1: Bureau of Reclamation costs FY94

A. Personnel	# months	\$/month	total cost	
1.) D. Reynolds	9	\$5,808	\$52,272	
2.) Staff support Denver	2	\$4,350	\$8,700	
Reynolds overhead factor (130%)			\$67,954	
Denver overhead factor (173%)			\$15,051	
USBR contract costs for July to Sept. 1993			\$22,935	
SUBTOTAL (A)	11		\$166,912	
B. Other costs				total cost
1.) Travel and per diem (60 days * \$66/day)			\$3,960	
2.) Supplies			\$1,300	
3.) Equipment maintenance			\$3,000	
4.) Propane for Mtn. Observ.			\$2,000	
SUBTOTAL (B)			\$10,260	
TOTAL (A & B)				\$177,172

DWR FY93-94 Funds needed by USBR: \$138,613

DWR FY94-95 Funds needed by USBR: \$38,559

SECTION 2: Field support contract (North American Weather)

1.) Personnel	# months	\$/month	total cost	
(a.) NAWC staff	3	\$3,200	\$9,600	
(b.) Local hire	3	\$1,500	\$4,500	
Overhead 110% reg. labor			\$10,560	
Overhead 30% temp. labor			\$1,350	
SUBTOTAL LABOR	6		\$26,010	
2.) SF6 Continuous Analyzer & CAL Gases			\$3,900	
3.) Insurance on Bureau equipment			\$500	
4.) Travel/per diem 4WD vehicle			\$6,000	
5.) Sequential Samplers (2) and Flow Controller (1)			\$1,600	
6.) Miscellaneous supplies and communication			\$2,000	
SUBTOTAL NON-LABOR			\$14,000	
TOTAL DIRECT COST			\$40,010	
General Administrative (15%)			\$6,002	
TOTAL WITHOUT FEE			\$46,012	
Fee (10%)			\$4,601	
TOTAL NAWC CONTRACT AMOUNT				\$50,613
TOTAL PART 1				\$227,784

Part 2 Equipment

ITEM	#	unit cost	total cost	
1. Ground seeding dispensers				
(a.) Remote propane dispenser (misc.)	10	\$200	\$2,000	
(b.) Solar panels (Bur. provided)	20	\$400	\$0	
2. Ground Microphysics Lab (Bureau provided)				
(a.) Aspirated 2D-C	1	\$85,000	\$0	
(b.) Photomicrographic equipment	20	\$5,000	\$0	
TOTAL PART 2				\$2,000

Part 3 Operational costs

SECTION 1: Precipitation gauge network operation (DWR personnel)

A. Personnel	# months	\$/month	total cost
1.) Beckwourth Operations	0.5	\$5,544	\$2,772
2.) Oroville control tech.	0.1	\$5,544	\$554
Overhead (100%)			<u>\$3,326</u>
SUBTOTAL (A)	<u>0.6</u>		<u>\$6,653</u>
B. Supplies			
1.) Antifreeze			\$1,325
2.) Spare parts and repairs			<u>\$1,000</u>
SUBTOTAL (B)			<u>\$2,325</u>
C. Fee for Use permits			\$500
TOTAL SECTION 1			\$9,478

SECTION 2: Ground Seeding Dispenser operation & misc. field work (DWR personnel)

A. Personnel (Install. & maint.)	# months	\$/month	total cost
1.) Oroville control tech.	0.9	\$5,544	\$5,156
2.) Oroville civil maint.	1.3	\$5,544	\$6,930
3.) Comm. eng. (Gen. Serv.)	0.1	\$7,392	\$739
4.) Radio tech. (Gen. Serv.)	0.2	\$7,392	\$1,478
5.) Beckwourth Operations	1.2	\$5,544	\$6,653
Labor Overhead (100%)			\$20,956
Travel and overtime			<u>\$6,000</u>
SUBTOTAL (A)	<u>3.7</u>		<u>\$47,913</u>
B. Supplies (contract)			total cost
ITEM			
1.) Propane and methanol (20 tanks * 350gal./tank * \$1.11/gal.)			\$7,770
2.) Propane tank rental (21 tanks * \$55/tank)			\$1,155
3.) Parts and maintenance			\$2,500
4.) 12 Cyl. SF6 Gas			\$14,000
5.) Trailer for Mtn. Obs.			<u>\$2,000</u>
SUBTOTAL (B)			<u>\$27,425</u>
C. Transportation			
1.) Helicopter (contract)			
(a.) Site install and remove			\$40,000
(b.) Field maintenance (20 hrs. * \$400/hr.)			<u>\$8,000</u>
SUBTOTAL (C)			<u>\$48,000</u>
D. Annual Fee for Use Permits (Forest Service)			\$500
E. Annual Report publication charges			\$500
TOTAL SECTION 2			\$124,338

SECTION 3: Rawindsonde Operation (Contracts)

A. Contractor and Oroville staff	# months	\$/month	total cost
1.) State Park (Johnsville)	1.1	\$5,682	\$6,250
2.) Civil Maintenance	0.4	\$6,098	\$2,439
Overhead (Civil) 100%			<u>\$8,689</u>
SUBTOTAL (A)	<u>1.5</u>		<u>\$17,379</u>

B. Supplies (Purchase Order)

	total cost
1.) Sondes, Balloons, Helium, Lights (75 launches * \$125/launch)	\$9,375
2.) Parts and Maintenance	<u>\$1,000</u>
SUBTOTAL (B)	\$10,375
TOTAL SECTION 3	\$27,754

SECTION 4: Icing Station operation (DWR personnel)

A. Personnel	# months	\$/month	total cost
1.) Oroville control tech.	0.75	\$5,544	\$4,158
2.) Oroville civil maint.	0.05	\$6,098	\$305
3.) Beckwourth Operations	0.10	\$5,544	\$554
Overhead (100%)			<u>\$5,017</u>
TOTAL SECTION 4	<u>0.90</u>		\$10,035

SECTION 5: Forecast Support and seeding directions (DWR personnel)

A. Personnel	# months	\$/month	total cost
1.) Meteorologist (Flood mgmt.)	6.0	\$4,200	\$25,200
Overhead (100%)			\$25,200
Travel and per diem			<u>\$2,000</u>
TOTAL SECTION 5	<u>6.0</u>		\$52,400

SECTION 6: Environmental studies (Northern Dist.)

A. Personnel	# months	\$/month	total cost
1.) Program management	1.0	\$5,216	\$5,216
2.) Environmental monitoring			
(a.) Rare plants Environmental specialist	0.4	\$4,884	\$1,954
(b.) Water quality & sedimentation Environmental specialist	2.0	\$4,884	\$9,768
(c.) Wildlife and fisheries Environmental specialist	1.4	\$4,884	\$6,838
(d.) CRMP participation	1.1	\$4,884	\$5,372
(e.) Biological assessment	1.2	\$4,884	\$5,861
(f.) Annual report	0.4	\$4,884	\$1,954
Overhead on labor (100%)			<u>\$36,962</u>
SUBTOTAL LABOR	<u>7.5</u>		\$73,924
			total cost
3.) Travel and per diem (90 days * \$84/day)			\$7,560
4.) Laboratory fees			\$28,176
5.) Supplies			<u>\$3,600</u>
SUBTOTAL NON-LABOR			\$39,336
TOTAL SECTION 6			\$113,260
TOTAL PART 3			<u>\$337,264</u>
COMBINED TOTAL (PARTS 1, 2 & 3)			<u>\$567,048</u>



## **APPENDIX B**

### **Suspension Criteria**



The following information describes criteria that if met, will suspend seeding prior to serious flooding situations.

### B.1 Excess Snowpack Water Equivalent

When the water content of the snowpack in the Feather River Basin, as measured at 25 identified snow courses, exceeds the accumulation defined by the following percentage of April 1 average amounts on:

January 1	110 percent
February 1	130 percent
March 1	150 percent
April 1	160 percent

Mid-month snow water content will be estimated from automatic snow sensors in the basin based on sensor change from the first of the month.

### B.2 Rain-Induced Winter Floods

When quantitative precipitation forecasts issued by the NWS (National Weather Service) or the Rhea QPF (Quantitative Precipitation Forecast) model would produce excessive runoff in the project area or downstream areas as determined by the Flood Forecasting staff of the DWR (Department of Water Resources). The following information constitutes criteria that were used as indicators of potential flooding:

- a. 60,000 ft<sup>3</sup>/s or more would be considered excessive inflow to Oroville Reservoir.
- b. Whenever Oroville Reservoir is encroached into flood control space and releases are being made at the spillway of Oroville Dam (normally releases in excess of about 20,000 ft<sup>3</sup>/s, most of which can pass through the power plant).
- c. Whenever flood flows or stages are occurring or forecast to occur which exceed flood warning stages on the Feather River below Oroville:
  - River stages near Gridley at or over 95 feet.
  - River stages at Yuba City at or over 65 feet.
  - River stages at Nicolaus at or over 43 feet.
- d. Whenever precipitation at Quincy is predicted or observed to exceed 4 inches in 24 hours, 5 inches in 48 hours, or 6 inches in 72 hours, or, for back up, the gauge at La Porte reports 5 inches in 24 hours, 6 inches in 48 hours, or 7 inches in 72 hours.

### B.3 Severe Weather

Whenever the NWS has issued a flash flood warning for the project area.

### B.4 Other Special Circumstances

The DWR Project Manager feels conditions are or may be perceived to be so hazardous as to warrant suspension of seeding. This circumstance may include the issuance of avalanche warnings within the project area.



## **APPENDIX C**

### **Liquid Propane Dispenser Design Documentation**



## **Dispenser Hardware Configuration**

The hardware configuration of the liquid propane dispenser is shown on figure C.1. The hardware specifications for the individual components are given in table C.1. This design used an Odessa Engineering model DSM 3260 data logger/controller; however, any data acquisition unit capable of data collection and external hardware control via a standard voice-band radio channel could be used.

Because of nozzle clogging concerns, early designs of the dispenser used three dispensing nozzles. Any nozzle could be selected through a valve/manifold arrangement. Field use of the dispenser showed that nozzle clogging was not a problem and the valve/manifold was eliminated, leaving a simpler and more reliable configuration. Early designs also experienced propane supply line freeze-up. The copper tubing was insulated using foam and reflective tape and was connected directly from the propane tank to the valve box at the top of the tower to completely eliminate supply line freeze-up.

The dispenser was solar-powered, using three 45-watt solar panels and one 105-amp-hr deep cycle battery. Two panels were oriented toward the south with the appropriate back-tilt. The third panel was mounted on the back of the first two panels and was oriented downward. This downward pointing solar panel was shown to be necessary to keep the battery charged when the other two panels became iced or covered with snow.

The final design used a radio antenna capable of operating during severe icing conditions.

The complete liquid propane dispenser system, including two 2,176-liter (575-gal) propane tanks, was mounted on a metal pallet that was helicoptered to the site as a single unit.

## **Dispenser Operation**

When seeding conditions were right (ambient air temperature below 0 °C and liquid water present), the mountaintop dispensers would be turned on remotely from Sacramento through the State of California, Department of Water Resources microwave radio system. Confirmation of liquid propane release was determined when the nozzle temperature dropped below -30 °C. Each dispenser would log propane flow rate and temperatures. By logging flow rate and dispensing time, total propane used for the season and the amount of remaining propane was known. Each unit would dispense liquid propane for 6 hours and turn off automatically unless dispensing was terminated manually or another 6 hour seeding block was requested. Automatic turn-off is important because radio communication may intermittently be lost due to severe weather conditions on the mountaintop. Each unit was automatically polled every hour by the computer in Sacramento. The computer kept daily statistics on data received from each dispenser.

Table C.1. - Liquid propane dispenser hardware specifications.

Filter: PACA, Inc - Sacramento CA 95828

Filter lock-off  
Model 5000-12  
12-V dc  
6 W  
LPG filter lock-off  
LP Gas WP312 lb/in<sup>2</sup>

Valve: Honeywell skinner valve

valve number: V5RBM58440  
12-V dc  
15 W  
body orifice: 3/32 in  
pressure: 125 lb/in<sup>2</sup>  
20% duty cycle  
coil: DC1-A3K  
code OH2

Flowmeter: FloScan Instrument Co. Inc

Model Number: 3005  
Transducer Type: 201B-18  
Output span: 0.6 to 60 gal/h  
Calibration: 5 V = 1422 Hz = 60 gal/h  
Analog Range Max: 5 V = 2600 Hz  
Analog Range Min: 5 V = 800 Hz

Nozzle: LNN3 Brass

Antennas: Sinclair Model SRL-2010C and  
Motorola Model TAD 1003

Data logger/controller: Odessa Engineering  
Model DSM 3260

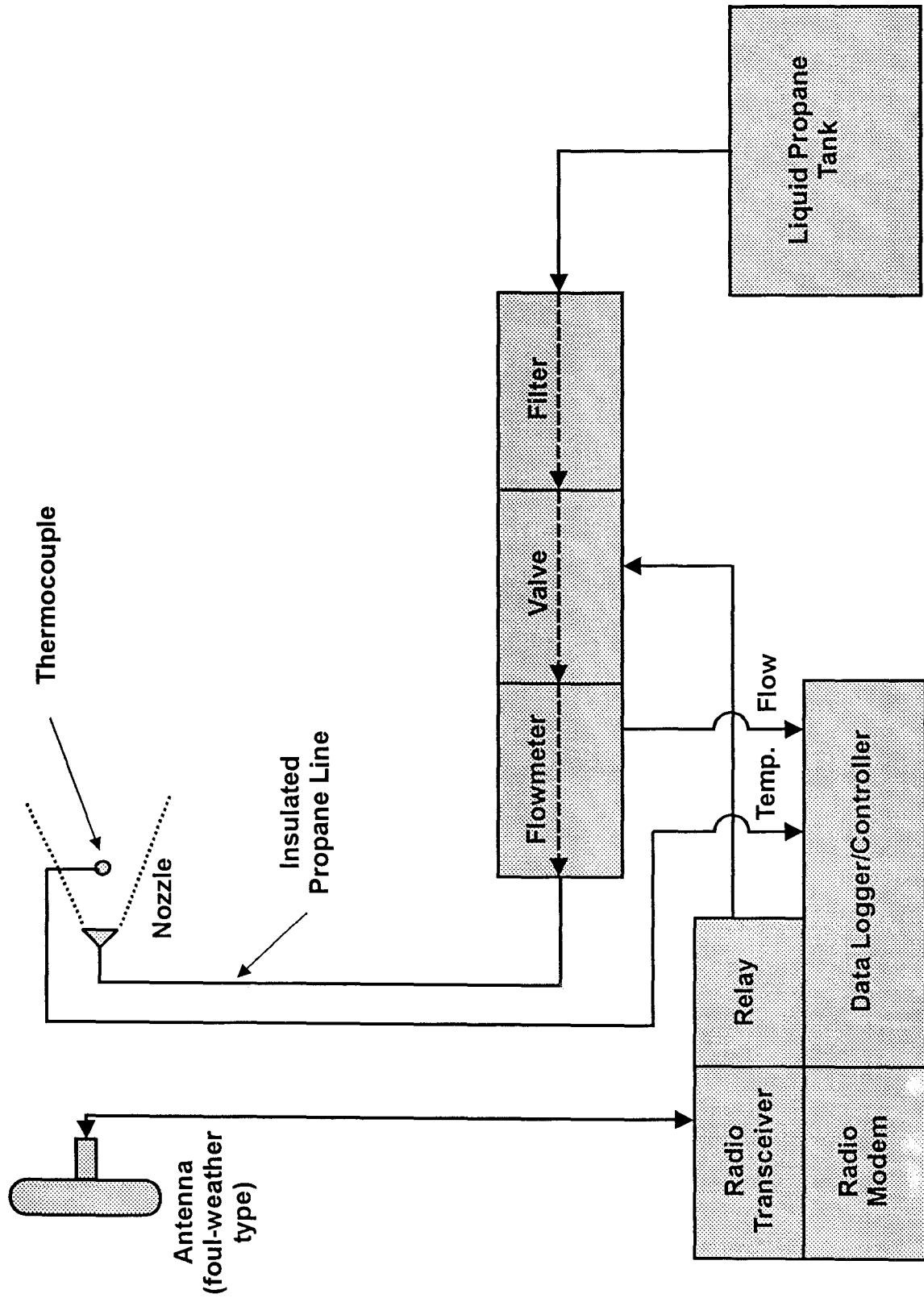


Figure C.1. - Liquid propane dispenser configuration.



## **APPENDIX D**

### **Calculations for Estimating Increased Runoff from an Augmented Snowpack in the Middle Fork Feather River Catchment Area**



An "estimate" is given of the increase in precipitation rate that is expected from seeding the cold winter storms to augment the snowpack in a part of the Middle Fork Feather River selected as the project area for a prototype program. The reader is cautioned that this estimate is considered to be the most reasonable increase that might be expected, but for any given storm and for any given period within a storm, the magnitude of the increase might vary from near zero increase to up to three times the increases discussed here. However, on the average and during most storm episodes, the values given here will apply. In addition, total estimated runoff for a fully operational prototype program is provided. The following estimated increases in the precipitation rate from seeding winter clouds with liquid propane are based on a recent review article by Reynolds (1988) and on laboratory and theoretical studies of the effectiveness of propane as a seeding agent (Hicks and Vali, 1973).

### 1. Ice Nuclei Flux per Dispenser

Based on the expected release rate of liquid propane and the number of ice crystals produced per gram of liquid propane (effectiveness), the flux (number of crystals/time) of ice crystals can be determined.

Expected release rate per dispenser per hour = 2.5 gal/h

$$2.5 \text{ gal/h} \times 4.23 \text{ lb/gal} \times \frac{1000 \text{ g}}{2.2 \text{ lb}} = 4807 \text{ g/h propane}$$

Based on the work of Hicks and Vali (1973), for every gram of liquid propane dispensed,  $10^{12}$  ice nuclei are created.

$$4807 \text{ g/hr} \times 10^{12} \text{ crystals/g} = 4.81 \times 10^{15} \text{ crystals/h}$$

$$4.81 \times 10^{15} \text{ crystals/h} \times \frac{1 \text{ h}}{3600 \text{ s}} = 1.34 \times 10^{12} \text{ crystals/s}$$

Assuming each crystal will grow in the presence of supercooled liquid water and fall out, after 1000 seconds (17 min), the crystals should reach a size of 500  $\mu\text{m}$  and obtain a mass of  $5 \times 10^{-6}$  g/crystal.

$$\begin{aligned} \text{"mass flux water"} &= 1.34 \times 10^{12} \text{ crystals/s} \times 5 \times 10^{-6} \text{ g/crystal} \\ &= 6.70 \times 10^6 \text{ g/s} \end{aligned}$$

This result can be converted to acre-ft/h per dispenser:

$$6.70 \times 10^6 \text{ g/s} \times 3600 \text{ s/h} \times 1 \text{ cm}^3/\text{g} \times \frac{1 \text{ in}^3}{16.387 \text{ cm}^3} \times \frac{1 \text{ ft}^3}{1728 \text{ in}^3} \times \frac{1 \text{ acre}}{4.356 \times 10^4 \text{ ft}^2} = 19.5 \text{ acre-ft/h/dispenser}$$

### 2. Precipitation Rate Increase

Distributing the mass of precipitation over a given area will allow calculation of an augmented precipitation rate based on seeding with liquid propane.

Reynolds (1988), showed that a lateral plume spread of about 15 degrees can be expected from a single dispenser. Based on crystal size and fall speed, crystals will be expected to fall out within 30 km downwind from the dispenser.

$$\text{Area} = (30 \text{ km})^2 \tan 7.5 \text{ degrees} = 118 \text{ km}^2$$

APR (augmented precipitation rate) = seeding rate x mass/crystal x 1/area of effect:

$$\text{APR} = 4.8 \times 10^{15} \text{ crystals/h} \times 5 \times 10^{-6} \text{ g/crystal} \times \frac{1}{118 \text{ km}^2} \times \frac{1 \text{ km}^2}{1 \times 10^{10} \text{ cm}^2} \times \frac{10 \text{ mm}}{1 \text{ cm}} \times \frac{1 \text{ cm}^3}{\text{g}} = 0.20 \text{ mm/h}$$

or:

$$\text{APR} = 0.20 \text{ mm/h} \times \frac{1 \text{ in}}{25.4 \text{ mm}} = 0.008 \text{ in/h}$$

Best Estimate APR = 0.01 in/h

### 3. Snowfall Increase

Using an estimate for APR of 0.01 in/h and a simple 10 to 1 snow depth to water equivalent ratio, the ASR (augmented snowfall rate) will be:

ASR = 0.1 inch of snowfall/h

### 4. Augmented Storm Totals and Seasonal Totals

#### a. Storm Total

Assuming 8 h/storm are treated:

Total augmented precipitation = 1.6 mm/storm water equivalent or 0.08 in/storm water equivalent

Snowfall Increase ~ 0.8 in/storm

#### b. Seasonal Total

Assuming 40 storms/season:

Total seasonal water equivalent/dispenser/season = 1.6 mm/storm/dispenser  
 = 64 mm/dispenser/season  
 (or 2.5 in/dispenser/season)

Snowfall increase ~ 32 in/season

c. Using acre-feet/dispenser and a total of 10 dispensers:

$$\begin{aligned} \text{Augmented Precipitation over Watershed} &= \\ 20 \text{ acre-ft/dispenser/h} \times 10 \text{ dispensers} \times \\ 8 \text{ h/storm} \times 40 \text{ storm/season} &= 64,000 \text{ acre-ft/season} \end{aligned}$$

Operating under proposed suspension criteria and 3:1 randomization is expected to reduce this potential increase by 50 percent or, on average, the expected increase is 32,000 acre-ft/season.

Assuming 70-percent runoff (Swart et al., 1986) of the augmented precipitation:

$$32,000 \times 0.70 = 22,400 \text{ acre-ft runoff in Oroville}$$



**APPENDIX E**

**Observations of Microphysical Effects of Liquid Propane Seeding  
on Utah's Wasatch Plateau during Early 1995**

by  
Arlin B. Super

Bureau of Reclamation  
Denver, CO



## **E.1 Introduction**

A series of limited cloud seeding experiments was conducted from December 13, 1994, through March 11, 1995, on the Wasatch Plateau (hereafter Plateau) of central Utah. The primary purpose of the experiments was to investigate the ability of AgI (silver iodide) to create significant ice particle concentrations within orographic (mountain-induced) cloud at slightly supercooled temperatures. However, a secondary purpose was to document microphysical effects of high altitude liquid propane seeding. The evidence obtained from a limited number of liquid propane seeding experiments is the subject of this report.

The experiments were simple in design. Liquid propane was released in 1-h "pulses" from a single HAS (High Altitude Site) on the Plateau's windward (west-facing) slope. Microphysical effects of the propane seeding were observed at a fixed downwind site (the Target) on the Plateau top's west edge. Both sites are indicated on figure E.1. Instruments at the Target permitted verification that propane-seeded cloudy air passed by the Target, and permitted monitoring of ice particle characteristics before, during, and after each passage of seeded air (each pulse). Various instrumentation at both sites provided supporting measurements of wind, air temperature, and the presence of SLW (supercooled liquid water).

## **E.2 Experimental Equipment**

The HAS propane dispenser was based on the design of Reynolds (1989, 1991) as described by Super et al. (1995). Liquid propane was released at about  $6000 \text{ g h}^{-1}$  ( $3 \text{ lb h}^{-1}$ ) through a single spray nozzle which chilled a limited volume of SLW cloud below  $-40 \text{ }^\circ\text{C}$ . High concentrations of ice crystals were formed in this chilled volume by condensation of very tiny liquid droplets, which immediately froze into embryonic ice particles.

Laboratory estimates by Hicks and Vali (1973) indicated the effectiveness or yield (ice crystals produced per gram) of liquid propane is about  $3 \times 10^{11}$  ice crystals  $\text{g}^{-1}$  at temperatures colder than  $-2 \text{ }^\circ\text{C}$  with yield decreasing to  $10^{10}$  crystals  $\text{g}^{-1}$  near  $0 \text{ }^\circ\text{C}$ . However, laboratory work by Kumai (1982) indicated near  $10^{11}$  crystals  $\text{g}^{-1}$  at temperatures colder than  $-5 \text{ }^\circ\text{C}$  and an exponential decrease at warmer temperatures to only  $10^8$  crystals  $\text{g}^{-1}$  near  $0 \text{ }^\circ\text{C}$ . Estimates based on field measurements by Hicks and Vali (1973) were more variable. However, they concluded, "Thus, it can be stated that the liquefied propane will produce  $10^{12}$  crystals per gram of propane under average conditions and at temperatures colder than  $-2 \text{ }^\circ\text{C}$ . Particular circumstances may lead to approximately tenfold increases or decreases in efficiency."

The California seeding program described by Reynolds (1989) was based on the  $10^{12}$  crystals per gram propane yield claimed by Hicks and Vali (1973). However, published yields show enough variability to justify further field testing, especially at temperatures warmer than  $-5 \text{ }^\circ\text{C}$ , where AgI is expected to be ineffective. Observations at several mountain locations in California (e.g., Reynolds, 1989) and the intermountain West (e.g., Sassen and Zhao, 1993) have shown that SLW warmer than  $-5 \text{ }^\circ\text{C}$  is common in winter orographic storms. Therefore, it is important to document propane's ability to create ice crystals and snowfall in slightly supercooled liquid water cloud.



All propane releases were from the 2540-m-elevation HAS. The HAS is very exposed to winds from south through west because terrain elevations decrease rapidly with distance in that quadrant. The HAS had an R.M Young model 5103 wind monitor to measure wind speed and direction and a Rosemount tower-type icing detector to monitor the presence of SLW. These instruments were mounted about 7 m a.g.l. (above ground level), and air temperature was observed about 3 m a.g.l. All measurements were averaged or summed for 6-min intervals and recorded by a Campbell CR-10 data logger. The site was manned during all experiments and the field technician made notes on cloud base location, visibility, snowfall, and other weather phenomena of interest.

Ice particles and AgI were detected at the Target located at 2855 m on the west edge of the Plateau top. This site, located at the head of a major canyon, is 315 m higher than the HAS seeding site and 4.2 km east-northeast of it. Sampling with an instrumented van during the early 1994 Utah field program (e.g., Holroyd et al., 1995) revealed that AgI and tracer gas released from the HAS frequently crossed the Plateau top's west edge in the vicinity of the Target during southwesterly flow. Channeling by local terrain is believed to be a major factor in the routine targeting of the Target site with HAS releases.

Because equipment was not available to detect propane at the Target, a "tracer" or "tag" was co-released which could be detected. That tracer material was AgI, released for the first and last 3 min of each propane release, and hereafter called "beginning tags" and "end tags," respectively. The AgI was released from a manual seeding generator at  $8 \text{ g h}^{-1}$  of AgI complexed with  $\text{NH}_4\text{I}$  in acetone. If both AgI tags were detected at the Target during a propane experiment, propane was assumed to be transported to the Target during the entire 1-h experiment. Although AgI has the potential to nucleate ice particles, it did not produce detectable IPC (ice particle concentrations) at the slightly supercooled temperatures existing during the propane seeding experiments.

The passage of AgI by the Target was detected by an NCAR acoustical IN (ice nucleus) counter (hereafter NCAR IN counter) operated with a cloud chamber temperature near  $-20^\circ\text{C}$ . Details of the NCAR IN counter are given by Langer (1973) and Super et al. (1988). The Target technician closely monitored the NCAR IN counter operation and logged various information about it each half-hour.

The Target was equipped with a Particle Measuring Systems 2D-C particle imaging probe with 800- $\mu\text{m}$  image width perpendicular to the wind and infinite along-the-wind sampling capability. The 2D-C probe was attached to a large vane which kept it pointed into the wind about 8 m a.g.l. A nearby heated Hydrotech anemometer provided wind speed measurements used to control the 2D-C probe's strobe rate to ensure production of non-distorted two-dimensional images of ice crystals. This method worked well with wind speeds greater than about  $2 \text{ m s}^{-1}$ , which were frequent at the canyon head location. The approach of using a vane-mounted 2D-C probe on a tower, first used during the early 1994 Utah field program, is believed superior to past 2D-C ground-based observations, which used a large aspirator to draw air past a vertically-pointed probe. Shattering of fragile crystal types against the aspirator walls has been visually observed on several occasions.

The 2D-C probe generates a considerable amount of data because the image of each ice crystal passing through the laser beam is recorded at 25- $\mu\text{m}$  resolution by a 32-diode array along with corresponding time data. The 2D-C probe data were recorded by a Science Engineering Associates M-200 data acquisition system using a DAT tape recorder with

1.3-gigabyte capacity. All other Target data were recorded with the same system at 1-s resolution.

Other instrumentation at the Target included a heated Hydrotech wind vane, a Rosemount tower-type icing detector, and a shielded air temperature sensor, all mounted about 8 m a.g.l. The on-site technician made weather observations at least once and usually twice per hour.

Three Belfort Universal weighing precipitation gauges were operated at locations shown on figure E.1. Each gauge had an orifice twice the area of the standard 8-in. orifice and a chart with one rotation per 24-h gears. The melted water equivalent resolution of these gauges is 0.005 in. (0.13 mm), and the time resolution is about 3 min. All gauges were equipped with Alter wind shields and were located in small, protected clearings in conifer forest to minimize wind-induced gauge catch losses. One gauge was 250 m east of the Target, expected to provide essentially the same snowfall as affected the Target. A second gauge was 6 km east-northeast of the Target, expected to often be targeted by the seeding plume at a more downwind location on the Plateau top. The third gauge was 4.3 km north of the Target near the head of Fairview Canyon. The 1994 van observations suggest that the latter location would be crosswind from the seeding plume when the plume passed over the Target. Therefore, the gauge north of the Target is considered a control gauge to monitor natural temporal variations in snowfall.

### **E.3 Experimental Design**

Field technicians were sent to the HAS and Target when private forecasters in Salt Lake City, Utah, expected a storm passage over the Plateau. The technicians did not stay overnight at the sites although they could have had weather conditions prevented safe travel. The technicians were usually deployed sometime after daylight and remained on-site until storm conditions were judged no longer suitable for sampling or late at night, whichever occurred first.

Once the technicians were on-site, they would observe whether cloud base was above both sites, between the sites or below the HAS. They would also observe the winds at each site. If cloud base was below the HAS, the HAS winds were in the southwest quadrant, and all required equipment was operational, a seeding experiment could commence. Liquid propane was intended to be released only when the HAS was in cloud because embryonic seeded ice crystals would quickly sublimate unless the atmosphere was saturated with respect to ice. As noted previously, the preference was to test AgI seeding unless temperatures were quite warm (above about -5 °C at the Target), in which case liquid propane was released.

It was desired to conduct seeding under a wide range of cloud conditions to provide information on the degree of response to seeding. Accordingly, no consideration was given to natural snowfall or the presence of SLW at the two sites in deciding when to release seeding material. Seeding experiments were conducted when natural snowfall ranged from none to heavy, and SLW was absent or present at one or both manned sites, provided that cloud base was below the HAS at the beginning of each experiment.

Although propane seeding was attempted on 5 different days between January 7 and March 11, 1995, post-season analysis revealed valid tests were accomplished on only the last 2 days, March 5 and 11. Earlier attempts failed, either because the cloud base lifted above the HAS or the wind direction shifted so the seeded air was not transported to the Target. Because

conditions were not suitable for valid testing, the earlier attempted propane seeding experiments will not be discussed further.

## E.4 Experimental Results

### E.4.1 March 5, 1995

Three experiments were attempted on this day, but the third, a propane release, did not affect the Target. Very low AgI IN concentrations were detected from the beginning tag of the third experiment (AgI released from 1125 to 1128), and no AgI IN were detected from the end tag. Moreover, cloud base lifted above the HAS by 1137, and the previously southwesterly wind gradually shifted to north of west by 1220. Experience has shown that HAS wind directions more northerly than about 250 degrees result in seeding material transport south of the Target.

Figure E.2 shows the first HAS propane release rate was near  $3 \text{ gal h}^{-1}$  from 0805 to 0905 as monitored by a gas flow meter. The AgI experiment's release was from 0930 to 1030. The HAS was in dense cloud from prior to 0800 until about 1130, with estimated visibility consistently less than 50 m. The icing detector cycled ("tripped") 8 times during the 3-h period shown on figure E.2; most of the SLW detection occurred during the AgI release. Only 2 trips occurred during the propane release. Winds are seen to have been southwesterly with speeds estimated by the on-site technician at near  $5 \text{ m s}^{-1}$  (the wind speed sensor readings were not recorded on this day).

Icing detector trips refers to the deicing cycle which occurs after a certain mass of SLW collects by accretion and freezes on the detector sensor. Each deicing cycle produces a "trip" of the heater relay, which is recorded. An approximate value of cloud LWC (liquid water content) can be calculated from the icing detector trip rate. Assuming a collection efficiency of 1.0 for the sensor, the LWC can be related to the mass load of ice required to trip the detector and the wind speed. Wind tunnel calibrations done in 1985 and 1986 revealed differences in the mass load trip point among 3 different Rosemount tower type icing detectors, with an average value of 0.075 g and range about that value of  $\pm 0.015 \text{ g}$ . Because no similar calibrations were done for the HAS and Target icing detectors, it will be assumed that they also tripped (deiced) every time 0.075 g of ice was accreted. The LWC can be calculated from:

$$LWC = NM/AS \quad (1)$$

where  $N$  is the number of trips per hour,  $M = 0.075 \text{ g}$ ,  $A$  is the sensor cross sectional area of  $1.77 \text{ cm}^2$ , and  $S = \text{wind speed in } \text{m s}^{-1}$ . It can readily be shown that for the units used, the expression can be simplified to:

$$LWC (\text{g m}^{-3}) = 0.12 N/S \quad (2)$$

This simple approach of using equation 2 will be used in all estimates of LWC given in this report. When the trip rate was slow, it was sometimes necessary to estimate what fraction of a trip occurred during a period of interest (e.g., if a trip occurred soon after the end of a seeded hour).

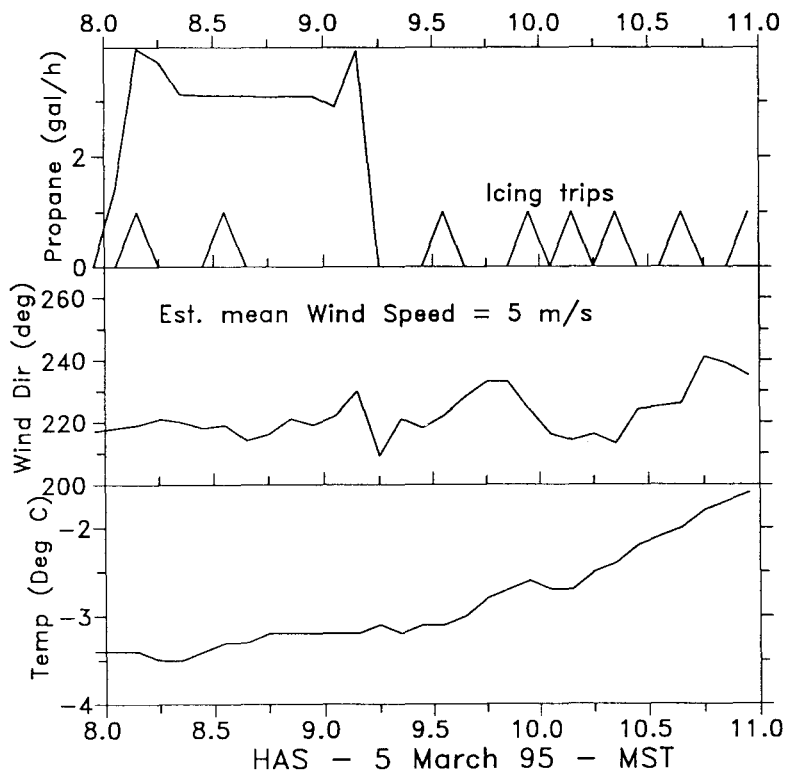


Figure E.2. - HAS temporal distributions of wind direction, air temperature, icing detector trips, and propane release rates during two seeding experiments of March 5, 1995.

Estimates of the HAS LWC during the propane and AgI releases are  $0.04 \text{ g m}^{-3}$  and  $0.08 \text{ g m}^{-3}$ , respectively. The HAS temperature was relatively warm, near  $-3.3 \text{ }^\circ\text{C}$  during the propane release and between  $-2$  and  $-3 \text{ }^\circ\text{C}$  during the AgI release.

Supercooled liquid water was present at the Target throughout the 3-h period as shown by the 11 trips of its icing detector on figure E.3. Estimated Target LWC values during the propane-seeded and AgI-seeded periods are  $0.04 \text{ g m}^{-3}$  and  $0.08 \text{ g m}^{-3}$ , respectively, the same as the HAS estimates.

Estimated visibility at the Target remained near 100 m during the experimental period. Winds were near westerly, averaging about  $6$  to  $7 \text{ m s}^{-1}$ . The average temperature was slightly warmer than  $-4.5 \text{ }^\circ\text{C}$  during the propane seeding and near  $-4 \text{ }^\circ\text{C}$  during the AgI plume passage. Laboratory measurements have indicated a cloud temperature of  $-4 \text{ }^\circ\text{C}$  is too warm for significant AgI nucleation (DeMott et al., 1995). As will be shown, this day's measurements within orographic cloud support those laboratory results.

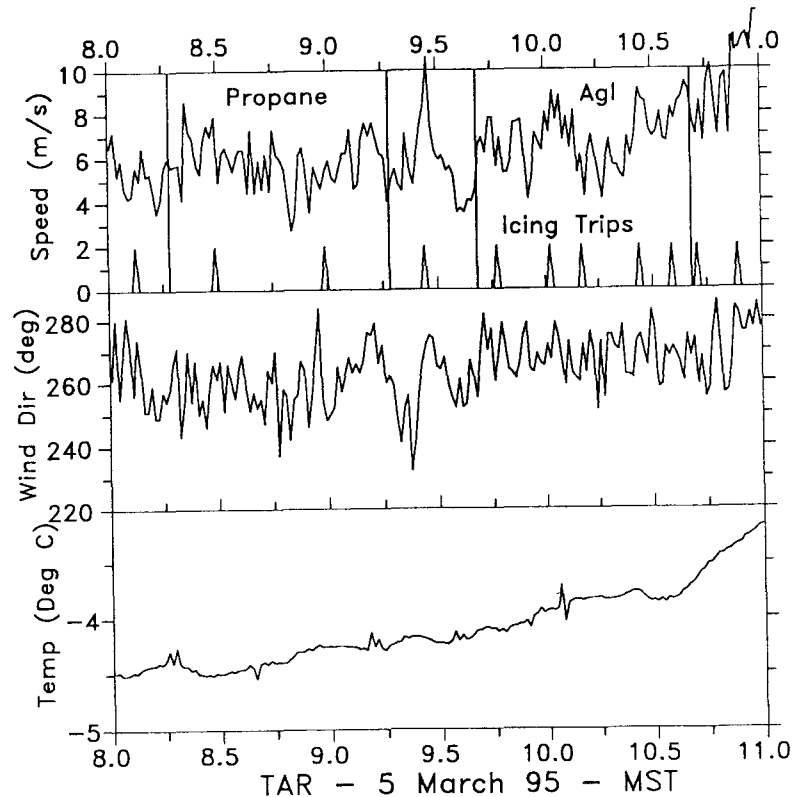


Figure E.3. - TAR temporal distributions of wind speed and direction, air temperature and icing detector trips during two seeding experiments of March 5, 1995. The estimated hour of maximum seeding plume presence is shown for each experiment by vertical lines.

Figure E.4 clearly shows the AgI beginning and end tags for the propane release as they passed the Target. Periods not seeded by the HAS generator had very low concentrations measured by the NCAR IN counter.

About 11 min elapsed from first release of each tag to first detection at the Target, translating into a  $6.4 \text{ m s}^{-1}$  speed if the AgI was transported directly between the HAS and the Target located 4.2 km apart. About 6 more minutes passed before maximum AgI IN concentrations were detected. Each 3-min release resulted in above-background IN values at the Target for about 30 min, although most AgI passed the Target within 10 min.

Figure E.4 also shows 1-min averages of IPC and estimated snowfall from the 2D-C probe observations, both based on the software of Holroyd (1987). Particles smaller than  $100 \mu\text{m}$ , only 4 times the probe's resolution, were ignored in the calculations, as were particles with an estimated center of mass outside the probe's  $800 \mu\text{m}$  sampling width.

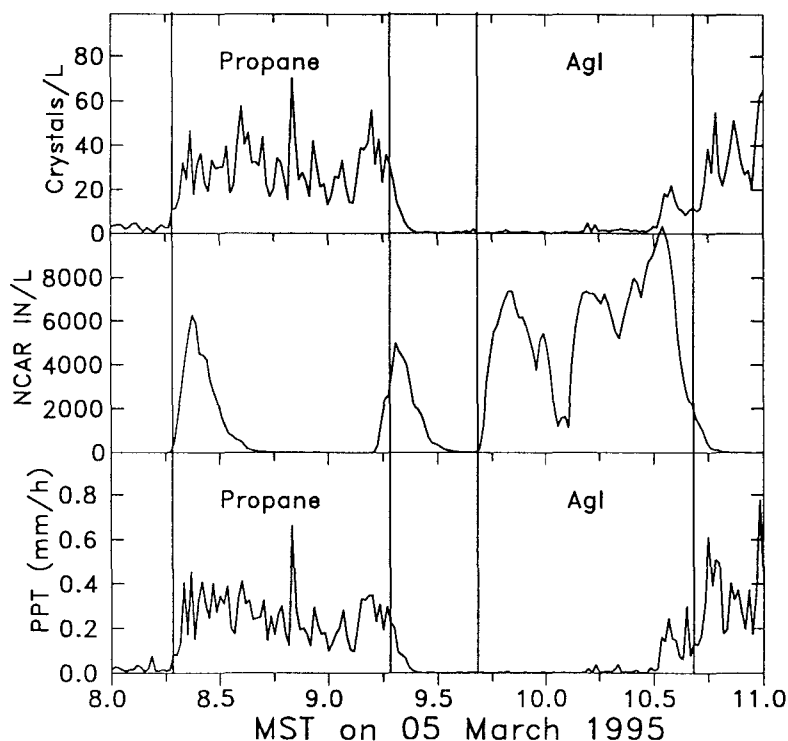


Figure E.4. - Temporal distributions of the IPC (top panel) and precipitation intensity (bottom panel), both calculated from the TAR 2D-C probe observations and the NCAR IN counter observations of  $\text{IN L}^{-1}$ , effective at  $-20^{\circ}\text{C}$  (middle panel), for two seeding experiments of March 5, 1995. The estimated hour of maximum seeding plume presence is shown for each experiment by vertical lines.

Vertical lines on figure E.4 show the estimated hour of maximum effect by the propane seeding (0818 to 0918), judged by the NCAR IN data and changes in IPC. It is obvious that the propane seeding had a marked effect on both IPC and snowfall because both were at very low levels before and after the propane seeding (Note: the term "snowfall" will refer to the rate of accumulation of *snow water equivalent*, also called precipitation intensity, throughout this report, not snow depth). Moreover, the timing of the 1-h increase in IPC and snowfall was in excellent agreement with the AgI tags. Propane seeding increased the average IPC by about  $30 \text{ L}^{-1}$ , the average snowfall by about  $0.25 \text{ mm h}^{-1}$ , and both rates were rather consistent for the hour of effect.

The first snowfall detection was near 1040 for both the crosswind and downwind gages and no snowfall was noted by the HAS technician until 1042 when occasional small graupel begin to fall. In contrast, the Target technician noted no snowfall at 0755 and "very, very light snow with small rim balls and very small needles" at his next entry at 0835. His 0905 entry noted very light snowfall (crystal types not noted) and he observed that snowfall had stopped

by 0947. The Target gage chart trace first moved to indicate snowfall between 0830 and 0845. Apparently, some mechanical lag occurred with the very light snowfall. The trace stopped moving an hour later. The hourly gage total was 0.25 mm, in very good agreement with the rate estimated with the 2D-C probe (fig. E.4). Although this snowfall was not high, it was typical of many wintertime hours. For example, Super (1994) reported a median rate just under 0.4 mm h<sup>-1</sup> on the Plateau top during the 1991 field season.

Reynolds (see appendix D) estimated average snowfall for propane seeding in California based on physical reasoning. Interestingly, he arrived at 0.20 mm h<sup>-1</sup>, which is slightly less than the 0.25 mm h<sup>-1</sup> value observed in this experiment. However, his estimate was based on snowfall over a target extending up to 30 km downwind from the propane dispensers, although this observation was made only 4.2 km horizontally from a single dispenser. One would anticipate higher snowfall farther downwind because of longer crystal growth times.

Because of the lack of natural snowfall and continued presence of dense cloud, a decision was made to conduct an AgI seeding experiment very soon after the propane seeding. The AgI generator was operated from 0930 to 1030. The first detection of this AgI release at the Target was at 0941, and figure E.4 shows high AgI IN concentrations for most of the next hour. In fact, the concentrations were higher than plotted because the NCAR IN counter has an electronic delay to eliminate counting echoes from the chamber top as ice crystals. The result is marked underestimates of rates even approaching 8000 L<sup>-1</sup>. Assuming the average IN concentration (at -20 °C) was 10,000 L<sup>-1</sup>, recent calibration data from the Colorado State University Cloud Simulation Laboratory (DeMott et al., 1995) suggest the yield of the AgI generator used was about 4 orders of magnitude lower, or 1 L<sup>-1</sup>, at -6 °C, the warmest temperature tested. As noted, the Target temperature was -4 °C during the AgI seeding, so no noticeable increase in IPC would be anticipated from the laboratory calibration. The continued low IPC after the propane seeding and until just after 1030 is in agreement with this expectation.

The increased IPC and snowfall after 1030 (1035 according to the Target gage) is interpreted as the beginning of natural snowfall which, as previously noted, was detected by crosswind and downwind gages 10 min later. The natural snowfall continued for several hours.

Figures E.5a through E.5d illustrate the time histories of the cumulative distributions of IPC and precipitation intensity by crystal sizes (a and c) and habits (b and d), respectively. That is, the total IPC or snowfall for each 10-min period was set to 100 percent and the percentages of IPC or snowfall were considered by crystal size and habit categories, again calculated by the software of Holroyd (1987). This approach does not address whether seeding changed either the IPC or snowfall, but only considers microphysical changes that might be related to seeding.

Figure E.5 shows that most of the propane-seeded IPC was classified as hexagonal or irregular with the majority of crystals between about 0.2 and 0.6 mm. When considered by snowfall, most crystals were in the hexagonal or needle/column categories and between about 0.4 and perhaps 0.8 mm. Hexagonal plates and needles would be expected from laboratory work at the slightly supercooled temperatures which existed between the HAS and Target (e.g., Ryan et al., 1976). The propane-seeded ice crystals grew in SLW cloud for about 1000 s before detection at the Target. Growth rates are about 0.5 μm s<sup>-1</sup> near -4 °C according to Ryan et al. (1976). This rate would result in a 0.5-mm crystal in 1000 s, in good agreement with figures E.5a and E.5c.

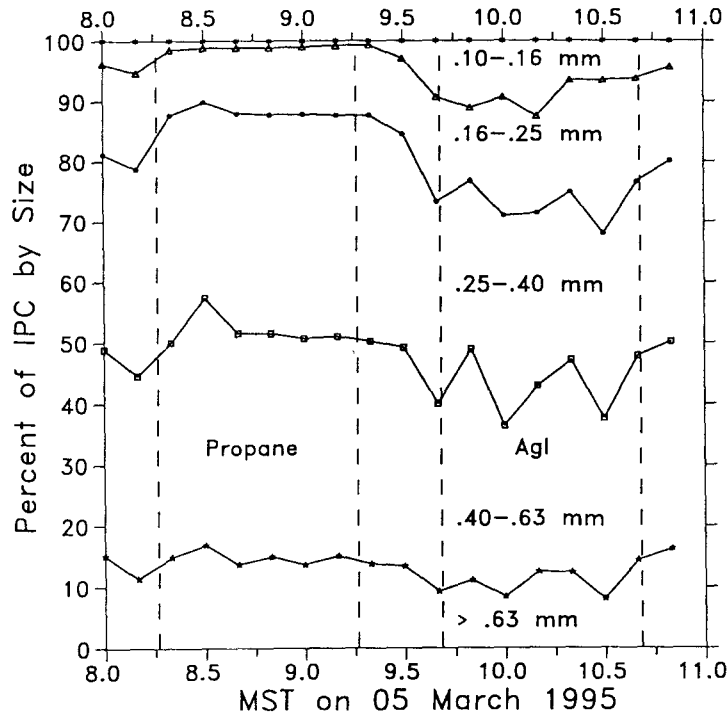


Figure E.5a. - Cumulative percentage of IPC, partitioned by size, versus time during March 5, 1995. The estimated hour of maximum seeding plume presence is shown for two experiments by vertical lines.

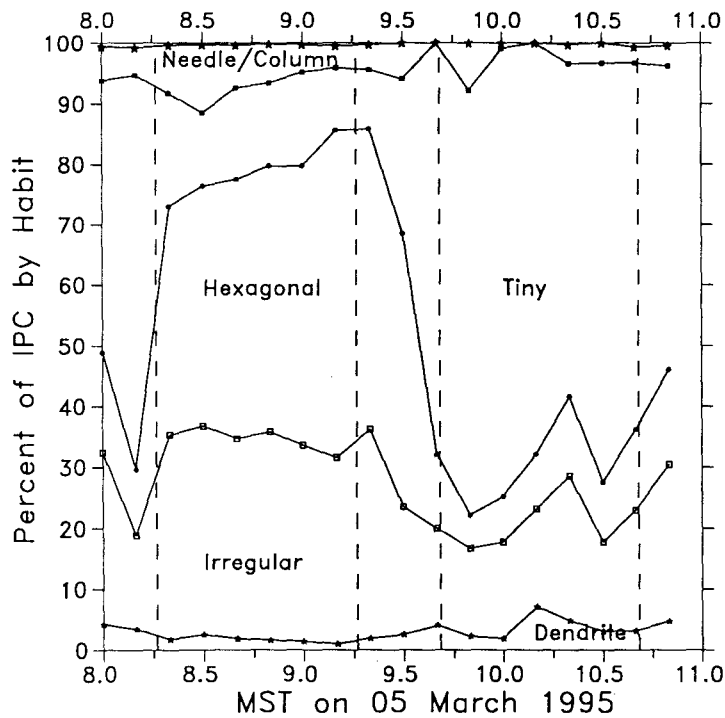


Figure E.5b. - Cumulative percentage of IPC, partitioned by crystal habit, versus time during March 5, 1995. The estimated hour of maximum seeding plume presence is shown for two experiments by vertical lines.

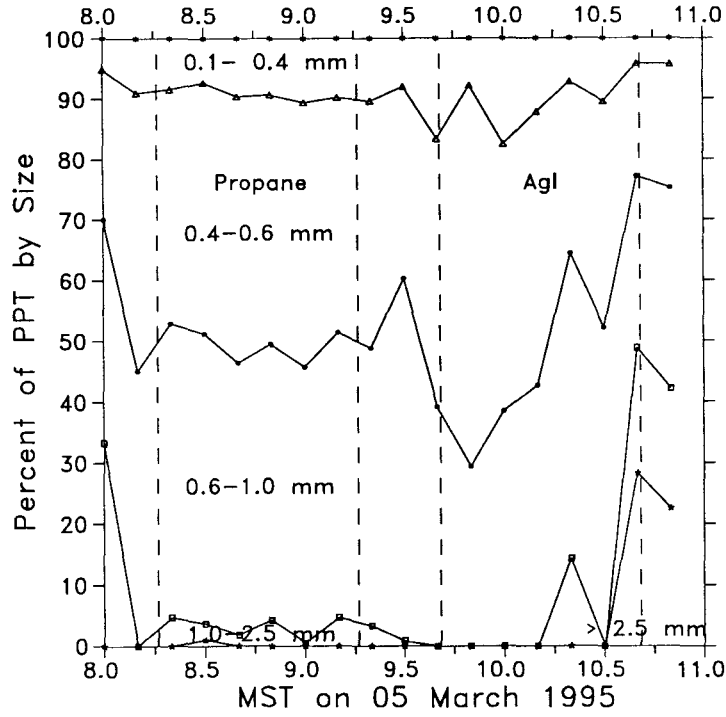


Figure E.5c. - Cumulative percentage of precipitation intensity, partitioned by size, versus time during March 5, 1995. The estimated hour of maximum seeding plume presence is shown for two experiments by vertical lines.

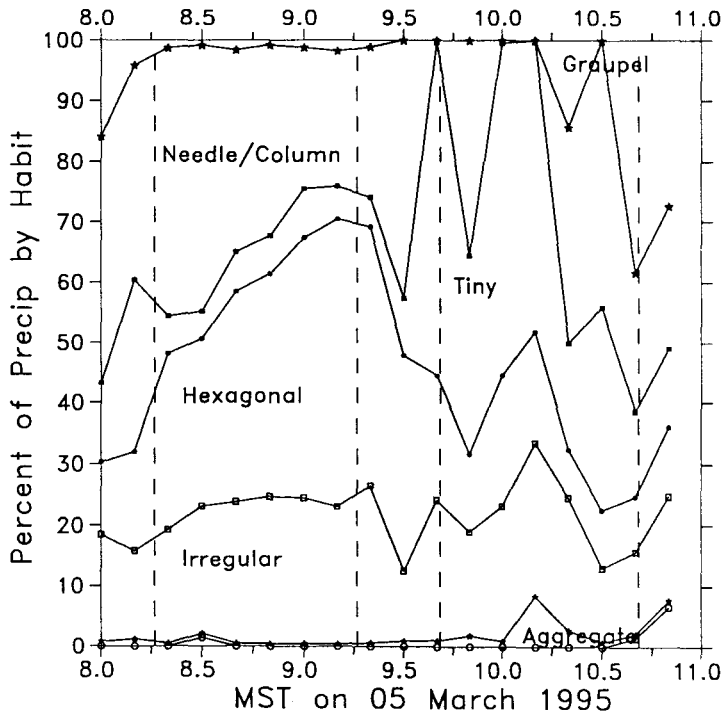


Figure E.5d. - Cumulative percentage of precipitation intensity, partitioned by crystal habit, versus time during March 5, 1995. The estimated hour of maximum seeding plume presence is shown for two experiments by vertical lines.

Figure E.6 shows images of ice crystals for selected times. For reference, the vertical width of each "line" of crystals represents 800  $\mu\text{m}$  and the smallest crystals are 100  $\mu\text{m}$  in size. The top panel shows all images observed between 0800 and 0805, prior to seeding. The middle three panels show typical 1-min intervals as the propane seeding pulse passed the Target (0830 to 0831, 0845 to 0846, 0900 to 0901), and the lowest panel shows a 10-min period after seeding (0931 to 0941). It is obvious that the IPC was much higher during seeding than before or after. Snowfall had essentially stopped by the time of the lower panel. The images are seen to have been much more uniform in size and shape during seeding than before or after. The uniformity shown on figure E.6 was characteristic of the entire seeded hour. Many of the seeded images appear to be small plates with a transparent (to the laser) center, suggesting a thin inner structure. Many other seeded images appear to be short columns and/or thick needles. Capped columns were also frequently observed on edge with the columns quite short.

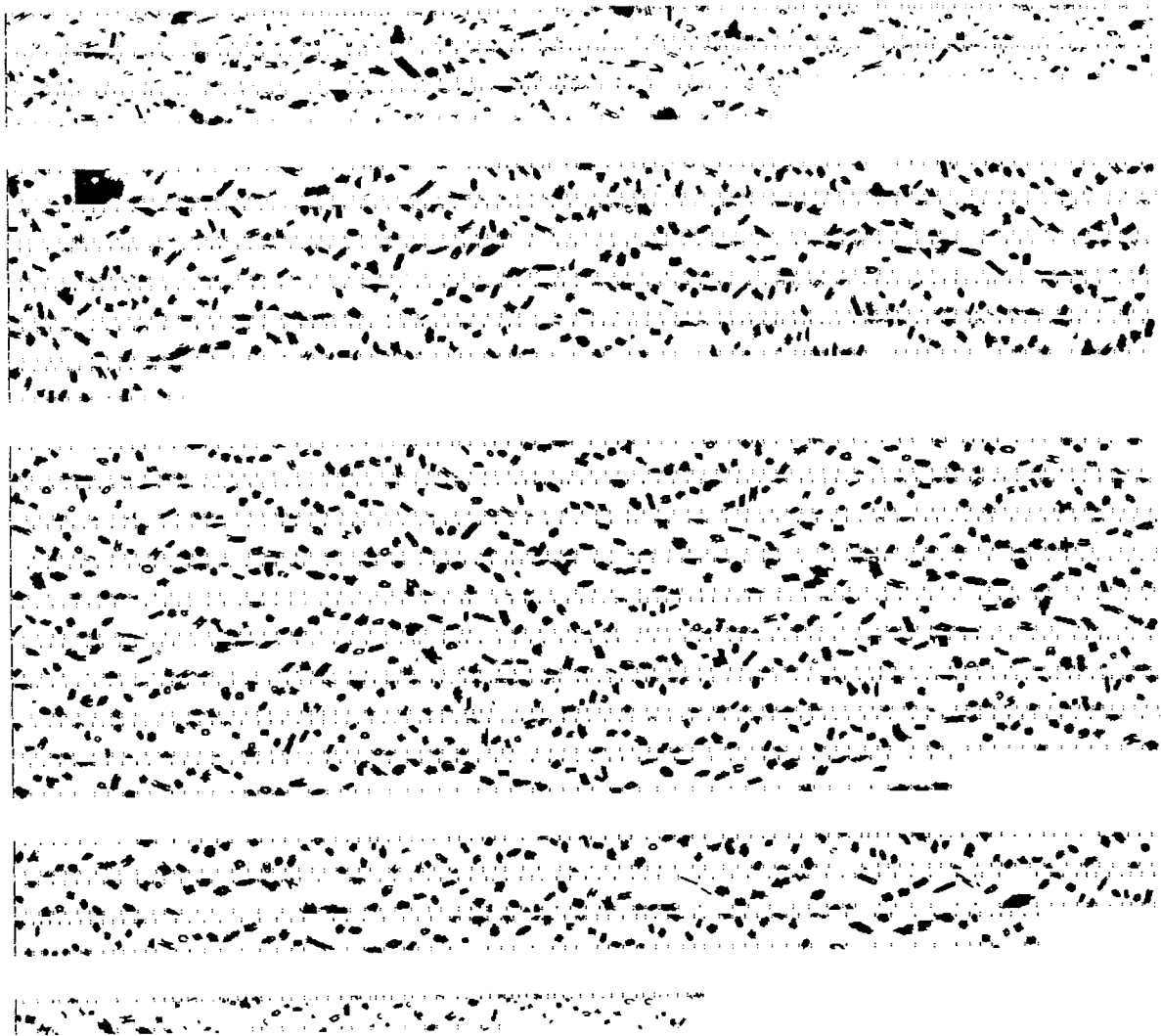


Figure E.6. - TAR 2D-C images of ice particles (100  $\mu\text{m}$  minimum size) for selected periods during March 5, 1995. The top panel is from 5 min (0800 to 0805) shortly before arrival of the propane seeding plume, the three middle panels are from 1-min periods during seeding (0830 to 0831, 0845 to 0846, and 0900 to 0901), and the bottom panel is from 10 min (0931 to 0941) just after seeding.

In summary, the two experiments on this day, conducted in slightly supercooled cloud (-2.5 to -4.5 °C) between the release and observing sites, clearly demonstrated two different results of seeding. The propane seeding produced 0.25 mm h<sup>-1</sup> at the Target, and the AgI seeding produced no detectable increase in IPC. This result is obviously an example of cloud conditions for which propane seeding offers a useful adjunct to AgI seeding.

The relatively low IPC and snowfall from the propane seeding suggest that a higher release rate might be appropriate for the conditions experienced. Of course, an operational seeding program would likely have a significantly greater distance between propane dispensers and the target than the 4.2 km used in these experiments. The associated greater travel time might be expected to result in more ice crystal growth and higher snowfall.

#### **E.4.2 March 11, 1995**

Three propane releases, each near 4 gal h<sup>-1</sup>, were made late on this day and extended into the early morning of March 12, 1995, as shown on figure E.7. All plots for this day will show 0100 m.s.t on March 12th as 2500 on March 11th.

Figure E.7 shows abundant SLW was present at the HAS during and between all three propane releases. A total of 44 trips of the icing detector occurred over the 7-h period shown. The greatest icing rate occurred during the final release when each 6-min sampling period had a trip and one period had two.

The HAS wind was southwesterly from 4 to 7 m s<sup>-1</sup> and the temperature was usually between -2 and -3 °C. Observations by the field technician each 30 min noted the HAS was in cloud throughout the period. Snowfall, typically small graupel, was observed between 1906 (first observation) and 2008 and again between 2242 and 2310. New snow depths were about 0.5 in per 30 min. It was not snowing between 2040 and 2210 and again after 2340.

Figure E.8 shows conditions at the Target. Each hour of propane seeding is shown as estimated from the AgI tags. Westerly winds prevailed near 8 m s<sup>-1</sup> during the first and third experiments and near 11 m s<sup>-1</sup> during the second experiment. The Target temperature was near -3 °C during the first and second experiments and cooled to just below -4 °C during the third experiment. Some SLW was detected during all experiments, but 26 of the 32 icing detector trips shown occurred before, during, and after the second experiment. As will be shown, natural snowfall apparently used much of the SLW during the first and third experiments.

The Target technician made several references to small graupel and small needles during the course of the experiments. The typical visibility observation was near 30 m in cloud and blowing snow.

The IPC and snowfall based on Target 2D-C observations are shown on figure E.9 along with the three pairs of beginning and end AgI tags detected by the NCAR IN counter. Estimated hours of maximum propane passage by the Target are shown by vertical lines, based on the arrival of the beginning tag and the arrival of the end tag plus 3 minutes. For each seeding experiment, the first 3-min AgI release began almost simultaneously with the propane release. However, for the end tag, the AgI generator was run for about the final 3 min of propane release. The lag time of the NCAR IN counter, about 30 s for high AgI concentrations, was also used in estimating the hour of maximum propane passage.

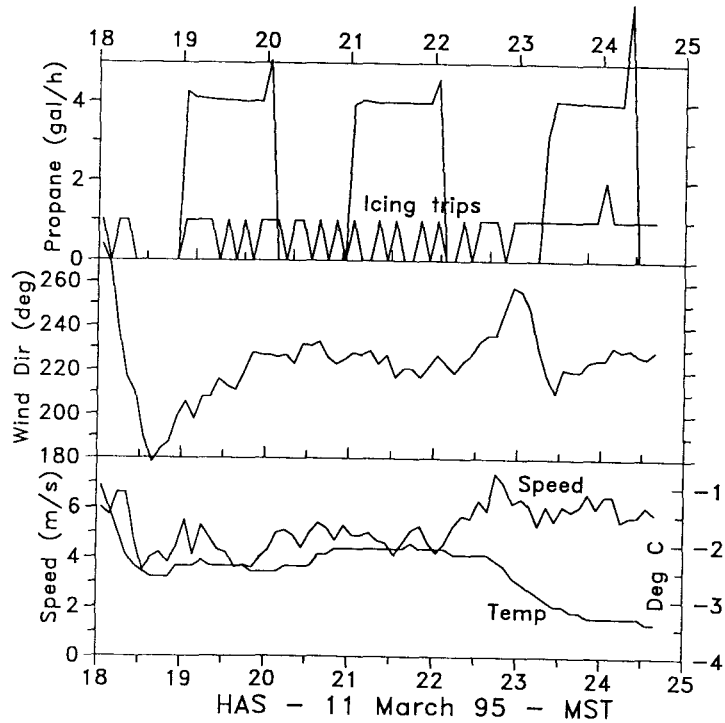


Figure E.7. - HAS temporal distributions of wind speed and direction, air temperature, icing detector trips, and propane release rates during three seeding experiments of March 11, 1995.

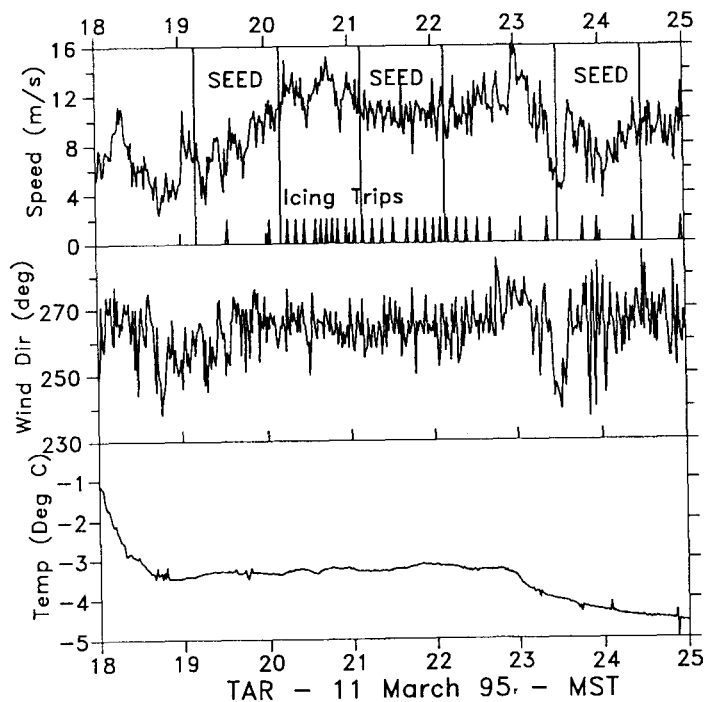


Figure E.8. - TAR temporal distributions of wind speed and direction, air temperature, and icing detector trips during three seeding experiments of March 11, 1995. The estimated hour of maximum seeding plume presence is shown for each experiment by vertical lines.

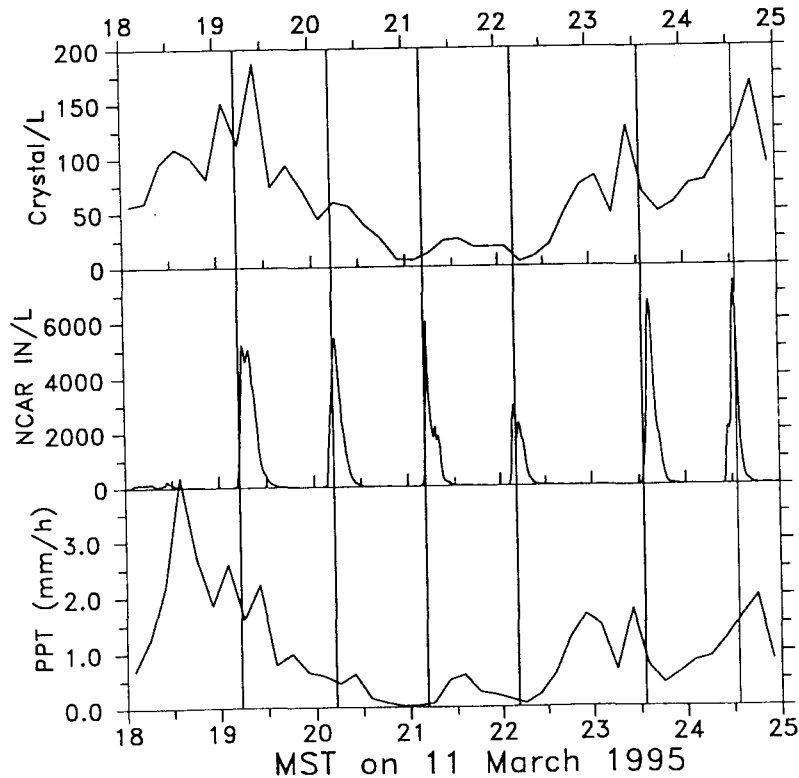


Figure E.9. - Temporal distributions of the IPC (top panel) and precipitation intensity (bottom panel), both calculated from the TAR 2D-C probe observations, and the NCAR IN counter observations of  $\text{IN L}^{-1}$ , effective at  $-20^{\circ}\text{C}$  (middle panel), for three propane seeding experiments of March 11, 1995. The estimated hour of maximum seeding plume presence is shown for each experiment by vertical lines.

The highest snowfall occurred prior to any propane release. Each of the 3 gages received more snowfall during the hour prior to the first seeding experiment than during any later hour until termination of all 3 experiments. The Target gage received the highest snowfall,  $7.7 \text{ mm h}^{-1}$ , during the hour before first arrival of the propane. That figure is almost twice the rate estimated with the 2D-C probe data and indicates the software underestimates high snowfalls. The first propane experiment is seen to have taken place during a period of decreasing natural snowfall which had been at an exceptionally high rate for the Plateau. For comparison, the highest snowfall observed on the Plateau during the 1991 field season was  $4.5 \text{ mm h}^{-1}$  (Super, 1994).

Figure E.9 shows that snowfall decreased throughout the first propane seeding, indicating that any increase caused by seeding was minor compared to the natural snowfall. The highest IPC shown was just after first propane arrival, but the IPC thereafter also decreased with time. Ice particle concentrations during the first experiment ranged from  $180 \text{ L}^{-1}$  to  $45 \text{ L}^{-1}$ , all well above the IPC associated with propane seeding on March 5th. It might be anticipated that any seeding affect would not be detectable because of the high natural

snowfall, which was quite variable with time. For reference, the Target gage recorded 2.9 mm during the hour of first propane passage.

The third seeding experiment will next be examined. Figure E.9 shows a minimum in both IPC and snowfall just after arrival of the propane, but both decreases had started prior to seeding. Moreover, both minimums were reached about 10 min into the seeded period and both the IPC and the snowfall increased throughout the remainder of the seeded hour. The variations shown are interpreted as primarily caused by natural snowfall with any seeding influence minor by comparison. The Target gage recorded 1.3 mm during the third seeded hour.

Reference to figure E.8 shows 2 trips of the icing detector during the first seeded hour and 3 trips during the third seeded hour. In spite of the high natural snowfall, some SLW was present at the Target, with estimated LWC values of  $0.03$  and  $0.05 \text{ g m}^{-3}$ , respectively, during the first and third seeded hours. As previously shown, SLW was abundant at the HAS throughout the period of interest. Because SLW was present at both sites, it is very likely that seeding converted some of the available SLW into ice crystals which grew as they were transported from the HAS to the Target. It is also likely that a large portion of the presumed seeded crystals were "swept out" by (became aggregates with) larger natural crystals. Thus, although not detectable from the available observations, it seems probable that the first and third seeding experiments increased snowfall, albeit at minor rates.

The second propane seeding will now be examined as the sole experiment on this day where a seeding effect might be detectable. It is seen on figure E.9 that both the IPC and the snowfall were at very low levels just before and after the second seeded hour, but somewhat higher during the seeded hour. The increase during the seeded hour could be caused by natural variability because much higher rates were observed earlier and later. Moreover, unlike the propane seeded hour of March 5th, this hour's rate of snowfall was not quasi-constant, suggesting natural variability.

It will be recalled that the Target SLW was abundant before, during, and after the second seeded hour. The estimated HAS LWC during the hour of propane release is  $0.20 \text{ g m}^{-3}$ , and the Target LWC for the propane-seeded hour is  $0.10 \text{ g m}^{-3}$ . Relatively abundant LWC often accompanies periods of limited natural snowfall (e.g., Super and Holroyd, 1989). Moreover, the crosswind gage observed its lowest value (0.25 mm) for several hours on either side of the second propane experiment, indicating natural snowfall was at a minimum. All these factors suggest that seeding may have had a noticeable effect.

Figures E.10a through E.10d show the cumulative distributions of IPC and snowfall during the pre-seeded, seeded, and post-seeded periods, again partitioned by crystal sizes and by habits. The figures show that natural snowfall characteristics were varying with time because they were different before and after the seeded hour. Such natural variability makes identification of seeding-caused changes more difficult. All sizes making up the IPC increased markedly from pre-seeding to seeding. However, further increases are seen during post-seeding, so at least part of the increase during seeding was associated with a natural trend.

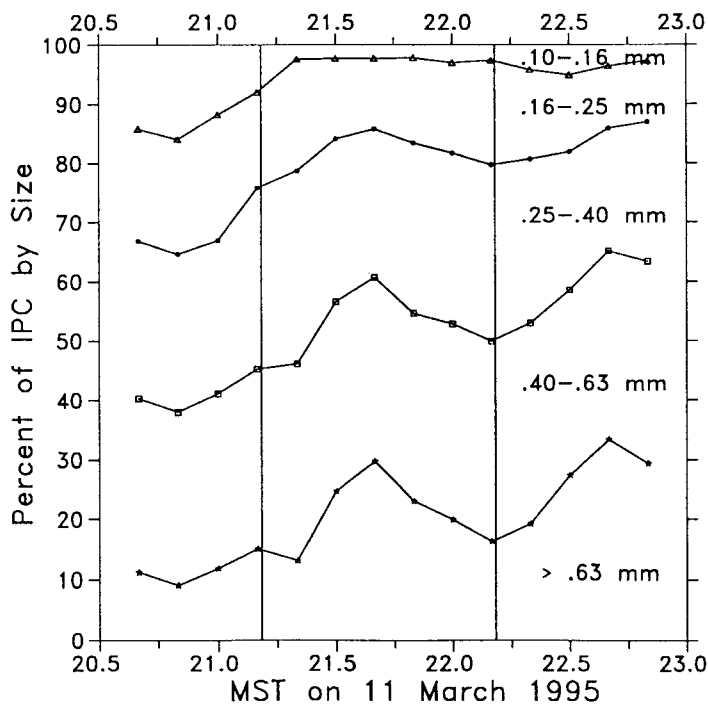


Figure E.10a. - Cumulative percentage of IPC, partitioned by size, versus time during March 11, 1995. The estimated hour of maximum seeding plume presence is shown by vertical lines for the second experiment.

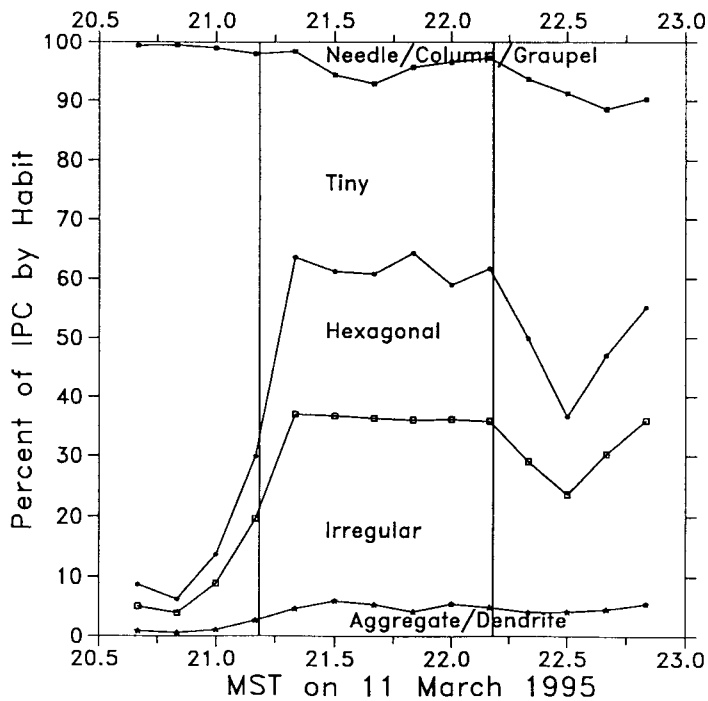


Figure E.10b. - Cumulative percentage of IPC, partitioned by crystal habit, versus time during March 11, 1995. The estimated hour of maximum seeding plume presence is shown by vertical lines for the second experiment.

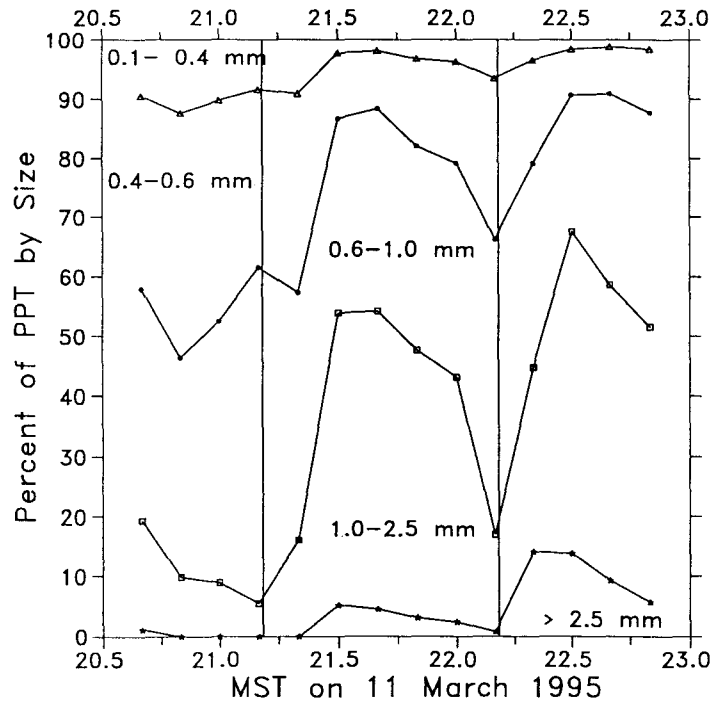


Figure E.10c. - Cumulative percentage of precipitation intensity, partitioned by size, versus time during March 11, 1995. The estimated hour of maximum seeding plume presence is shown by vertical lines for the second experiment.

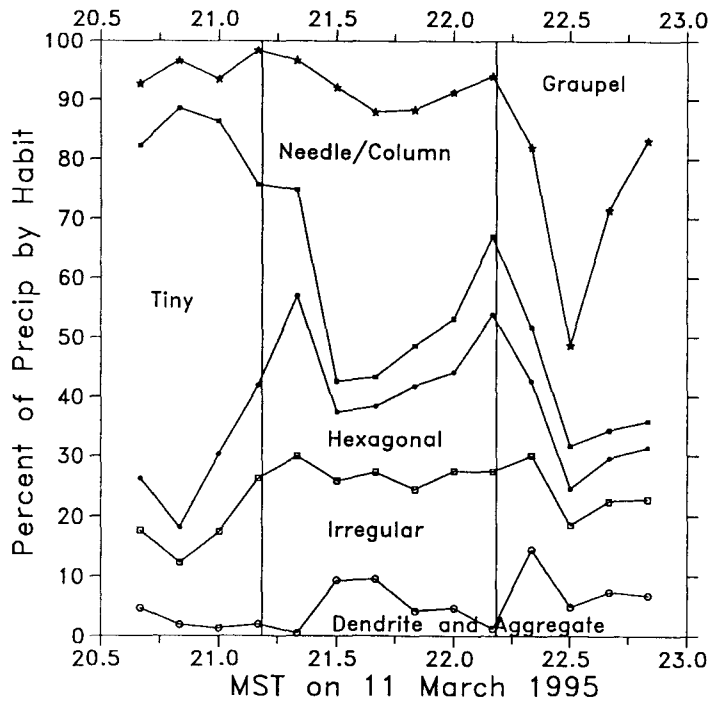


Figure E.10d. - Cumulative percentage of precipitation intensity, partitioned by crystal habit, versus time during March 11, 1995. The estimated hour of maximum seeding plume presence is shown by vertical lines for the second experiment.

The seeded period had a large decrease in percentage contribution of the total IPC by crystals classified as tiny (too small and with insufficient structure to classify), and increases in hexagonal and irregular crystals. These changes are especially evident when compared with the pre-seeding period, but are also apparent in comparison with the period after seeding.

Turning attention to crystal sizes and types that made up the snowfall, the seeded hour had a large increase in all sizes compared with pre-seeding but not with post-seeding. As noted earlier, this size change was likely partially caused by a natural trend. However, the seeded hour had a markedly higher percentage of the combined needle/column category (only during the middle portion of the seeded hour), and more hexagonal and irregular crystals, than both the pre- and post-seeding periods. The abrupt decrease in tiny crystals from pre-seeding to seeding is again seen.

The second experiment's seeded crystals were exposed to SLW cloud for at least 700 s while transported from the HAS to the Target, at temperatures between -2 and -3 °C. This range is known to produce very slow growth for ice crystals. According to Ryan et al. (1976) plane plate crystals should form at -3 °C (the warmest temperature they examined), which would grow at about 0.2  $\mu\text{m s}^{-1}$ . That rate would produce 0.15-mm crystals in 750 s. Figures E.10b and E.10d both show increases in hexagonal crystals and in irregulars, which could be plates too small to identify. These changes support the hypothesis that seeding produced plate crystals.

Perhaps the best impression of microphysical changes during this seeding experiment can be gained from examination of the ice particle images themselves. Figure E.11 shows 3 panels of 2D-C images at least 100  $\mu\text{m}$  in size. The top panel is for 5 min (2104 to 2109) just prior to arrival of the propane-seeded pulse when the average IPC was 3  $\text{L}^{-1}$ . The middle panel is for a typical minute (2116 to 2117) early in the seeded hour when IPCs were near 18  $\text{L}^{-1}$ , and the bottom panel is for a minute (2130 to 2131) near the time of highest IPC during the seeded hour.

The uniformity of the middle panel's crystals is striking. This panel is interpreted as primarily seeding-caused crystals. Uniformity in crystal sizes and types would be expected if crystals originated at a point source (the propane dispenser) and thereafter were exposed to a similar growth environment. Similar uniformity has been seen in earlier seeding experiments. The crystals appear to be thin (centers transparent to the laser) embryonic plates as expected with prevailing temperatures. Most of the crystals in the middle panel appear to be near 0.15 to 0.30 mm, somewhat larger than expected from Ryan et al. (1976).

By the time of the bottom panel, many crystals similar to those of the middle panel are interspersed with much larger particles, some of which are small graupel and some of which appear to be columns or aggregates of columns. The average IPC during this period was near 28  $\text{L}^{-1}$ . The interpretation is that a small natural snow shower occurred during the middle of the seeding experiment. The "additional" crystals of the lower panel are too large to have been caused by seeding with the limited available growth time and they appear characteristic of a colder growth environment.

Images (not shown) were examined just before and after the end of seeding. By 2208, the image population was very similar to the middle panel of figure E.11 except that some small graupel was evident. By 2222, after the seeded pulse had passed beyond the Target, larger graupel were common as natural snowfall increased.

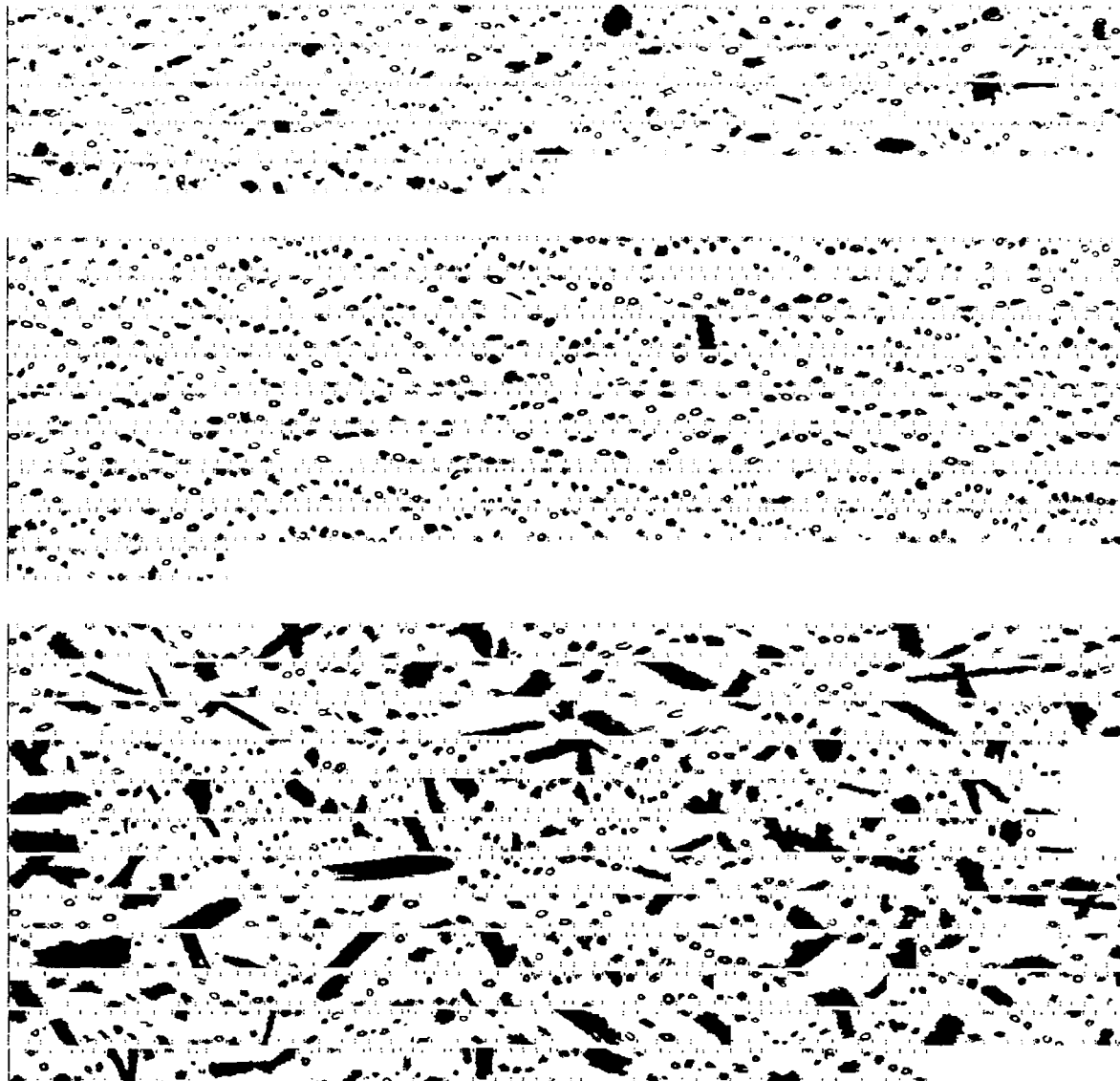


Figure E.11. - TAR 2D-C images of ice particles (100  $\mu\text{m}$  minimum size) for selected periods during March 11, 1995. The top panel is from 5 min (2104 to 2109) shortly before arrival of the propane seeding plume, the middle panel is from 1 min (2116 to 2117) shortly after seeding plume arrival, and the bottom panel is from 1 min (2130 to 2131) near the time of highest IPC during the seeded hour.

Because crystals larger than perhaps 0.4 mm would not be expected to be caused by this particular seeding, most snowfall shown on figure E.10c must have been from natural crystals. Thus, although seeding apparently affected the microphysics, its contribution to the total snowfall was limited during this experiment.

One can establish an *upper limit* on possible seeding production by optimistically assuming that *all* snowfall observed at the Target during the second experiment was caused by seeding. Figure E.9 shows the average IPC was about 20  $\text{L}^{-1}$ , and the average estimated snowfall was near 0.3  $\text{mm h}^{-1}$  during this seeded hour. The Target gage observed 0.38 mm during the same hour. These values represent the highest IPC and snowfall production possible from

the type of propane seeding applied to a cloud with abundant LWC but temperature only slightly below 0 °C. But the evidence of large crystals during part of the seeded hour argues that these values are unrealistically high. The crosswind gage observed 0.25 mm of snowfall during the same hour, suggesting the propane-caused component of Target snowfall may be closer to 0.1 mm h<sup>-1</sup>.

A more realistic estimate of the propane-caused IPC and rate of snowfall is based on the very first portion of the seeded hour before the larger natural crystals shown on the bottom panel of figure E.11 were evident. The period 2115 to 2120 had only a few of the larger, natural crystals, and the propane-seeded pulse appeared to have been well established by then. By 2123, larger natural crystals were plentiful. The difference between the natural background IPC of 3 L<sup>-1</sup> for 2100 to 2110 and the 18 L<sup>-1</sup> of 2115 to 2120 is 15 L<sup>-1</sup>, believed to be the best estimate of propane-caused crystals during this day. The estimated snowfall was 0.12 mm h<sup>-1</sup> for 2115 to 2120. If the few natural crystals were eliminated, the propane-caused snowfall is estimated at no more than 0.10 mm h<sup>-1</sup>. Examination of some brief periods with few large crystals near the end of the seeded hour (images not shown) suggested propane-caused IPCs and snowfall slightly lower than the values stated.

To summarize the microphysical evidence, the second propane experiment resulted in some marked changes in ice particle characteristics, but natural snowfall during much of the seeded hour also affected ice particle population. Crystal sizes abruptly increased from the pre-seeded period, but sizes continued to increase after seeding. Seeding apparently increased hexagonal and irregular crystal types. The percentage of needle/column category toward the total concentration increased slightly during the middle portion of the seeded hour, and this category's contribution to snowfall was quite noticeable. That result means that the needles or columns were relatively large, indicating they were of natural origin.

The layer temperature between the HAS and the Target was between -2 to -3 °C during the second experiment, more than 1 °C warmer than during the successful propane seeding experiment of March 5th. It might be speculated that the warmer temperature is partially responsible for the lower IPC during this experiment compared with an average of 30 L<sup>-1</sup> on March 5th. As discussed in section 2, Hicks and Vali (1973) reported decreased yields at temperatures only above -2 °C, and relatively constant yields at colder temperatures. However, Kumai (1982) found a marked decrease in propane effectiveness for temperatures warmer than -5 °C. Of course, direct comparison of the IPC assumes similar dispersion of the ice crystal plumes created by the two propane releases, and no direct evidence exists to support or refute that assumption. Target wind speeds were higher on March 11th, which could reduce the IPC by about 1/3 compared with March 5th, all else being equal. Obviously, additional observations are needed before definitive statements can be made about the temperature dependence of propane yield.

The very low snowfall likely caused by this propane seeding may be caused by the combined factors of decreased propane effectiveness and very slow crystal growth rates, both a result of the warm temperatures. However, it is worth recalling that the horizontal distance between the HAS and Target is only 4.2 km, and the locations were chosen for test purposes because of the ability to routinely target the Target site. An operational seeding program would be designed to affect a more distant target. For example, the California program discussed by Reynolds (1994) shows typical distances between propane dispensers and target gages between 15 to 30 km, which would provide much more crystal growth time than the experiments reported herein.



### **Mission**

The mission of the Bureau of Reclamation is to manage, develop, and protect water and related resources in an environmentally and economically sound manner in the interest of the American Public.